USAARL-TECH-FR--2023-18

En Route Care in Confined Spaces: Loading and Unloading Effect on Patients

Rachel Kinsler, Kerri Caruso, Amy Lloyd, Laura R. Kroening,
& Jeffrey Molles

Notice

Qualified Requesters

Qualified requesters may obtain copies from the Defense Technical Information Center (DTIC), Fort Belvoir, Virginia 22060. Orders will be expedited if placed through the librarian or other person designated to request documents from DTIC.

Change of Address

Organizations receiving reports from the U.S. Army Aeromedical Research Laboratory on automatic mailing lists should confirm correct address when corresponding about laboratory reports.

Disposition

Destroy this document when it is no longer needed. Do not return it to the originator.

Disclaimer

The views, opinions, and/or findings contained in this report are those of the author(s) and should not be construed as an official Department of the Army position, policy, or decision, unless so designated by other official documentation. Citation of trade names in this report does not constitute an official Department of the Army endorsement or approval of the use of such commercial items.

IRB Determination and Number

This study, USAARL 2021-022, was determined to be research not involving human subjects by the USAARL Exempt Determinations Official and approved on 10 June 2021.

REPORT DOCUMENTATION PAGE

Form Approved
OMB No. 0704-0188

1. REPORT DATE *(DD-MM-YYYY)*	2. REPORT TYPE	3. DATES COVERED *(From - To)*
06-03-2023	Final Report	Oct 2016 - Apr 2022

4. TITLE AND SUBTITLE
En Route Care in Confined Spaces: Loading and Unloading Effect on Patients

5a. CONTRACT NUMBER

5b. GRANT NUMBER
DM167047

5c. PROGRAM ELEMENT NUMBER
6.3/37300

6. AUTHOR(S)
Kinsler, R. E.[1], Caruso, K.[1,2], Lloyd, A. L.[1,2], Kroening, L. R.[1,2], & Molles, J. J.[1,2]

5d. PROJECT NUMBER
2021-022

5e. TASK NUMBER

5f. WORK UNIT NUMBER

7. PERFORMING ORGANIZATION NAME(S) AND ADDRESS(ES)
U.S. Army Aeromedical Research Laboratory
P.O. Box 620577
Fort Rucker, AL 36362

8. PERFORMING ORGANIZATION REPORT NUMBER
USAARL-TECH-FR--2023-18

9. SPONSORING/MONITORING AGENCY NAME(S) AND ADDRESS(ES)
Defense Health Program

10. SPONSOR/MONITOR'S ACRONYM(S)
DHP

11. SPONSOR/MONITOR'S REPORT NUMBER(S)

12. DISTRIBUTION/AVAILABILITY STATEMENT
DISTRIBUTION STATEMENT A. Approved for public release: distribution is unlimited.

13. SUPPLEMENTARY NOTES
[1]U.S. Army Aeromedical Research Laboratory, [2]Goldbelt Frontier, LLC

14. ABSTRACT
The purpose of this study was to characterize the biodynamic response of a supine human during the loading and unloading procedures on a MEDEVAC aircraft. An instrumented manikin with accelerometers and gyroscopic sensors replicated the human biodynamic response to vibration and mechanical shock. Two platforms, the Basic Medical Interior (BMI) on the HH-60 and the Interim MEDEVAC Mission Support System (IMMSS) on the UH-60 were used for testing. Other parameters were varied throughout the study including loading height, loading direction (head first versus feet first), and litter pole sensor placement (inboard versus outboard). Results showed that loading the litter imparted significantly more vibrational exposure to the manikin than walking the litter. There were no significant differences in vibratory exposure between the two MEDEVAC platforms. No significant difference was also observed when comparing loading the manikin head first versus feet first, or when comparing loading at the top height versus the bottom height within the platforms. This study indicates that litter loading and unloading procedures result in statistically significant exposure to vibratory motions and may result in exacerbating casualty injury. Aircraft design and litter bearer training may help reduce some exposure to these motions.

15. SUBJECT TERMS
Patient loading, MEDEVAC, helicopter, litters, en route care, vibration, acceleration, rotational velocity, shock, vibration transmissibility, jolt exposure, RMS, VDV

16. SECURITY CLASSIFICATION OF:			17. LIMITATION OF ABSTRACT	18. NUMBER OF PAGES	19a. NAME OF RESPONSIBLE PERSON
a. REPORT	b. ABSTRACT	c. THIS PAGE			Loraine St. Onge, PhD
UNCLAS	UNCLAS	UNCLAS	SAR	67	19b. TELEPHONE NUMBER *(Include area code)* 334-255-6906

This page is intentionally blank.

Summary

The exposure to vibratory motion and repeated shocks associated with medical evacuation (MEDEVAC) may contribute to exacerbation of casualty injuries and possible consequences to patient health outcome. The purpose of this study was to characterize the biodynamic response of a supine human during the loading and unloading procedures on a MEDEVAC aircraft. An instrumented manikin with accelerometers and gyroscopic sensors replicated the human biodynamic response to vibration and mechanical shock. Video data was also recorded for all trials. Two platforms, the Basic Medical Interior (BMI) on the HH-60 and the Interim MEDEVAC Mission Support System (IMMSS) on the UH-60 were used for testing. Other parameters were varied throughout the study, including loading height, loading direction (head first versus feet first), and litter pole sensor placement (inboard versus outboard). The research team completed 20 loading and unloading trials under different combinations of these parameters.

For analysis, each trial was divided into separate motion segments; litter lifting, walking to platform, loading litter, unloading litter, walking from platform, and litter dropping. The metrics used for data analysis included metrics based on International Organization for Standardization (ISO) 2631-1 (e.g., vibration dose value [VDV] and root mean square [RMS]), maximum acceleration, and jolt exposure (JE). The latter is an acceleration-based metric developed for this study to better characterize the unique motions recorded. The video data was also synchronized with the inertial data to link the measurements with the actions of the litter bearers, litter, and manikin.

Analysis was conducted in a manner allowing for both biodynamic characterization and statistical analysis (via t-test) of the varied parameters. Results showed that loading the litter imparted significantly more vibrational exposure to the manikin than walking the litter, between three and eleven times as much according to JE. There were no significant differences in vibratory exposure between the two MEDEVAC platforms. No significant difference was observed when comparing loading the manikin head first versus feet first, or when comparing loading at the top height versus the bottom height within the platforms. The litter pole sensor reveals that the outboard side showed a higher JE by a factor of 1.75 when compared to the inboard side. Finally, JE for loading was significantly higher than that for unloading by as much as a factor of 2.4.

This study indicates that litter loading and unloading procedures result in statistically significant exposures to vibratory motions and may result in exacerbating casualty injuries. Aircraft design and litter bearer training may help reduce some exposure to these motions. Due to the large standard deviations of the results, future studies should include factors such as training, experience, and anthropometry of the litter bearers.

This page is intentionally blank.

Acknowledgements

The Fort Rucker Department of Aviation Medicine Dustoff Training Complex supported this research by providing a venue for data collection to take place using medical evacuation simulators. Several U.S. Army Aeromedical Research Laboratory Soldiers also assisted in performing the trials.

This page is intentionally blank.

Table of Contents

List of Figures

List of Tables

This page is intentionally blank.

Introduction

Surveys on health care providers in the field have reported severe discomfort and pain experienced by casualties during military ground and air transport attributed the pain to vibration and repeated shock associated with the transport (Kinsler et al., 2015). The forces and vibrations transmitted to the patient's body through the transport system could have severe consequences, especially for neurotrauma patients sensitive to increased intracranial pressure (Ratanalert et al., 2004; Reno, 2010). Studies looking at different litters, transport systems, and immobilization systems determined how these systems exacerbate or mitigate the vibration and motion stresses during medical evacuation (MEDEVAC) (Kinsler et al., 2015 and 2018). However, these findings are limited to the transport ride profiles, with little evidence describing the impact of these systems during the loading and unloading phase of MEDEVAC. Subjective observations during field evacuations have revealed cases of patients experiencing unexpected mechanical shocks and motions during loading and unloading, such as accidental litter dropping by litter bearers. These transmitted forces and motions can have consequences on patient health outcomes and patient well-being. The purpose of this study is to define the mechanical inputs and unexpected shocks patients are exposed to during the loading and unloading procedures of MEDEVAC. These findings may contribute to improving loading procedures as well as the future design of transport systems.

Studies reported in the literature and observations from Operation Iraqi Freedom and Operation Enduring Freedom indicated that repeated shock and vibration during aeromedical and ground transport can cause considerable patient motion and may adversely affect patient comfort and medical outcome. Patient management during military en route care is a complex process because of inconsistencies in patient clinical conditions, vehicle configurations, patient transport systems (e.g., litters and immobilizations systems), and environments associated with transport.

In 2019, the U.S. Army Aeromedical Research Laboratory (USAARL) conducted a survey to investigate the negative features of common MEDEVAC platforms (Conti et al., 2019). The majority of the 60 respondents were critical care flight paramedics (CCFPs) who performed their duties on the HH-60 and/or UH-60. The results of the survey highlighted that compartment configurability, the litter system, cabin ergonomics, compartment size, patient loading capability, and personal protective gear (PPG) were all reported to negatively affect the mission by over 60% of respondents. Out of those six features, four (compartment configurability, the litter system, cabin ergonomics, and patient loading capability) highlighted the litter pan system or lifting littered patients as the main problems with the systems. Identifying the negative aspects of patient loading and unloading is especially exigent given that future MEDEVAC operations will require caring for multiple patients, enhancing these current issues. Task-specific research is needed to improve patient handling safety, loading, and unloading procedures and the development of future transport systems.

MEDEVAC platforms and en route care operations continuously look to optimize patient care and provider capabilities. The confined space of common MEDEVAC platforms presents the difficult task of loading and unloading patients onto these transport systems. Working as a CCFP requires heavy lifting, continuous or prolonged gripping, and repetitive motions that increase the chances of mishaps during patient loading and unloading. In 2011, the USAARL conducted a study to assess fixed position litter loading on a MEDEVAC helicopter where a

common observation was the tendency for the litter to be caught on the litter pan belts and interfere with other protruding structures (Kinsler & Barazanji, 2011). This environment does not allow for easy, smooth loading and may result in unexpected shocks or motion to the patient. Different MEDEVAC configurations possess different features that may influence patient loading and unloading; therefore, this study explores loading and unloading on two common platforms, the HH-60 with the Basic Medical Interior (BMI) and the UH-60 with the Interim MEDEVAC Mission Support System (IMMSS). The results of this study provide critical information for patient handling system designers to develop safer platforms and procedures that minimize the amount of forces transmitted to the patient's body during loading and unloading.

While motion transmitted to the human body during vehicle motion is the focus in most transmitted-vibration analysis studies (Meusch & Rahmatalla, 2014a, 2014b; DeShaw & Rahmatalla, 2016), the measurement of the forces transmitted to the different body segments of the supine patient during loading is limited in the literature. The complexity of the biodynamic response of different body segments presents a challenging task for analysis. Unexpected large body motion can dramatically change the orientations of the sensors attached to the body and the transport system, which can generate significant assessment and conclusion errors. However, with the current advances in new motion measurement technologies, effective methodologies have been established to deal with such complicated environments (DeShaw & Rahmatalla, 2012). For this study, a simulated patient manikin, the Instrumented Supine Manikin (ISMv1.2), represents the patient.

Objectives

This is a characterization study to define the forces on a simulated patient during the loading and unloading phases of MEDEVAC. The transmitted forces/motions to the manikin body segments will be collected and analyzed.

Specific Aims

Specific Aim 1: Collect acceleration and gyroscopic data from a simulated patient during loading and unloading on different MEDEVAC configurations.

Specific Aim 2: Characterize the biodynamic response of a simulated patient during loading and unloading procedures.

Methods

A team of four litter bearers and a simulated flight medic performed loading and unloading procedures with the ISMv1.2 on two different MEDEVAC platforms, the HH-60M with BMI and UH-60A/L with IMMSS. Previous studies have shown that differences in litter bearer size or height may affect the person in the aircraft loading the paitent, but do not significantly affect the patient on the litter (Kinsler & Barazanji, 2011). Since this study focused on the patient, the anthropometric characteristics team consisting of the litter bearers and the simulated medic were not controlled.

The ISMv1.2 replicates the human biodynamic response to vibration. The ISMv1.2 has several internal six degree-of-freedom (6DOF) sensors (combined accelerometers and

gyroscopes), which all connect to a built-in data acquisition system located inside the manikin's chest. Figure 1 shows the sensor locations within the manikin and the relevant coordinate systems, local and global. To record the response of the simulated patient, three 6DOF sensors were located in the head, chest, and pelvis and one triaxial accelerometer was located in the leg.

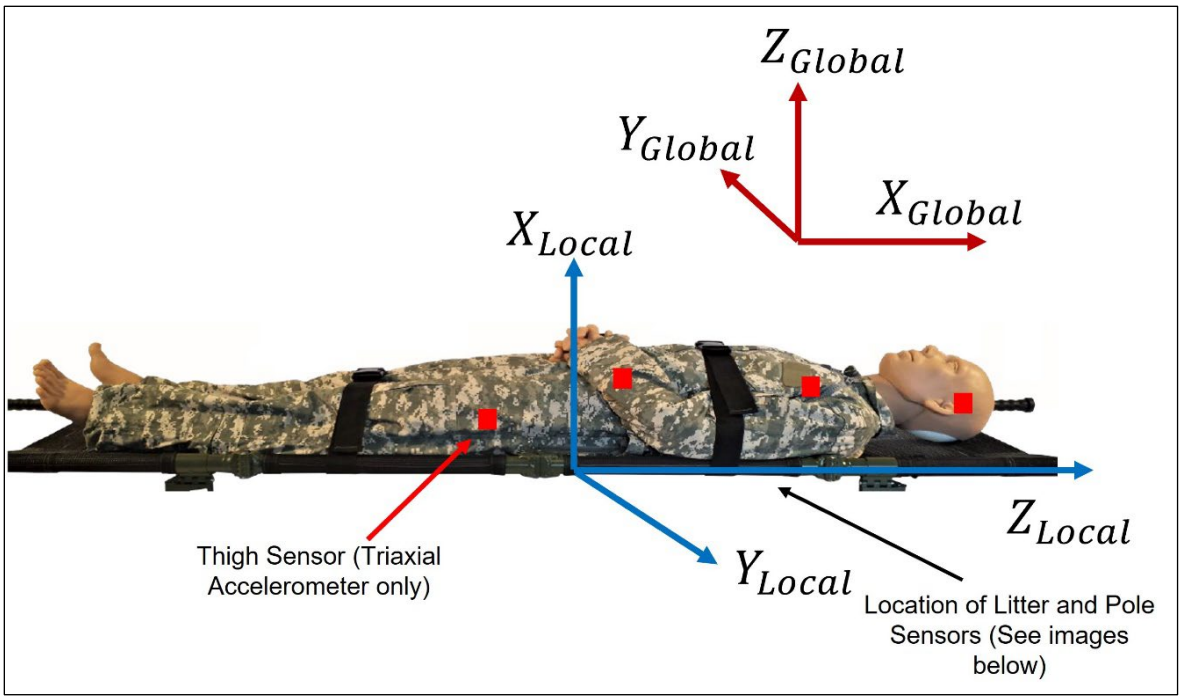

Figure 1. ISMv1.2 sensor locations and relevant coordinate systems.

Figure 2 shows the sensors located on the litter. To record the input excitations of the system, a 6DOF reference sensor was mounted onto the litter mesh near the center of the manikin and an accelerometer was mounted onto one of the litter poles. Both of these input sensors were mounted at the center of the litter, approximately 37 inches from the end of the poles. This location is the maximum deflection of the litter when weighted down by the manikin. The right image (Figure 2) shows the mounting plates for the 6DOF sensor (gray mounting pate) and the accelerometer (yellow mounting plate) attached to the litter. Both sensors were mounted on the bottom side of the litter. To protect the input sensors from hitting objects on the platform or interfering with the litter bearers, a plastic cover was attached onto each sensor plate. The input sensor on the litter pole was switched between both litter poles throughout the study to provide the input response to both the outboard and inboard side of the litter system.

This space is intentionally blank.

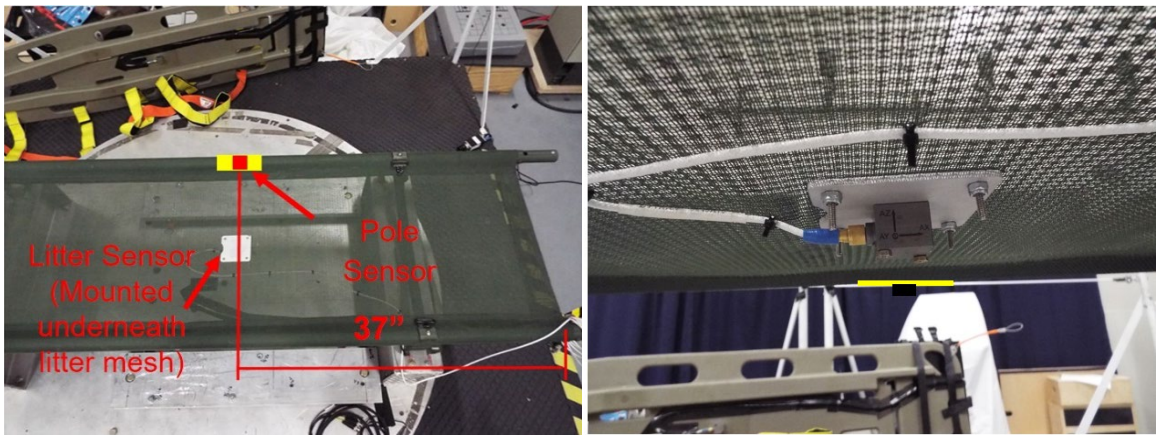

Figure 2. Sensor placement locations on litter.

Each trial was ordered by MEDEVAC platform (BMI and IMMSS), litter pan's position, direction of loading (head first and feet first), and the litter pole sensor placement (inboard and outboard). For each trial, the manikin was loaded and unloaded once. Table 1 shows the testing configurations and the order of testing.

Table 1. Order of Testing Configurations

Trial Number	Platform	Litter Position	Direction of Loading	Sensor Placement
1	BMI	Top	Head First	Outboard
2	BMI	Middle	Head First	Outboard
3	BMI	Bottom	Head First	Outboard
4	IMMSS	Top	Feet First	Inboard
5	IMMSS	Bottom	Feet First	Inboard
6	BMI	Top	Feet First	Inboard
7	BMI	Middle	Feet First	Inboard
8	BMI	Bottom	Feet First	Inboard
9	IMMSS	Top	Head First	Outboard
10	IMMSS	Bottom	Head First	Outboard
11	IMMSS	Top	Feet First	Outboard
12	IMMSS	Bottom	Feet First	Outboard
13	BMI	Top	Feet First	Outboard
14	BMI	Middle	Feet First	Outboard
15	BMI	Bottom	Feet First	Outboard
16	IMMSS	Top	Head First	Inboard
17	IMMSS	Bottom	Head First	Inboard
18	BMI	Top	Head First	Inboard
19	BMI	Middle	Head First	Inboard
20	BMI	Bottom	Head First	Inboard

Since loading can be a strenuous and an exhausting task, the order of testing was randomized between the platforms and configurations to help limit bias. The BMI has three litter positions (top, middle, and bottom), while the IMMSS has two (top and bottom). The direction of loading refers to the part of the manikin that entered the aircraft first during the loading task. For example, during the "head first" trial, the head entered the aircraft first during loading and the feet exited first during unloading. Current MEDEVAC aircraft platforms commonly load the patients in the feet first direction, depending on the patient's injuries and seating location of the medic. However, loading and unloading the manikin in both directions, head first and feet first, provides data for future MEDEVAC platform designs. The last column, the sensor placement, refers to the location of the sensor on the litter pole with respect to the outboard and inboard sides of the aircraft. The outboard side refers to the outer most side of the aircraft, while the inboard side refers to the midline of the aircraft. This variable allowed the study team to characterize the input of potential interruptions caused by the aircraft such as the seatbelts (outboard side) versus the input of medic handling such as lifting or sliding (inboard side). Figure 3 illustrates the set up for trials 1-5 to better understand the testing configurations.

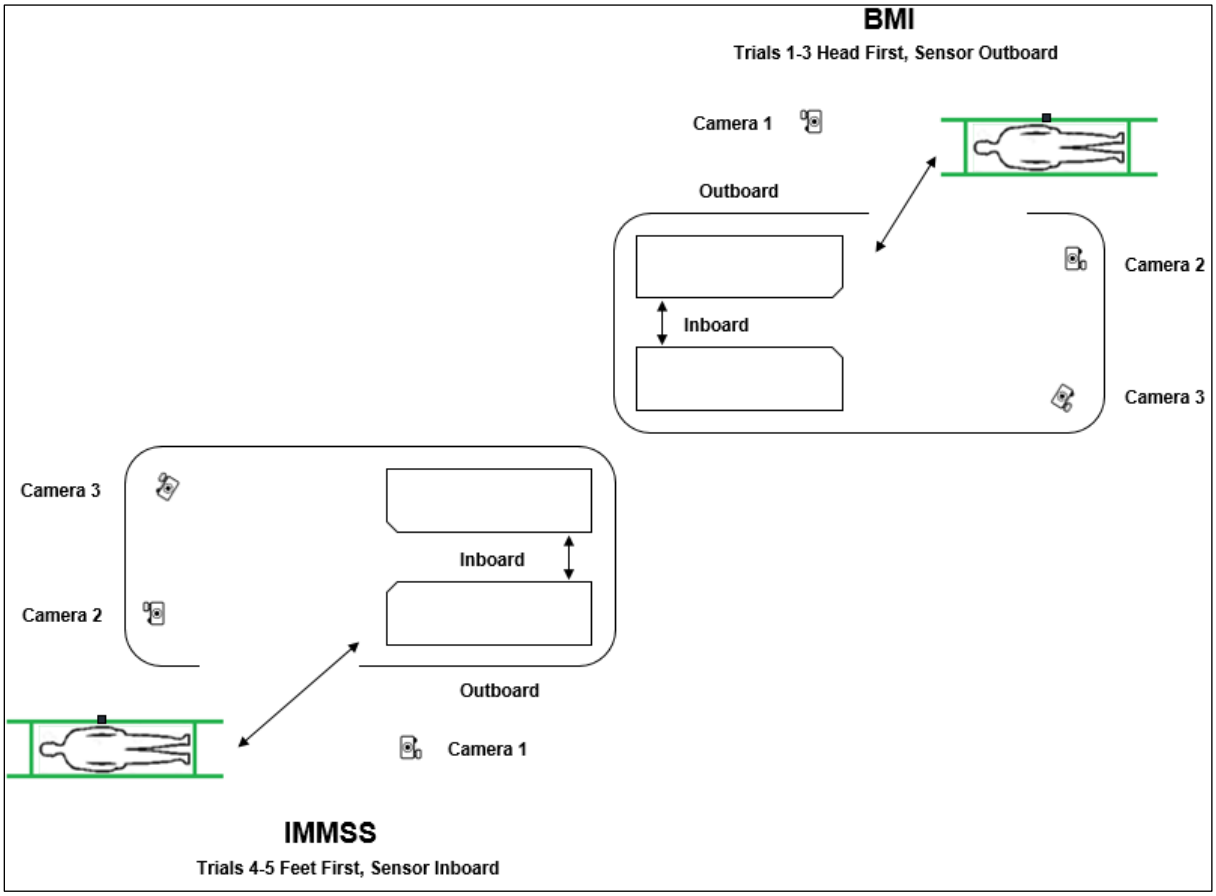

Figure 3. Testing setup for trials 1 through 5.

Before testing, digital cameras were set up around the space and the ISMv1.2's internal sensors were calibrated. For the BMI trials, the platform was configured to resemble the HH-60M BMI. On the testing side, all litter pans were lowered, and the top litter position was prepared to be loaded. On the opposite side, the litter pans were raised up to the appropriate heights, as if they were already loaded with patients. The manikin was strapped to a standard U.S. Army decontaminable litter using litter straps in a two-strap configuration. One strap went across the chest of the manikin and the other went across the legs. The litter was placed on the ground ten feet away from the platform.

To synchronize the video and sensor data, recordings were started as close to simultaneously as possible. Once recording began, a researcher tapped the chest plate of the ISMv1.2 three times in succession. These taps were registered on both the internal sensors and video, and as such could be used to synchronize the data streams. Four litter bearers then lifted the litter off the ground, carried it to the platform and passed it off to another volunteer who was acting as the receiving medic on the inside of the aircraft. Together, the team and the simulated medic loaded the manikin onto the MEDEVAC platform. Once the litter was securely settled on the litter pan, the simulated medic tapped the manikin three times again to signal the start of the unloading portion. The medic and team removed the litter from the litter pan and placed it back down on the ground at the starting position. Recording was stopped and the next testing configuration was set up.

Results

The data from this study was processed and evaluated by ActiBioMotion (ABM), who have extensive experience in vibrational data analysis. ABM developed the ISMv1.2. The full report from ABM can be found in Appendix B.

After filtering the raw data using a lowpass filter, the sensor coordinate systems were combined into one global frame through a process called sensor fusion. The global frame is defined by a vertical Z axis parallel to gravity with a horizontal plane that creates the X and Y axes. During sensor fusion, the accelerometers were used to identify the vertical gravity vector while the gyroscopic sensors were used to obtain the orientation over short time periods. Together, an estimation of the sensor orientation and global frame were defined.

Next, the data was reduced into several motion segments through the use of the video data. The relevant segments used for analysis included lifting litter, walking to platform, loading litter, unloading litter, walking from platform, and dropping litter. Other motion segments, such as the three taps used for synchronization, or pauses, were ignored during analysis.

To quantify acceleration, ABM followed ISO 2631-1 guidelines (International Organization for Standardization, 1997) and ISO specifications were applied to all motion segments for each sensor. First, the frequency-weighted translation acceleration was applied. Then the crest factor was calculated with transient vibration and mechanical shocks. Subsequently, the weighted RMS, running RMS, maximum transient vibration value and the frequency-weighted and unweighted VDV, were calculated. It was determined that the VDV was the most effective method of quantifying the acceleration. This determination was based on the high crest factor values as well as a qualitative analysis of the inertial data. VDV is often used to

characterize vibration data with a significant number of mechanical shocks. The formulae defining these metrics can be found in ISO 2631-1 and Appendix B.

The manikin experienced motions that go beyond transient vibration and shock. Additional metrics including unweighted RMS and VDV, as well as the weighted and unweighted gyroscopic data RMS were used to supplement the metrics above. Approximate transmissibility values were also calculated by dividing the VDV of each segment (the outputs) by the VDV of the litter (input). All of these metrics proved useful in quantifying the inertial data.

Finally, one last metric was developed to describe a motion experienced by the manikin that cannot be described solely as vibration or mechanical shock. This metric was termed jolt exposure (JE). JE is calculated by taking the absolute value of a single axis acceleration profile (unweighted) and removing all data points that do not exceed a certain threshold. The threshold chosen in this report was 1.6 meter per second squared (m/s^2). This value was chosen from section C.2.3. of ISO 2631-1, as it represents the upper range value of vibratory acceleration considered to be uncomfortable for healthy humans. It is assumed that the perception of discomfort would likely be greater in injured humans. The remaining data points are then squared (to assign greater weight to high accelerations) and summed. The equations are defined below:

$$if\ \|a(n)\| < 1.6\frac{m}{s^2}, then\ a(n) = 0 \qquad \text{Equation 1}$$

$$JE = \sum_{n=1}^{k} a\,(n)^2 \qquad \text{Equation 2}$$

Results are presented below in a series of box plots. Figures 4 through 9 represent the distribution over the full set of trials with the exception of trials 4 and 19. Trial 4 appeared to be an outlier, and trial 19 did not have a complete video recording and could not be properly segmented. The box plots include the VDV metric with weighted acceleration (Figure 4), the VDV metric calculated with unweighted accelerations (Figure 5), the RMS metric of the gyroscope data (Figure 6), and the JE metric for each body segment (Figure 7 only represents the head). The red line in the center of the box plots indicates the median value, the lower and upper lines of the box indicate the 25th and 75th percentile of the dataset, the lower and upper whiskers indicate the 5th and 95th percentile and the red plus symbols represent outlier data points.

This space is intentionally blank.

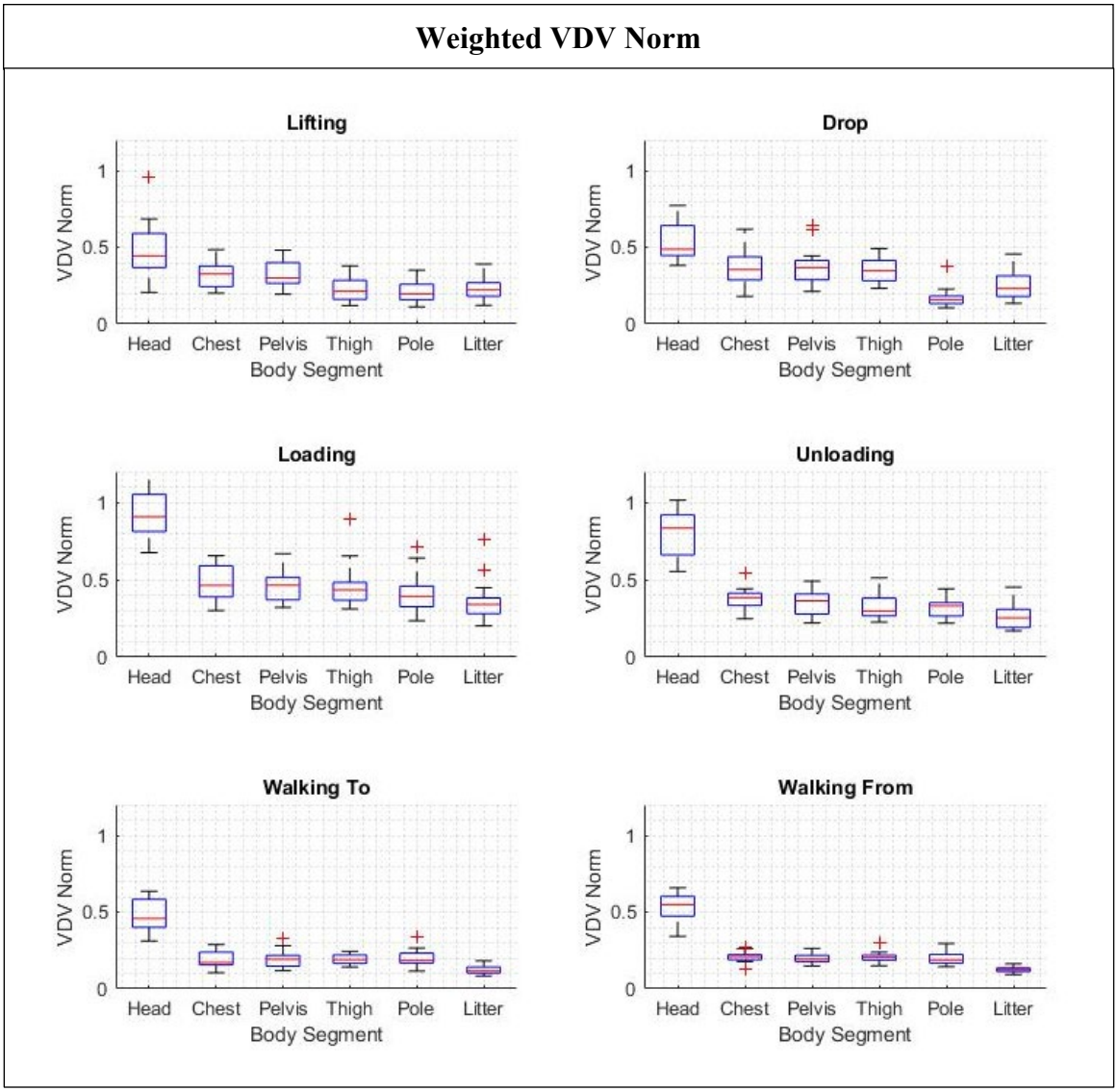

Figure 4. Weighted VDV norm by motion segment and sensor placement.

This space is intentionally blank.

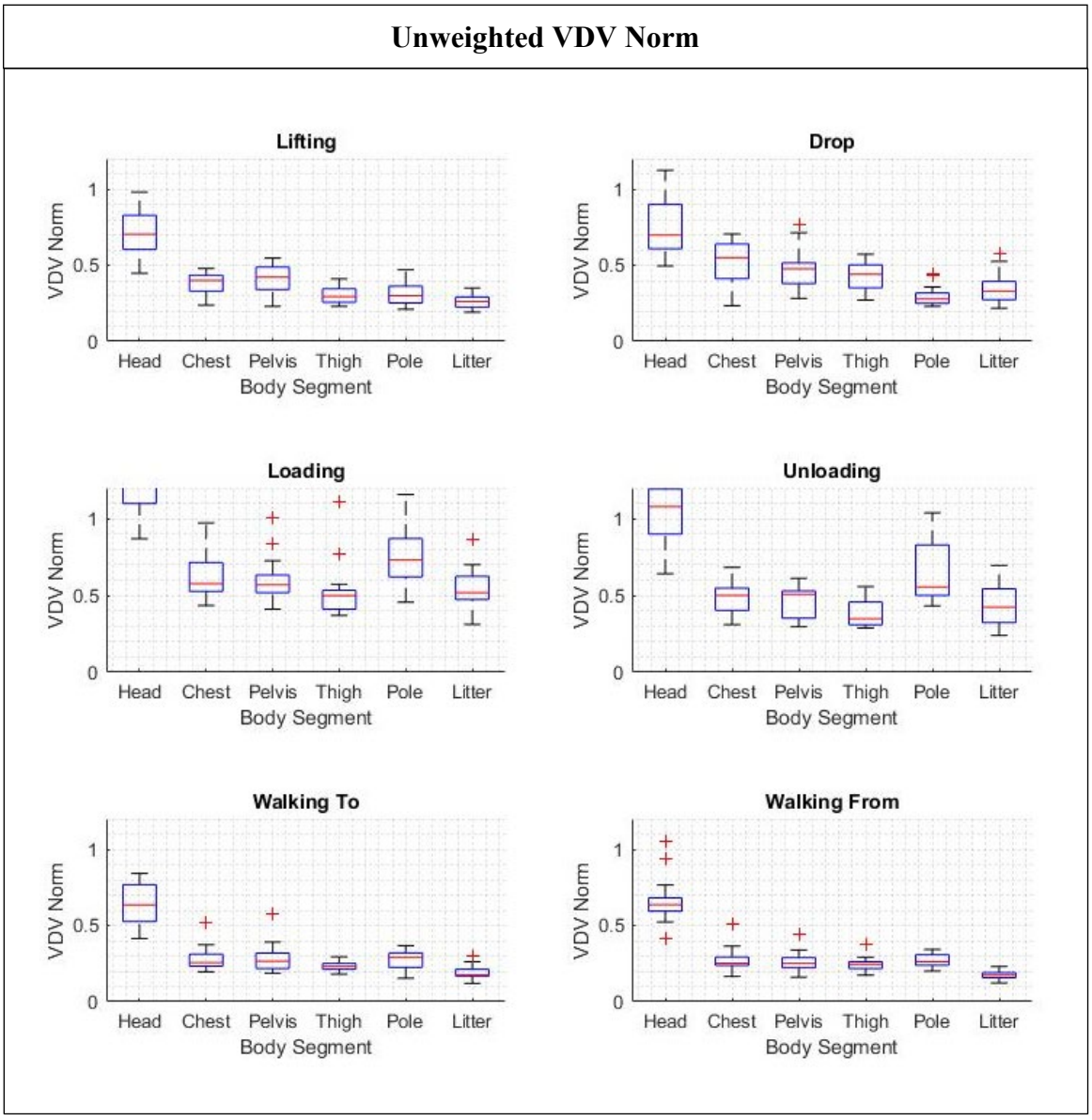

Figure 5. Unweighted VDV norm by motion segment and sensor placement.

This space is intentionally blank.

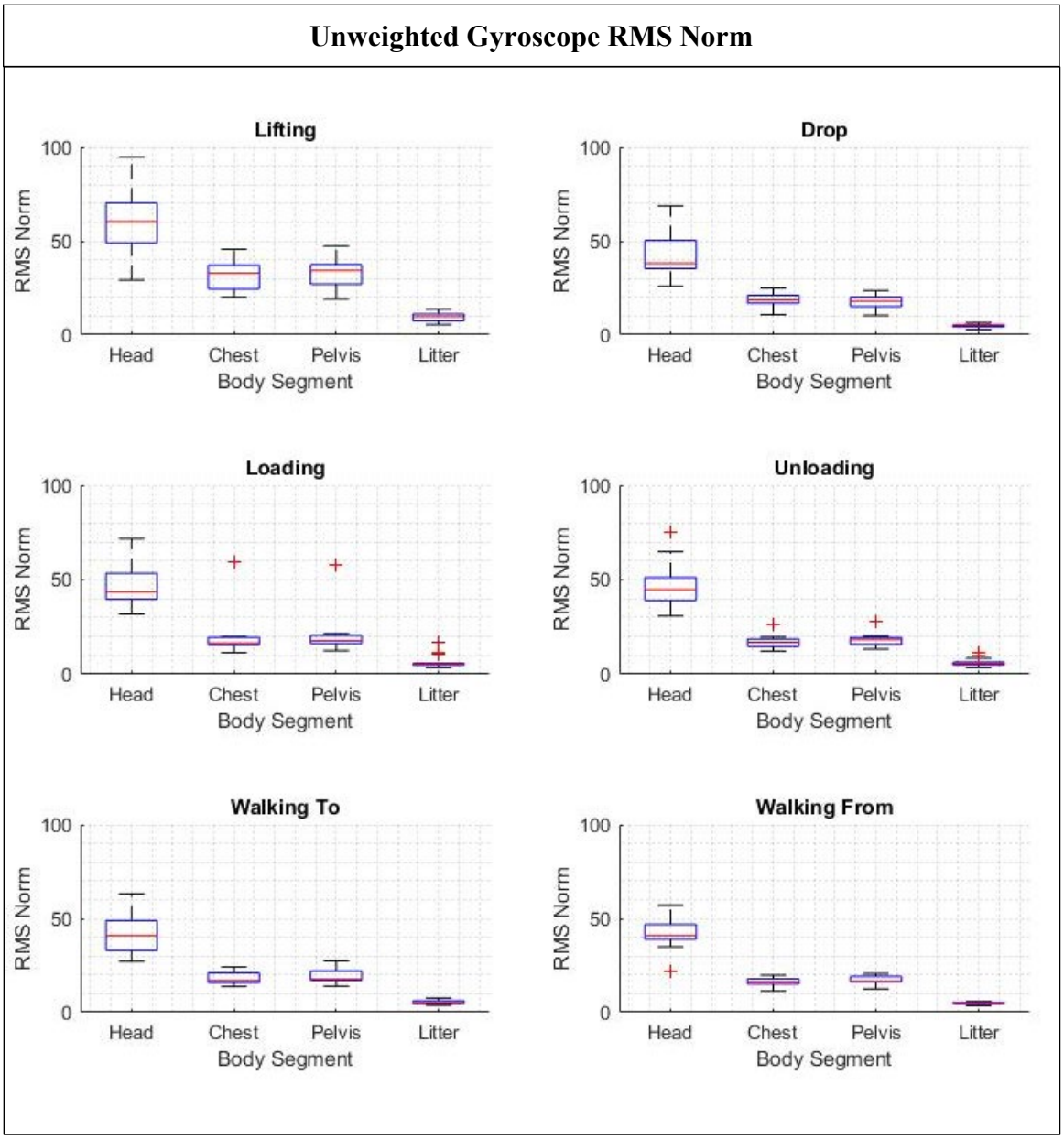

Figure 6. Unweighted gyroscope RMS norm by motion segment and sensor placement.

This space is intentionally blank.

Jolt Exposure Distribution for the Head

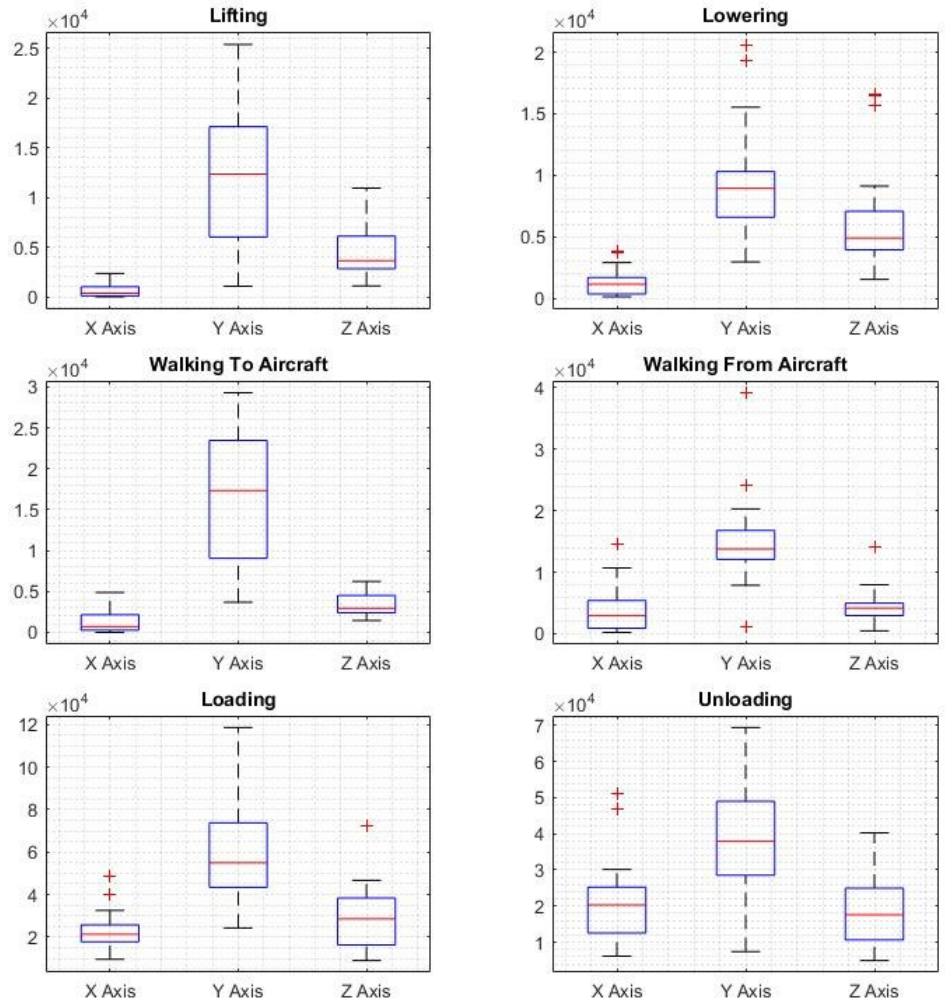

Figure 7. Jolt exposure to the head by motion segment and each axis.

This space is intentionally blank.

This page is intentionally blank.

Figure 8 shows the maximum acceleration values (defined by the norm and in units of g) that were encountered during each segment of each trial. Note that the color coding was applied to make table interpretation easier – color has no bearing on the risk or exposure of a certain value. The darkest green denotes the lowest observed acceleration and the darkest red denotes highest observed acceleration.

Maximum Acceleration (Norm in gs) of Each Segment for all Trials

Head

	Lifting	Walking To	Loading	Unloading	Wlaking From	Lowering
Trial 1	0.528	0.918	0.364	0.298	0.088	0.850
Trial 2	0.569	1.133	0.593	0.534	0.433	0.697
Trial 3	0.647	0.656	0.646	0.431	0.183	1.107
Trial 4	·	·	·	·	·	·
Trial 5	0.462	0.675	0.391	0.224	0.169	0.593
Trial 6	0.347	0.994	0.342	0.293	0.084	0.898
Trial 7	0.481	1.305	0.640	0.976	0.103	0.707
Trial 8	0.413	0.821	0.213	0.309	0.086	0.763
Trial 9	0.334	0.761	0.741	0.325	0.107	0.760
Trial 10	0.438	1.560	0.342	0.404	0.152	0.664
Trial 11	0.383	0.590	0.508	0.436	0.094	0.880
Trial 12	0.354	0.957	0.508	0.500	0.166	1.654
Trial 13	0.313	1.296	0.755	0.459	0.194	0.611
Trial 14	0.382	1.199	0.335	0.374	0.100	0.937
Trial 15	0.348	1.221	0.401	0.262	0.167	0.958
Trial 16	0.419	1.178	0.347	0.431	0.194	1.058
Trial 17	0.365	1.515	0.457	0.420	0.047	1.240
Trial 18	0.356	1.114	1.114	0.684	0.882	0.822
Trial 19	·	·	·	·	·	·
Trial 20	0.368	1.063	0.376	0.198	0.058	0.768

Chest

	Lifting	Walking To	Loading	Unloading	Wlaking From	Lowering
Trial 1	0.655	0.532	0.364	0.406	0.104	0.342
Trial 2	0.685	0.446	0.282	0.723	0.554	0.259
Trial 3	0.766	0.454	0.376	0.447	0.117	0.317
Trial 4	·	·	·	·	·	·
Trial 5	0.732	0.277	0.310	0.242	0.067	0.233
Trial 6	0.488	0.413	0.169	0.492	0.055	0.312
Trial 7	0.776	0.510	0.274	0.746	0.042	0.414
Trial 8	0.670	0.558	0.175	0.357	0.038	0.294
Trial 9	0.529	0.385	0.308	0.386	0.093	0.391
Trial 10	0.669	0.591	0.315	0.637	0.092	0.364
Trial 11	0.458	0.402	0.402	0.485	0.054	0.263
Trial 12	0.341	0.524	0.531	0.643	0.071	0.606
Trial 13	0.401	0.630	0.293	0.549	0.198	0.335
Trial 14	0.625	0.491	0.159	0.296	0.055	0.267
Trial 15	0.458	0.474	0.435	0.302	0.092	0.412
Trial 16	0.507	0.614	0.287	0.659	0.092	0.351
Trial 17	0.275	0.563	0.380	0.297	0.027	0.613
Trial 18	0.454	0.452	0.430	0.701	0.405	0.332
Trial 19	·	·	·	·	·	·
Trial 20	0.293	0.577	0.296	0.185	0.071	0.290

Pelvis

	Lifting	Walking To	Loading	Unloading	Wlaking From	Lowering
Trial 1	0.550	0.652	0.406	0.266	0.159	0.322
Trial 2	0.479	0.429	0.317	0.223	0.198	0.243
Trial 3	0.725	0.443	0.260	0.207	0.126	0.270
Trial 4	·	·	·	·	·	·
Trial 5	0.539	0.424	0.202	0.516	0.175	0.191
Trial 6	0.492	0.469	0.169	0.219	0.103	0.361
Trial 7	0.475	0.579	0.265	0.550	0.027	0.263
Trial 8	0.394	0.563	0.159	0.266	0.084	0.243
Trial 9	0.504	0.366	0.303	0.201	0.075	0.386
Trial 10	0.556	0.635	0.342	0.262	0.094	0.254
Trial 11	0.400	0.325	0.290	0.181	0.088	0.214
Trial 12	0.307	0.504	0.518	0.227	0.097	0.551
Trial 13	0.352	0.786	0.340	0.370	0.202	0.302
Trial 14	0.493	0.603	0.149	0.162	0.030	0.336
Trial 15	0.433	0.514	0.398	0.249	0.216	0.491
Trial 16	0.409	0.705	0.276	0.175	0.093	0.343
Trial 17	0.367	0.506	0.358	0.257	0.056	0.505
Trial 18	0.398	0.428	0.386	0.274	0.489	0.300
Trial 19	·	·	·	·	·	·
Trial 20	0.412	0.657	0.424	0.276	0.074	0.378

Thigh

	Lifting	Walking To	Loading	Unloading	Wlaking From	Lowering
Trial 1	0.386	0.463	0.463	0.194	0.172	0.388
Trial 2	0.332	0.459	0.193	0.123	0.098	0.254
Trial 3	0.389	0.348	0.195	0.150	0.078	0.279
Trial 4	·	·	·	·	·	·
Trial 5	0.295	0.378	0.219	0.555	0.158	0.197
Trial 6	0.358	0.409	0.165	0.150	0.116	0.345
Trial 7	0.292	0.724	0.142	0.405	0.085	0.316
Trial 8	0.258	0.607	0.082	0.267	0.151	0.367
Trial 9	0.304	0.371	0.275	0.164	0.105	0.270
Trial 10	0.326	0.531	0.151	0.230	0.181	0.237
Trial 11	0.332	0.436	0.264	0.157	0.161	0.245
Trial 12	0.307	0.395	0.277	0.220	0.074	0.484
Trial 13	0.283	0.411	0.147	0.286	0.211	0.329
Trial 14	0.368	0.545	0.118	0.117	0.058	0.376
Trial 15	0.430	0.569	0.327	0.232	0.226	0.706
Trial 16	0.297	0.435	0.178	0.128	0.071	0.284
Trial 17	0.396	0.401	0.285	0.293	0.127	0.357
Trial 18	0.286	0.454	0.126	0.225	0.314	0.319
Trial 19	·	·	·	·	·	·
Trial 20	0.402	0.429	0.415	0.258	0.100	0.229

Pole

	Lifting	Walking To	Loading	Unloading	Wlaking From	Lowering
Trial 1	0.216	0.430	0.386	0.146	0.136	0.362
Trial 2	0.188	0.410	0.278	0.142	0.135	0.302
Trial 3	0.230	0.332	0.253	0.142	0.127	0.340
Trial 4	·	·	·	·	·	·
Trial 5	0.166	0.397	0.320	0.277	0.251	0.298
Trial 6	0.177	0.313	0.234	0.191	0.128	0.286
Trial 7	0.185	0.657	0.134	0.438	0.122	0.263
Trial 8	0.181	0.670	0.194	0.153	0.165	0.404
Trial 9	0.157	0.376	0.208	0.156	0.128	0.296
Trial 10	0.210	0.615	0.237	0.144	0.348	0.271
Trial 11	0.263	0.416	0.280	0.036	0.035	0.261
Trial 12	0.075	0.274	0.224	0.050	0.042	0.378
Trial 13	0.081	0.346	0.212	0.071	0.050	0.267
Trial 14	0.099	0.447	0.215	0.052	0.029	0.326
Trial 15	0.094	0.606	0.342	0.053	0.043	0.309
Trial 16	0.288	0.489	0.274	0.052	0.104	0.265
Trial 17	0.154	0.432	0.134	0.113	0.055	0.331
Trial 18	0.100	0.435	0.171	0.241	0.547	0.343
Trial 19	·	·	·	·	·	·
Trial 20	0.121	0.540	0.314	0.068	0.146	0.294

Litter

	Lifting	Walking To	Loading	Unloading	Wlaking From	Lowering
Trial 1	0.416	0.431	0.426	0.157	0.101	0.268
Trial 2	0.389	0.315	0.236	0.073	0.093	0.205
Trial 3	0.563	0.358	0.209	0.143	0.073	0.214
Trial 4	·	·	·	·	·	·
Trial 5	0.339	0.267	0.215	0.345	0.145	0.162
Trial 6	0.363	0.272	0.171	0.173	0.085	0.170
Trial 7	0.288	0.517	0.202	0.180	0.010	0.223
Trial 8	0.278	0.529	0.168	0.199	0.053	0.269
Trial 9	0.366	0.329	0.281	0.148	0.063	0.291
Trial 10	0.335	0.333	0.296	0.176	0.148	0.175
Trial 11	0.260	0.329	0.263	0.082	0.097	0.157
Trial 12	0.257	0.348	0.349	0.137	0.062	0.277
Trial 13	0.297	0.274	0.219	0.236	0.190	0.200
Trial 14	0.334	0.492	0.113	0.081	0.037	0.204
Trial 15	0.379	0.382	0.326	0.177	0.161	0.335
Trial 16	0.356	0.378	0.092	0.115	0.073	0.248
Trial 17	0.321	0.347	0.225	0.144	0.062	0.279
Trial 18	0.259	0.368	0.196	0.212	0.397	0.189
Trial 19	·	·	·	·	·	·
Trial 20	0.331	0.416	0.418	0.227	0.062	0.187

Figure 8. Maximum value of the free acceleration norm for each body segment/litter location in each trial.

Transmissibility over each segment was presented as a bar graph (Figure 9). Figure 9 shows how the acceleration input to the manikin is either mitigated or exacerbated for each body segment. Values above 1.0 indicate exacerbation, while values below indicate mitigation. The black error bars indicate the standard deviation.

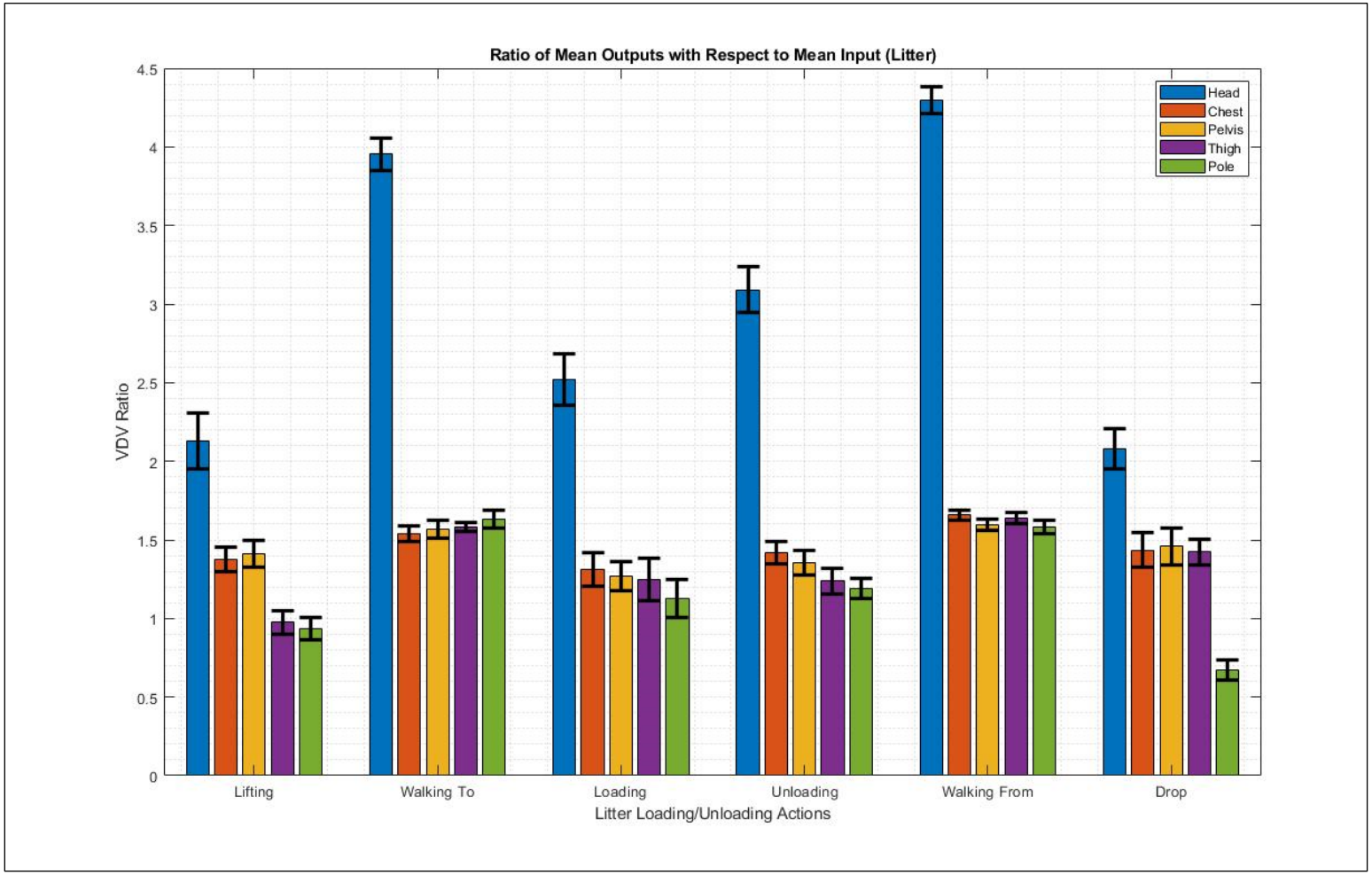

Figure 9. Approximated transmissibility showing metric broken down by motion segment and sensor placement.

Acceleration data from a single trial and body segment (chest) was broken down into each axis to identify the effects of unintentional actions of the litter bearers such as dropping the litter (Figure 10).

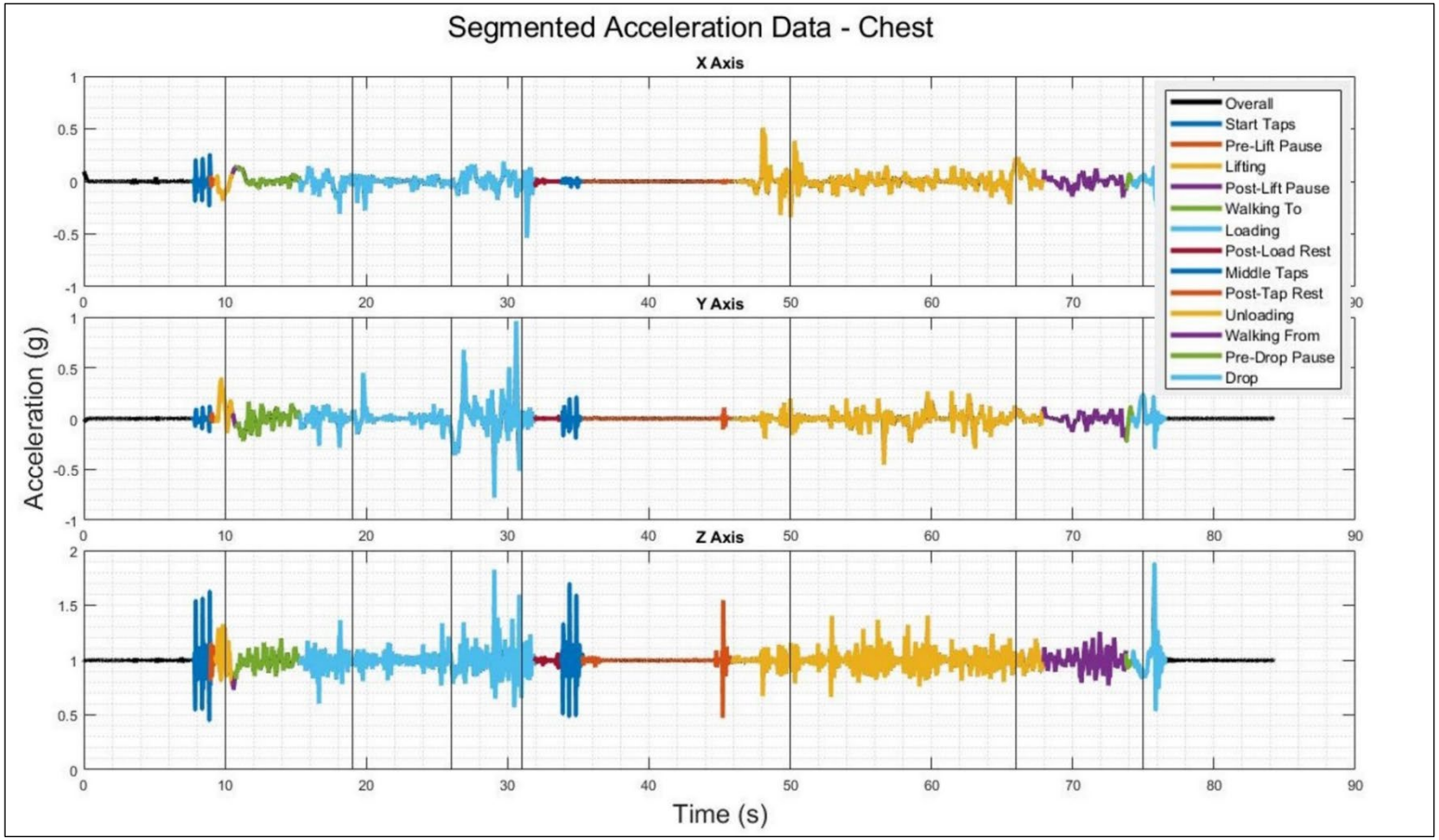

Figure 10. Segmented time history acceleration data for a single trial showing metric broken down by actions for chest sensor.

This page is intentionally blank.

The remaining results present the statistical analysis. This study compared several of the tested parameters to determine if there is a statistically significant difference in transmitted vibration or shock. Two sample t-tests were used to compare means. For this study, P-values below 0.05 were considered statistically significant, and P-values between 0.05 and 0.1 were considered marginally significant. The * symbol was placed above the bars with statistically significant differences, and the ^ symbol was placed above the bars with marginally statistically significant differences. The parameters were compared across the following metrics:

- Head VDV norm, chest VDV norm, pelvis VDV norm, pole VDV norm, and litter VDV norm;
- Head gyroscope RMS norm, chest gyroscope RMS norm, pelvis gyroscope RMS norm, and litter gyroscope RMS norm;
- Head JE norm, chest JE norm, pelvis JE norm, thigh JE norm, pole JE norm, and litter JE norm.

The comparisons made include walking versus loading (Figure 11), inboard versus outboard (Figure 12), BMI versus IMMSS (Figure 13), head first versus feet first (Figure 14), top versus bottom litter pans (Figure 15), and loading versus unloading (Figure 16).

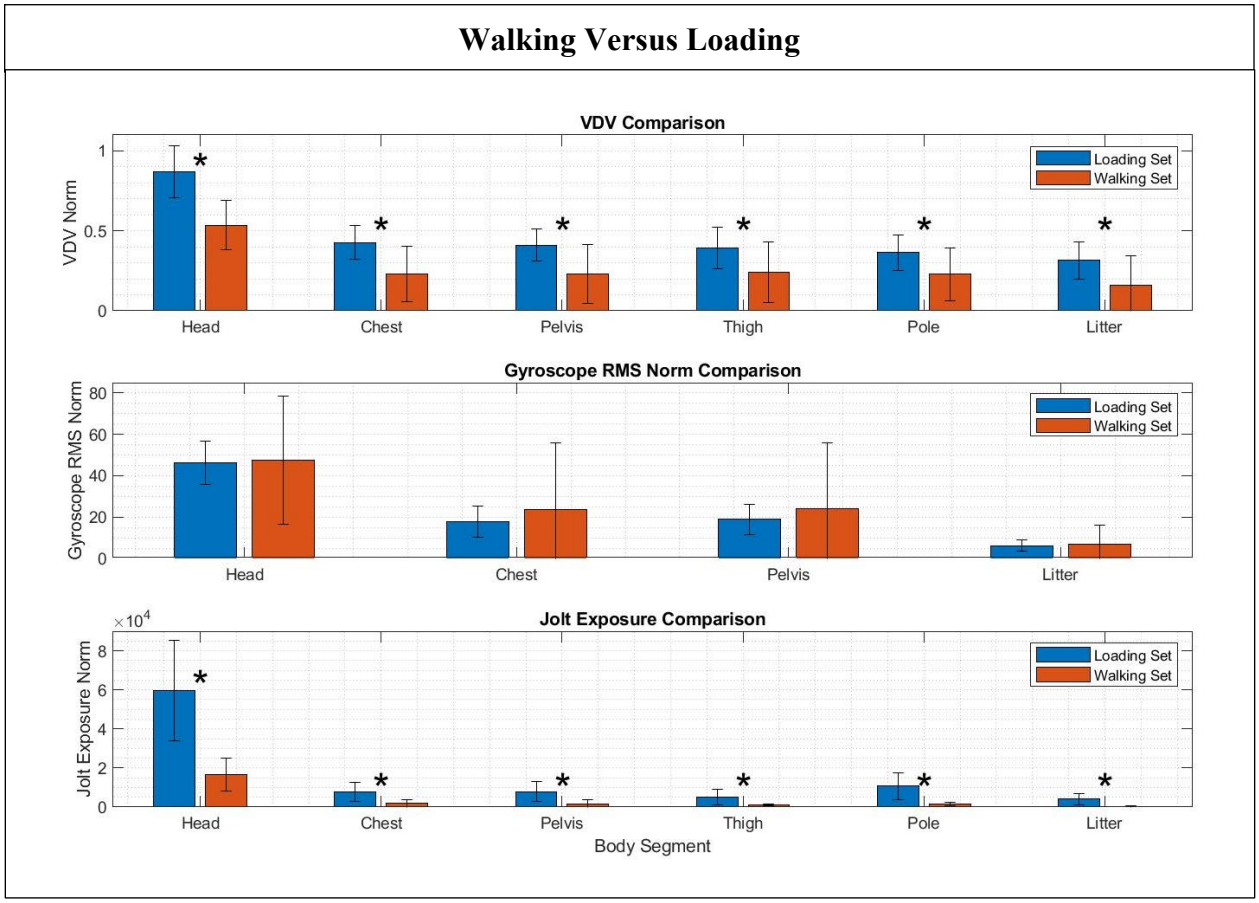

Figure 11. Comparison between walking and loading segments.

Figure 11 shows that all six VDV metrics and all six JE metrics were found to be significantly different between walking and loading. The differences between the VDV norm were large (loading was between 1.5 and 2 times greater); the differences between JE were larger (loading was between 3 and 11 times greater).

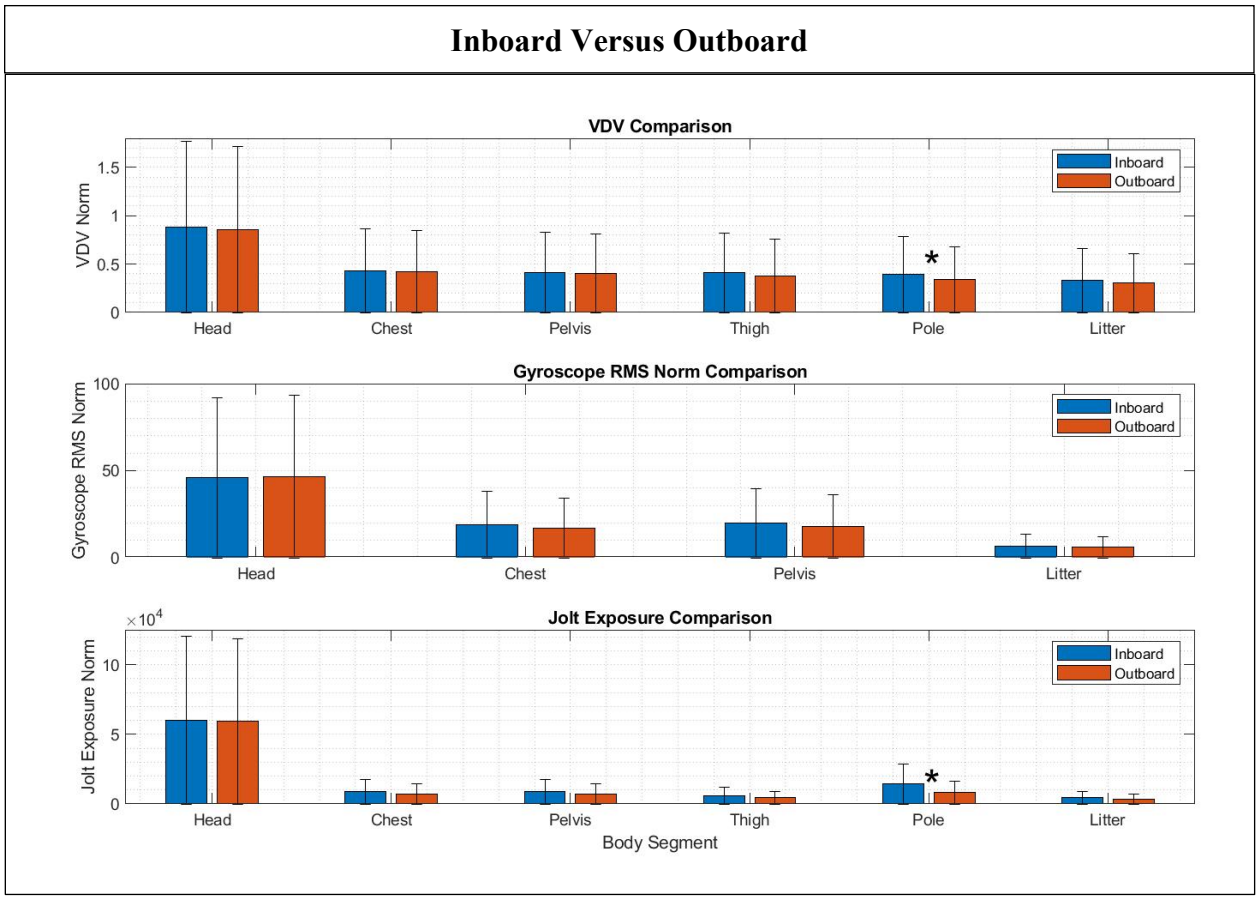

Figure 12. Comparison between inboard and outboard placement of litter pole sensor.

Half of the trials were conducted with the litter pole sensor on the inboard side and the other half were conducted with the litter pole sensor on the outboard side. As expected with this comparison, the pole VDV and the pole JE show statically significant results, but no other locations were significantly different.

This space is intentionally blank.

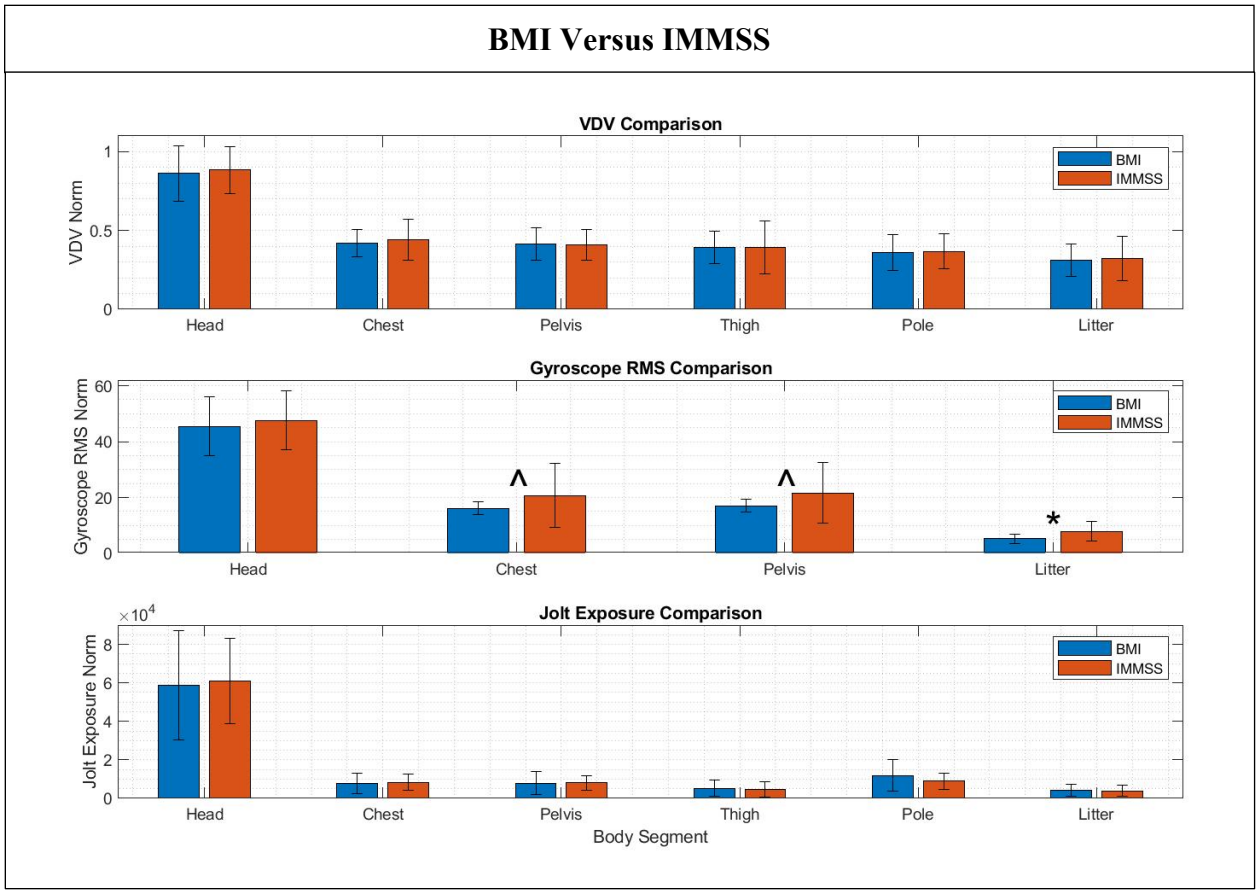

Figure 13. Comparison between BMI and IMMSS MEDEVAC platforms.

The difference in gyroscopic RMS values for the litter is statistically significant between the two platforms, while the difference in gyroscopic RMS values for the chest and pelvis are marginally statically significant.

This space is intentionally blank.

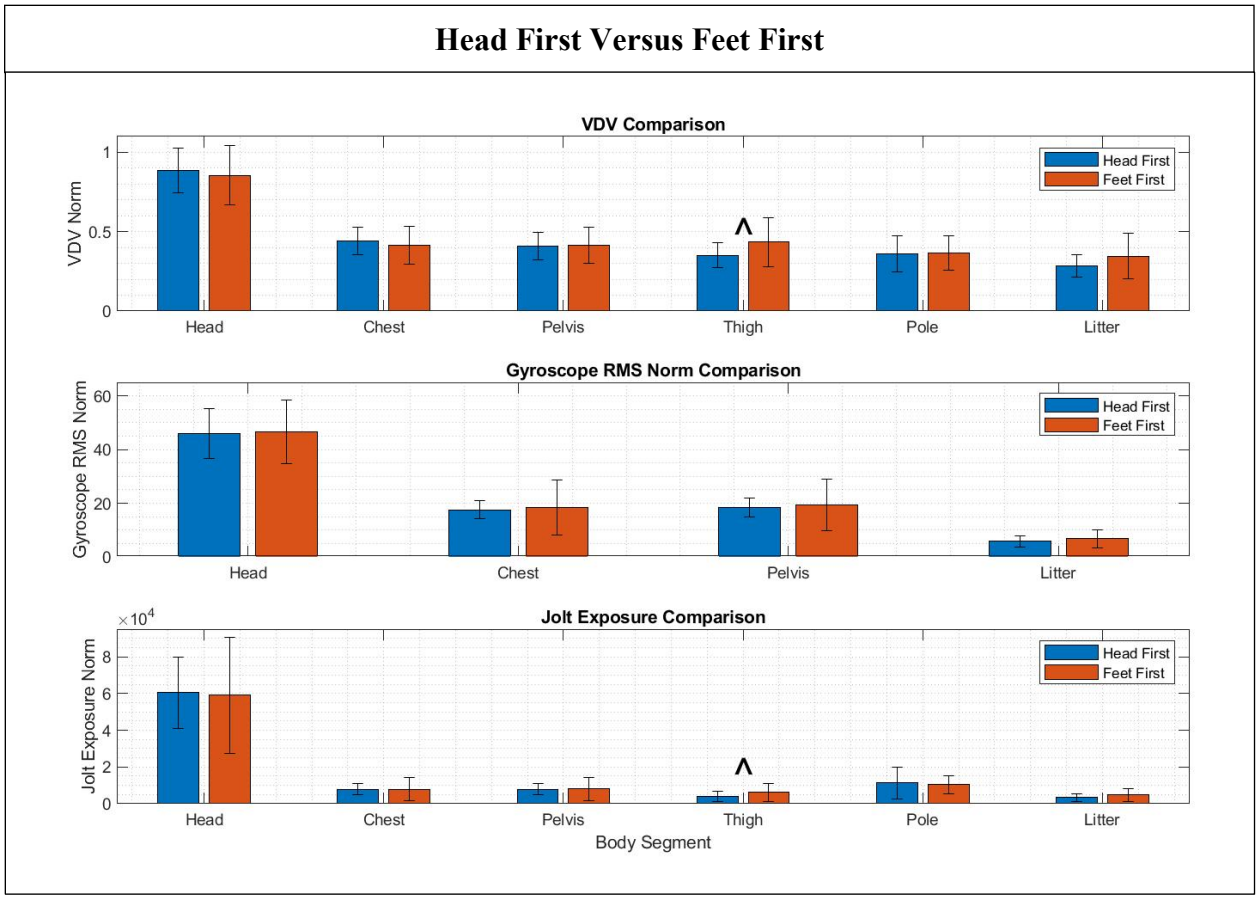

Figure 14. Comparison between loading directions, head first and feet first.

There are marginally statistically significant differences for the VDV and JE values at the thigh. Due to the lack of gyroscopic data in the thigh, it is unknown if those values would also be deemed significant.

This space is intentionally blank.

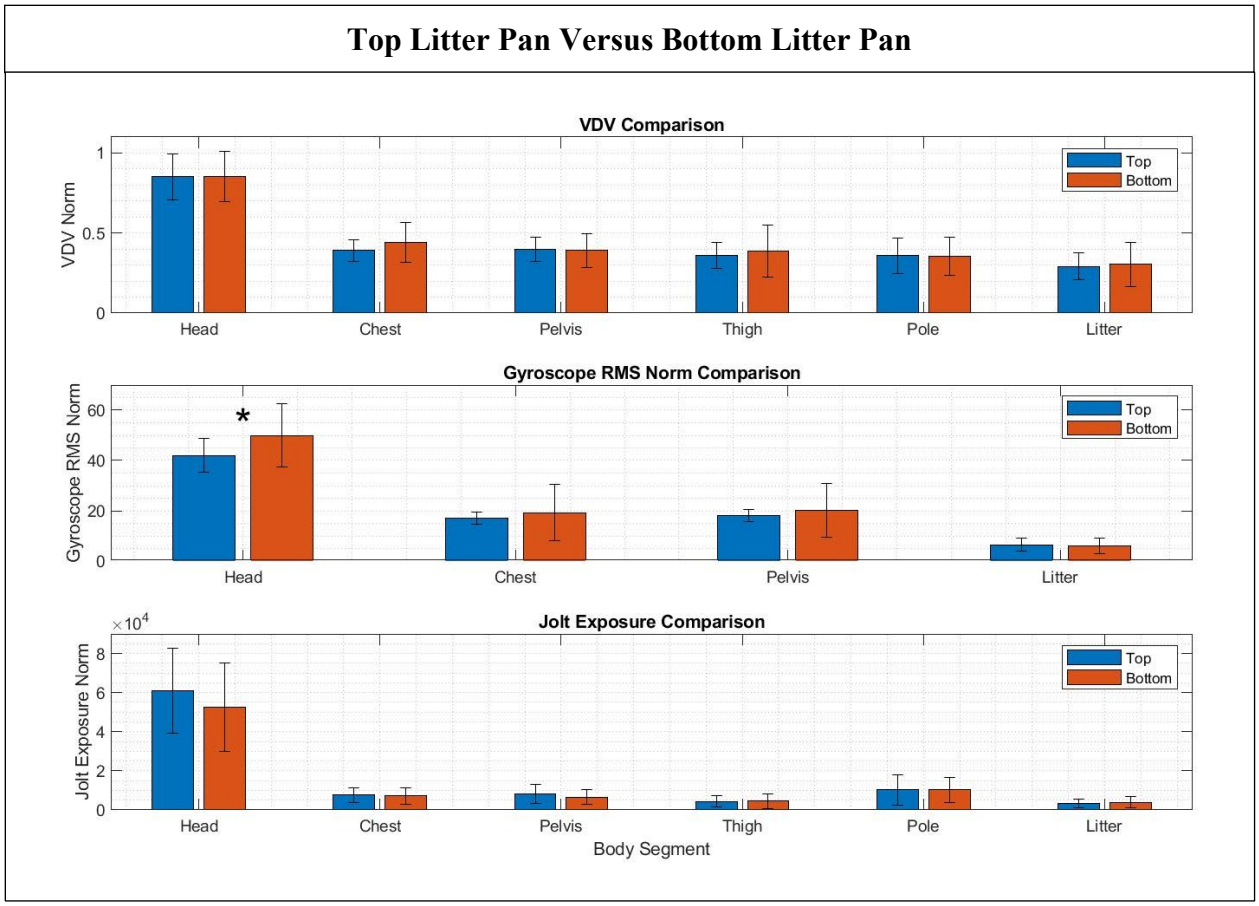

Figure 15. Comparison between top and bottom litter pans.

The gyroscopic RMS values were statically significant at the head, where the bottom position value is 1.19 times that of the top. At the head, the JE metric was 1.17 times greater for the top height but was not statically significant.

This space is intentionally blank.

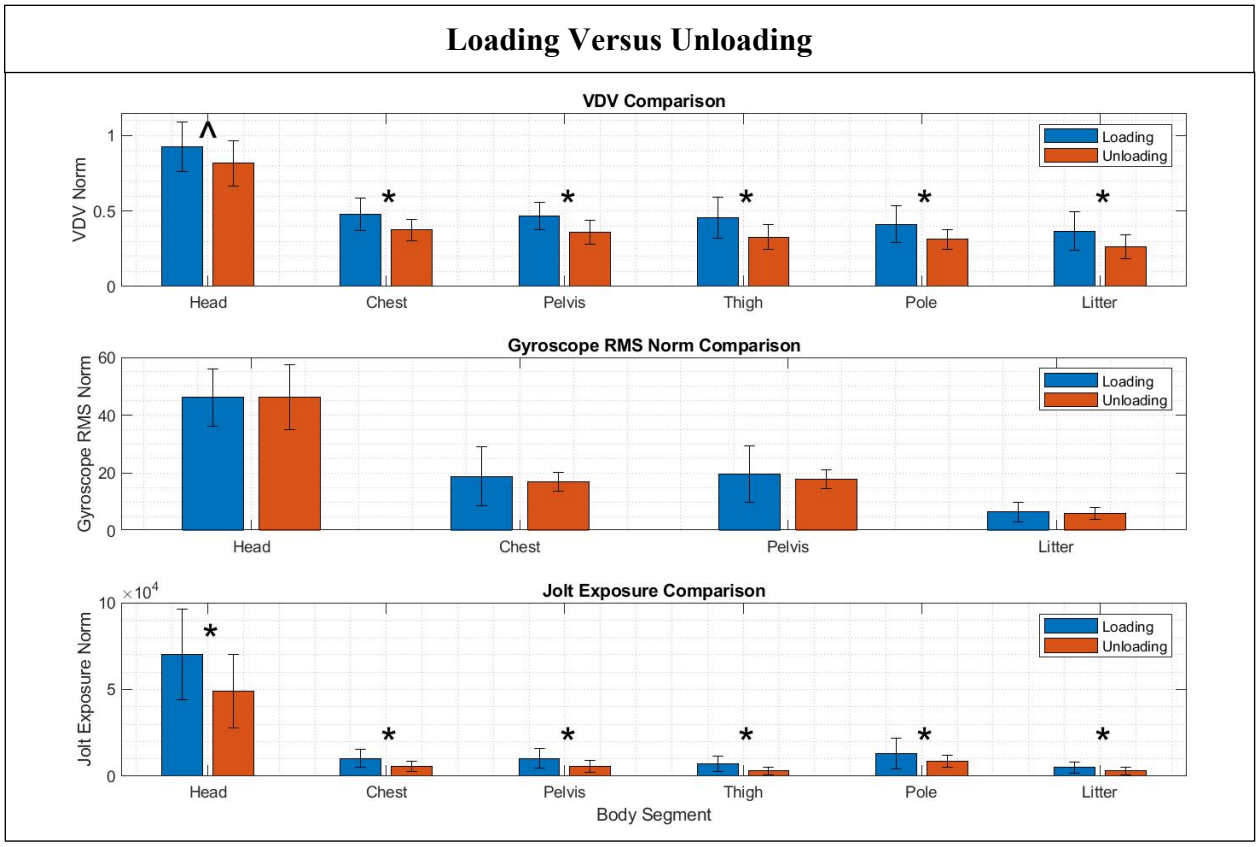

Figure 16. Comparison between loading and unloading motion segments.

All acceleration metrics showed significant differences, 11 showing statistically significant and one showing marginal statistical significance. In all 12 cases, the loading motion segment metrics were greater than the unloading motion segment metrics. In terms of JE, the loading metrics were between 1.4 and 2.4 times greater for the loading data.

The complete analysis and description of the results can be found in ABM's report titled *Analysis of En Route Care in Confined Spaces: Loading and Unloading Effect on Patients*. (Appendix B).

Discussion

Based on the calculated values for frequency-weighted VDV, unweighted VDV, and gyroscope RMS norms, the head received the most vibration excitation and mechanical shocks during loading and unloading procedures. Due the design of the manikin, and a lack of neck muscles to create head stability, it is not surprising to see values that were approximately two times greater than in the other body segments. While the manikin may represent an unconscious or human dosed with a paralytic medication, vibration responses may differ in conscious patients.

The biodynamic results can be differentiated by three characteristics, mechanical shock, rotation, and max acceleration. Shock was significantly present in the loading and unloading motion segments. Rotation was most present during the lifting segment, particularly at the

location of the head. Maximum acceleration occurred in the lifting and walking motion segments, mainly at the head. The standard deviations of these values were large, suggesting that the litter team may be capable of decreasing the exposure to vibrations and shocks through careful handling techniques. Experience, training, and anthropometry of the litter bearers could be included as factors in future studies.

The loading segments exhibited VDV norms values to be at least 1.5 times more than the walking segments. Likewise, the JE values revealed the head to be exposed 3.6 times more during loading than walking. The largest JE ratio was calculated at the litter where the loading JE was 10.7 times walking JE. Looking at the inboard and outboard sides of the aircraft, the VDV metric had a mean outboard pole value 1.146 times that of the inboard, with an associated P-value of 0.0284. Comparatively, the JE metric had a mean outboard pole value 1.748 times that of the inboard with an associated P-value of 0.0129. This suggest much of the vibration and shock may come from an aircraft artifact on the side of the aircraft.

There was little evidence to draw significant comparisons between the aircraft platforms (BMI versus IMMSS), the loading direction (head first versus feet first), and the litter pan heights (top versus bottom). Finally, the comparison results displayed that the loading segments impart significantly greater vibrations and shocks than the unloading segment. JE values were 1.44 times greater for the loading segment at the head, which was the least difference of all segments. Overall, the loading motion segment generates the most vibration and shock to the body with the unloading segment a close second. Comparing the parameters for statistical significance motivates the need for more in-depth research on loading and unloading procedures and MEDEVAC designs.

Conclusion

This study reveals the effects of patient loading and unloading onto an aircraft during MEDEVAC operations. The loading and unloading procedures caused statistically significant exposure to vibration and mechanical shock when compared to walking the litter to and from the platform. The standard deviations in all metrics suggest that the loading process or actions of litter bearing have the ability to mitigate or exacerbate the excitations experienced by the patient. Studies involving more control over the litter bearers such as training, ability, and anthropometry could help researchers to determine ways to mitigate these vibrations. Improved training procedures across all personnel who may be expected to carry and load litters could allow for significant reductions of potentially injurious inputs to litter patients. Other studies looking at aircraft design, specifically obstructions on the outboard side of the aircraft such as the litter pan belts, should be considered. Patient handling system designs that eliminate protruding structures and attachment points will reduce some of the mechanical shocks that may be present during loading and unloading.

References

Conti, S., Kroening, L., Kinsler, R., Lloyd, A., & Molles, J. (2019). *Optimal physical space for en route care: Medic posture and injury survey results* [Report No. 2019-18]. U.S. Army Aeromedical Research Laboratory.

Department of Defense. (2012). *Design criteria standards: Human engineering.* MIL-STD-1472G.

DeShaw, J., & Rahmatalla, S. (2012). Comprehensive measurement in whole-body vibration. *Journal of Low Frequency Noise, Vibration and Active Control, 31*(2), 63–74.

DeShaw, J., & Rahmatalla, S. (2016). Predictive discomfort of supine humans in whole-body vibration and shock environments. *Ergonomics, 59*(4), 568–581.

Deshaw, J, Frick, E., Rahmatalla, S., Kinsler, R., & Barazanji, K. (2019). *Biodynamically validated instrumented supine manikin for evaluation of patient systems* [Abstract]. Military Health System Research Symposium.

International Organization for Standardization. (2020). *Earth-moving machinery – Laboratory evaluation of operator seat vibration*. ISO 7096:2020.

International Organization for Standardization. (1997). *Mechanical vibration and shock – Evaluation of human exposure to whole-body vibration*. ISO 2631-1: 1997.

International Organization for Standardization. (1997). *Mechanical vibration and shock – Evaluation of human exposure to whole-body vibration – Part 5: Method for evaluation of vibration containing multiple shocks*. ISO 2631-5: 1997

Kinsler, R., & Barazanji, K. (2011). *Assessment of fixed position litter loading in the HH-60M MEDEVAC helicopter* [USAARL Technical Memorandum 2011-19]. U.S. Army Aeromedical Research Laboratory.

Kinsler, R., Barazanji, K., Lee, J., Fulton, L., & Hatzfeld, J. (2015). *Analysis of two surveys examining enroute care technologies, platforms, and space requirements [*Poster presentation]. Military Health System Research Symposium.

Kinsler, R., Khouri, R., Squire, C., Conti, S., & Wurzbach, J. (2018). *Immobilization and vibration mitigation systems: Test and evaluation of current and developmental products* [Unpublished report]. U.S. Army Aeromedical Research Laboratory.

Meusch, J., & Rahmatalla, S. (2014a). 3D transmissibility and relative transmissibility of immobilized supine humans during transportation. *Journal of Low Frequency Noise, Vibration and Active Control, 33*(2), 125–138.

Meusch, J., & Rahmatalla, S. (2014b). Whole-body vibration transmissibility in supine humans: effects of board litter and neck collar. *Applied Ergonomics, 45*(3), 677–685.

Ratanalert, S., Phuenpathom, N., Saeheng, S., Oearsakul, T., Sripairojkul, B., & Hirunpat, S. (2004). ICP threshold in CPP management of severe head injury patients. *Surgical Neurology International, 61*(5), 429–434.

Reno, J. (2010). Military aeromedical evacuation, with special emphasis on craniospinal trauma. *Neurosurgical Focus, 28*(5), E12.

Appendix A. Acronyms and Abbreviations.

6DOF	Six degree-of-freedom
ABM	ActiBioMotion
BMI	Basic medical interior
CCFP	Critical care flight paramedic
DTIC	Defense Technical Information Center
IMMSS	Interim MEDEVAC mission support system
ISM	Instrumented supine manikin
ISO	International Organization for Standardization
JE	Jolt exposure
MEDEVAC	Medical evacuation
PPG	Personal protective gear
RMS	Root mean square
VDV	Vibration dose value
USAARL	U.S. Army Aeromedical Research Laboratory

Appendix B. Report by ActiBioMotion

Analysis of En Route Care in Confined Spaces: Loading and Unloading Effect on Patients

By ActiBioMotion LLC

3 September 2021

Table of Contents

This page is intentionally blank

Abstract

The purpose of this study was to characterize the biodynamic response of a supine human during the loading and unloading procedure into a medical evacuation (MEDEVAC) aircraft. The human was represented by an instrumented supine manikin designed to replicate the human response to vibration and mechanical shock. Vibration measurements were taken at six different locations: four inside the manikin, one on the litter pole, and one on the litter mesh. Video data was collected for all trials. Several parameters were varied during loading, including MEDEVAC platform, loading orientation, loading height, and litter pole sensor location.

For analysis, each trial was subdivided into multiple independent, non-overlapping motion segments: Litter Lifting, Walking to Platform, Loading Litter, Unloading Litter, Walking from Platform, and Litter Dropping. The metrics used for data analysis included metrics based on ISO 2631-1 (e.g. VDV and RMS), max acceleration, and Jolt Exposure (JE). The latter is an acceleration-based metric developed for this study to better characterize the unique motions recorded. The video data was also synced with the inertial data to link the measurements with the actions of the litter bearers, litter, and manikin. Analysis was conducted in a manner allowing for both biodynamic characterization and statistical analysis (via t-test) of the varied parameters.

The results of the biodynamic results can be differentiated into three categories: shock, rotation, and max acceleration. Shock is impacted most during the loading and unloading motion segments. Rotation is impacted most during the lifting motion segment, particularly at the location of the head. Max acceleration is impacted most in the lifting and walking to motion segments, also particularly at the head. The investigation also included analyzing synced inertial data with the video data. This analysis showed actions including partially dropping the litter, hitting the litter pole on the aircraft, and catching the litter on the litter pan. These actions were observed multiple times and as a result, the JE metric was valuable in isolating the effects of these actions on the manikin motion.

Loading the litter imparted significantly more vibrational exposure to the manikin than walking the litter – between three and eleven times as much according to JE. Two MEDEVAC platforms, the HH-60 with the BMI and the UH-60 with the IMMSS, were compared and revealed no significant difference in vibratory exposure. No significant difference was also observed when comparing loading the manikin head first versus feet first, or when comparing loading at the top height vs the bottom height within the platforms. The location of the litter pole sensor was varied between the inboard and outboard side, and the outboard side showed a higher JE by a factor of 1.75. Finally, JE for loading was significantly higher than that for unloading by as much as a factor of 2.4.

In summary, the litter loading process caused statistically significant exposure to vibratory motion (when compared to the process of litter walking). Results indicate that this exposure is inherent to the loading process but is exacerbated by litter-bearer actions. The standard deviations in all metrics were large – in the most extreme cases one standard deviation could be as large as the value of the metric. This suggests that other factors such as training, experience and anthropometry of litter-bearers may be the cause for the large standard deviations, and therefore should be considered in future studies. From a hardware viewpoint, the outboard litter side was a larger source of exposure than the inboard. Adding a shock absorbing material, such as rubber, on either the litter's outboard pole or the outboard side of the MEDEVAC platform may reduce exposure.

1 Introduction

Recent surveys on health care providers in the field have reported severe discomfort and pain experienced by casualties during military ground and air transport and attributed the pain to vibration and repeated shock associated with the transport (Kinsler, Barazanji, Lee, Fulton, and Hatzfeld, 2015). The forces and vibrations transmitted to the patient's body through the transport system could have severe consequences, especially for neurotrauma patients sensitive to increased intracranial pressure (ICP) (Ratanalert et al., 2004; Reno, 2010). Litters, transport systems and immobilization systems have been studied to determine if they exacerbate or mitigate the vibration and motion stresses during rotary-wing medical evacuation (MEDEVAC) (Kinsler et al., 2015 and 2018). However, these factors are largely studied during the transport ride profiles with little evidence describing the impact of these systems during the loading and unloading phase of MEDEVAC. Subjective observations during field evacuations have revealed cases of patients experiencing unexpected mechanical shocks and motions during loading and unloading, such as their litter being dropped. These transmitted forces and motions can have dramatic consequences on patient health outcome and well-being.

MEDEVAC platforms and en route care operations are continuously evaluated to optimize patient care and provider capabilities. The confined space of common MEDEVAC platforms presents the difficult task of loading and unloading patients onto these transport systems. Critical Care Flight Paramedic (CCFP) are subjected to heavy lifting, continuous or prolonged gripping and repetitive motions that increase the chances of mishaps during patient loading and unloading. USAARL conducted a study to assess fixed position litter loading on a MEDEVAC helicopter and a common observation was the tendency of the litter to become caught on the litter pan belts and interfere with other protruding structures (Kinsler and Barazanji, 2011). This environment does not allow for easy, smooth loading and may result in unexpected shock or motion to the patient. Different MEDEVAC configurations possess different features that may influence patient loading and unloading. Therefore, this study investigated loading and unloading on two common platforms, the HH-60 with the BMI and the UH-60 with the IMMSS.

While motion transmitted to the human body is the main focus in most transmitted-vibration analysis studies (Meusch and Rahmatalla, 2014a, 2014b; DeShaw and Rahmatalla, 2016), the measurement of the forces transmitted to the different body segments of the supine patient during transport is limited in the literature. The complexity of the biodynamic response of different body segments presents a challenging task for analysis. Unexpected large body motion can dramatically change the directions of the sensors attached on the body and the transport system, which can generate significant assessment and conclusion errors. However, with the current advances in new motion measurement technologies, recent publications have outlined effective methodologies to deal with such complicated environments (DeShaw and Rahmatalla, 2012). A simulated patient manikin, the Instrumented Supine Manikin (ISMv1.2), was used for this study (Barazanji et al., 2019). The ISMv1.2 was created to replicate human biodynamic response to vibration. The ISMv1.2 has several 6DOF sensors (combined accelerometers and gyroscopes), which all connect to a built-in data acquisition system located inside the chest. The findings of this study will provide critical information for developing safer litter systems, handling equipment and procedures.

The primary objective of this report is to analyze the collected inertial and video data to (1) biodynamically characterize the motion encountered during the litter loading process, and (2) identify the parameters that impact the vibration exposure in terms of statistical significance and magnitude of effect. To the best of the authors' knowledge, no studies of this kind have been previously conducted. Therefore, an imperative part of the data analysis process is to consider a wide variety of calculations and metrics to identify which are effective

in this characterization. Once identified, these effective metrics must be presented such that the two aforementioned objectives can be achieved and their results succinctly and clearly communicated.

2 Methodology

2.1 Measurement Setup

A human surrogate, the ISMv1.2 (Instrumented Supine Manikin for Vibration version 1.2), was used in all testing, where the ISMv1.2 was strapped to a U.S. Army Decontaminable litter and subjected to patient loading and unloading on different MEDEVAC platforms. Henceforth, the ISMv1.2 will be referred to as the "manikin". The manikin is designed to replicate the human biodynamic response to vibration (DeShaw, Frick, Rahmatalla, Kinsler and Barazanji, 2019). The manikin is internally instrumented, and was setup such that six degree-of-freedom (6DoF) inertial sensors (triaxial accelerometer and triaxial gyroscope) were placed at the following locations: manikin head (internal), manikin chest (internal), manikin pelvis (internal), manikin thigh (internal), litter pole (external), and the litter mesh (external). The thigh and pole sensors did not record gyroscope measurements due to the limited number of channels of the manikin's internal data acquisition system. Video data was also captured by six time-synced cameras.

The locations of the inertial sensors can be seen in the three images comprising Figure 1. In the top image, the red squares signify the location of an inertial sensor; The sensors located at the head, chest and pelvis areas have all six channels connected, whereas the thigh sensor has only the three accelerometer channels connected. The litter mesh sensor has all six channels connected, and the pole sensor has only the three acceleration channels connected.

The top image of Figure 1 displays two sets of Coordinate Systems (CS), one labeled local (blue) and one labeled global (red). The local CS follows ISO 2631-1, meaning it is fixed to the location of the input, and is used for the ISO-based calculations. This is primarily relevant for the correct application of frequency weighting; the ISO metric VDV, as well as the gyroscope metrics, are presented in terms of the CS-invariant norm. The global CS is not fixed to the litter, and thus remains constant throughout each trial. This global CS is introduced to make interpretation of certain results (Jolt Exposure and axial acceleration over an entire trial) more intuitive, as the results do not need to be interpreted in terms of a continually changing CS).

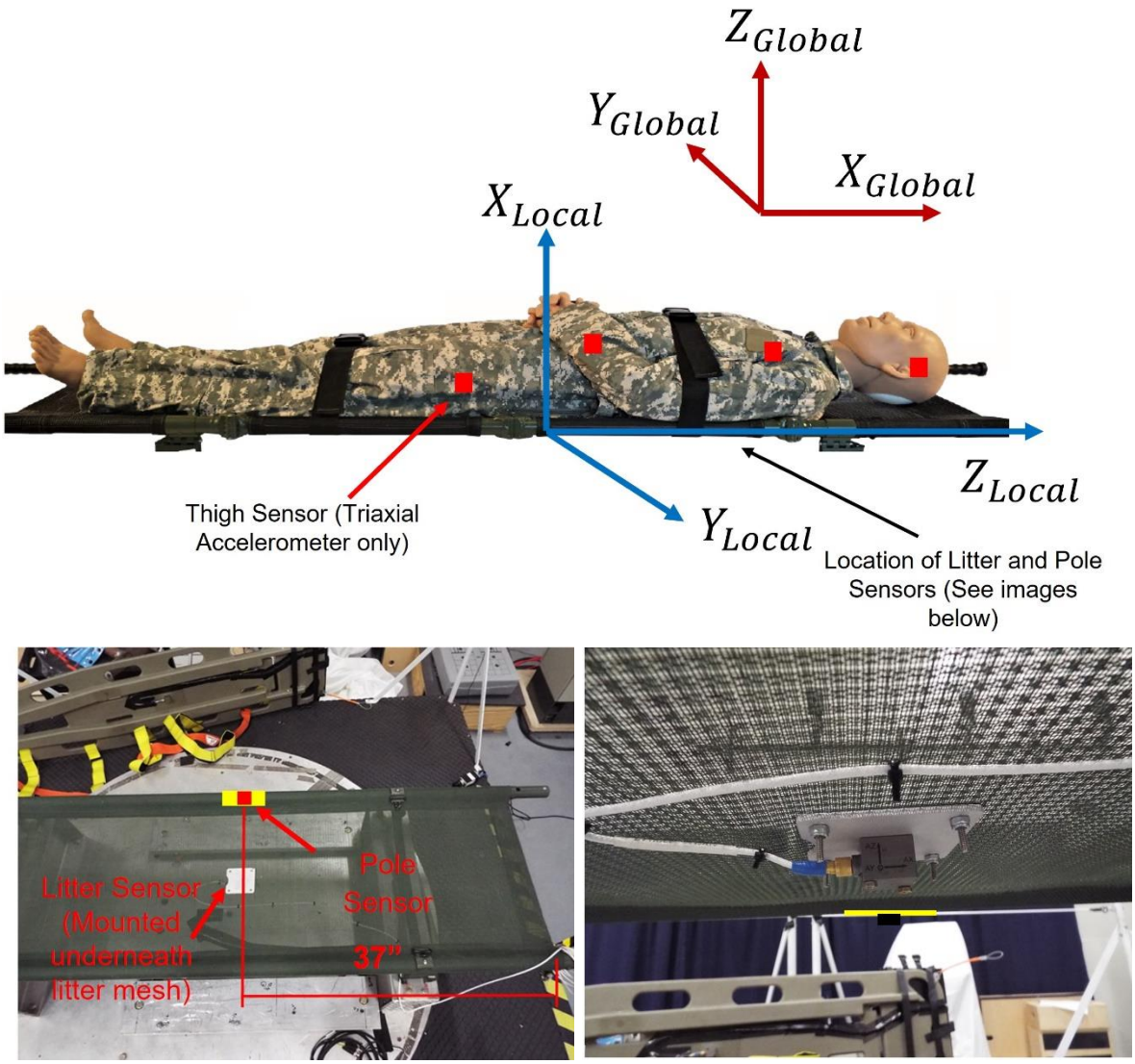

Figure 1: Locations of the six sensors connected to the manikin. The top picture depicts the locations of the four internal sensors (red squares), as well as the relevant coordinate systems. The bottom left picture depicts the location of the litter pole sensor (red square) and litter sensor (annotated gray square), and the bottom right picture depicts the location and mounting method of the litter mesh sensor.

2.2 Loading/Unloading Process Description

In this study, the process of loading and unloading the manikin is defined as follows: Before starting, the litter was placed on the ground at least ten feet away from the platform (aircraft analogue). The process began when four litter bearers lifted the litter off the ground, carried it to the platform, and passed it to a volunteer acting as the receiving Medic on the inside of the platform. Together, the team loaded the manikin onto the MEDEVAC platform. The placement/orientation of the manikin within the platform varied by trial but concluded when the litter was securely settled inside the litter pan. These steps were then reversed to unload the manikin. The manikin was lifted from the litter pan and passed off to the four litter bearers. The litter was then carried back to the starting location and lowered to complete the process. An example of a loaded manikin can be seen in Figure 2.

Figure 2: Example of a manikin loaded in the top litter position in the BMI phase.

This complete loading and unloading process (starting with the lifting of the manikin and ending with the dropping of the manikin) was performed 20 times (for a total of 20 trials). The JERCA 4 protocol lists a total of 40 trials, as the loading and unloading portions were considered separate. For the purposes of this report, those two portions are combined into a single trial. Four parameters were varied throughout the trials:

1. Two platforms: HH-60M with BMI and UH-60A/L with IMMSS
2. Three Litter Positions: Top, Middle, Bottom
3. Loading Direction: Head First or Feet First
4. Litter Pole Sensor Placement: Inboard or Outboard

A complete description of the process used to load/unload the manikin from the aircraft analogue, as well as the parameters that were varied and specifications followed, can be found in the USAARL JERCA 4 Protocol document.

2.3 Data Processing

The steps taken in processing and converting the raw inertial data into relevant metrics and results are enumerated below:

1. The raw data were lowpass filtered and inspected, yielding usable data in the local CS (Figure 1 - top image). To realize the global CS in the same image, a sensor fusion algorithm was applied.
2. The data was broken into 13 different motion segments, six of which contained relevant information. The seven segments deemed to not contain relevant information included motions such as pauses between the litter loading and unloading steps and the two sets of triple taps used for syncing the video and inertial data. A more complete description of the segmentation can be found in the Appendix (Section 6.1). The six relevant segments are as follows:
    1. Lifting the litter
    2. Walking the litter to the aircraft
    3. Loading the litter into the aircraft
    4. Unloading the litter from the aircraft
    5. Walking the litter from the aircraft back to the location it was originally lifted from
    6. Lowering the litter.

The time stamps necessary to achieve said segmentation were obtained from the video data that was collect concurrently with the ISMv1.2 data. During this analysis of the video data, notes were made as to when unexpected events occurred (such as dropping the litter or hitting it on the cab) for several trials.

3. For each trial, relevant metrics (including root mean square (RMS) acceleration and VDV) were calculated for each of the six motion segments enumerated in the previous step. For each of these six motion segments, sensors measurements existed at six locations (referred to as body segments) – Head, Chest, Pelvis, Thigh, Pole, Litter. Calculating metrics for each of the six body segments for each of the six motion segments yielded a total of $6 \times 6 = 36$ values per metric per trial.
4. To succinctly and clearly show the distribution of the values generated in the previous step over all the trials, the results were organized via boxplots. Other graphics were also added as needed, including a plot of the acceleration of a single trial with demarcations at the times potentially hazardous events were identified by video analysis.

2.3.1 Step 1 – Conversion to the Global Coordinate System

The process of converting the ISMv1.2's data (collected in the multiple local sensor frames) to a single, shared global frame was accomplished by a process called sensor fusion. Said global frame is defined by a vertical Z axis parallel to that of gravity, and X and Y axes placed in the horizontal place (see top image of Figure 1). Sensor fusion is the process of combining the measurements of two or more sensors with a model to compensate for each sensor type's weakness. Here, the accelerometer can be used to identify the vertical gravity vector, but only if there is little free acceleration (free acceleration is acceleration other that caused by gravity). Conversely, the gyroscope data can be integrated to obtain very accurate orientation data over short time periods, but the accuracy degrades over time. Succinctly, by applying sensor fusion, the orientation estimates of the accelerometer and gyroscope can be combined such that the gyroscope stabilizes the estimates of the accelerometer during periods of free acceleration, and the accelerometer estimates stabilize the gyroscope's drift over time (Madgwick et al., 2011). The end result is a robust estimation of sensor orientation over time.

Two issues of import are horizontal orientation drift, and the orientation estimates of the locations that only have accelerometric measurements. Horizontal orientation drift occurs because the accelerometer cannot provide a stabilizing measurement of a horizontal vector, subjecting the yaw measurement to a time-based drift. This is mitigated through a series of techniques designed to reduce integration drift by minimizing gyroscope bias (the cause of the drift). As for the location where only accelerometric data is available (i.e. the litter pole and thigh), frequency filtering is used to remove free acceleration and an optimization protocol (gradient descent) is implemented to maximize the accuracy of the orientation estimates.

2.3.2 Step 2 – Breaking Trials into Motion Segments

It was determined that each trial contain six motion segments of import: Lifting the litter, Walking to the aircraft, Loading the manikin to the aircraft, Unloading the manikin from the aircraft, Walking from the aircraft, and Lowering the litter. The time stamps of these individual motion segments were determined through careful scrutiny of the video data (Further explanation and definition of these segments can be found in the Appendix section). The inertial and video data were then synced by utilizing the chest taps performed in each trial. The chest taps have a very distinct inertial signature, which could then be matched with the segmentation data. This resulted in an inertial data set for each of the six motion segments.

2.3.3 Step 3 – Metric Calculation

The calculated metrics were based on un-weighted measured acceleration and weighted acceleration data as specified by ISO 2631-1:1997 guidelines (ISO 2631-1). For the weighted acceleration, the first step in the ISO analyses was to apply the defined frequency weighting function, which heavily attenuates frequencies below 4 Hz and above 8 Hz but leaves the 4-8 Hz band essentially untouched. While it is understood that the ISO specifications deal with sensors mounted directly on the input at the interface between the body and litter, we opted to apply them to our segment data, even though our segment data is part of the output. After applying the weighting filter, the Crest Factor was calculated with transient vibration and mechanical shocks. Subsequently, the weighted RMS, running RMS, Maximum Transient Vibration Value (MTVV) and the weighted and unweighted Vibration Dose Values (VDV), were calculated. As we were interested in the VDV of both the frequency-weighted and unweighted acceleration, both were calculated. Based on the results, it was determined that the VDV was the most effective method of quantifying the acceleration. This determination was based on the high Crest Factor values (though rarely exceeding the value of nine), as well as a qualitative analysis of the inertial data. The formulae defining these metrics can be found below, and in ISO 2631-1.

The formula for the weighted RMS is as follows:

$$a_w = \left[\frac{1}{T}\int_0^T a_w^2(t)\,dt\right]^{\frac{1}{2}} \qquad \text{Equation 1}$$

Here $a_w(t)$ is the frequency-weighted translational acceleration as a function of time in units of meters per second squared, and T is the duration of the measurement in seconds.

The formula for the running RMS is as follow:

$$a_w(t_0) = \left\{\frac{1}{\tau}\int_{t_0-\tau}^{t_0}\left[a_w(t)\right]^2\,dt\right\}^{\frac{1}{2}} \qquad \text{Equation 2}$$

Here $a_w(t)$ is instantaneous frequency-weighted translational acceleration, τ is the integration time for running average, t is the time (integration variable), and t_0 is the time of observation (instantaneous time).

The formula for the Maximum Transient Vibration Value (MTVV) is as follows:

$$MTVV = \max[a_w(t_0)] \qquad \text{Equation 3}$$

That, is the MTVV is the highest magnitude of $a_w(t_0)$ read during the measurement period T ($a_w = \left[\frac{1}{T}\int_0^T a_w^2(t)\,dt\right]^{\frac{1}{2}}$ Equation 1).

The formula for the fourth power vibration dose value (VDV) is as follows:

$$VDV = \left\{\int_0^T [a_w(t)]^4\,dt\right\}^{\frac{1}{4}} \qquad \text{Equation 4}$$

Here $a_w(t)$ is instantaneous frequency-weighted translational acceleration, and T is the duration of the measurement.

The loading process contained both transient vibration and shocks, but also exhibited motion that did could not be fully described as a combination of transient vibration and shock. An example of such motion would be dropping the litter on one side but catching it before contact with the ground. Therefore, additional metrics

were calculated to supplement those stated above. These included the unweighted version of the RMS and VDV, as well as the weighted and unweighted values of the gyroscope data RMS. A metric roughly approximating transmissibility was also calculated by dividing the VDV of each segment (the outputs) by the VDV of the litter (input). Transmissibility is essentially a transfer function that describes how vibrational energy propagates through the body as a function of the input vibration. The above metrics (specifically VDV and Gyroscope RMS) were calculated for each axis (as specified by the ISO), but then combined via calculation of the norm to simplify the comparison process.

The above metrics proved useful in quantifying the inertial data in broad terms, but lacked descriptive power for the transient and irregular jolts that characterized the observed manikin motion. The term "jolt" is used because the type of motion being referenced cannot be characterized solely as vibration or mechanical shock. To quantify this jolt motion, a metric termed "Jolt Exposure" (JE) was developed. JE is calculated by taking the absolute value of a single axis acceleration profile (unweighted) and removing all data points that do not exceed a certain threshold. The threshold chosen in this report was 1.6 m/s2. This value was chosen from Section C.2.3. of ISO 2631-1:1997, as it represents the upper range value of vibratory acceleration considered to be "uncomfortable" for healthy humans. It is assumed that the perception of discomfort would likely be greater in injured humans. The remaining data points are then squared (to assign greater weight to high accelerations) and summed. The equations describing this process is as follows: (if $\|a(n)\| < 1.6\frac{m}{s^2}$, then $a(n) = 0$ Equation 5 and $JE = \sum_{n=1}^{k} a(n)^2$ Equation 6)

$$\text{if } \|a(n)\| < 1.6\frac{m}{s^2}, \text{ then } a(n) = 0 \qquad \text{Equation 5}$$

$$JE = \sum_{n=1}^{k} a(n)^2 \qquad \text{Equation 6}$$

Here JE is Jolt Exposure, a is a single-axis time-varying acceleration profile, n is an inter used to refer to the n'th element of a, and k is the number of data points in a.

The issue that this metric is intended to address the averaging out effect that metrics like VDV are subjected to. For example, in terms of VDV value, an acceleration profile with a large, ephemeral shock followed by a long period of mild vibration can have the same VDV value as an acceleration profile with consistent moderate vibration. In this example, the JE metric would be able to distinguish between these two acceleration profiles, as the mild vibration is excluded from the data set. Finally, note that this metric is not normalized against the number of measurements, as is a metric like VDV. The goal of JE is to quantify a form of "exposure", and by avoiding normalization, tasks that take longer to complete will have a correspondingly higher exposure metric, which is not necessarily the case with normalized metrics.

2.3.4 Step 4 – Analysis and Plot Generation

Between the many trials, body segments, and motion segments, it was determined that the most succinct method of presenting the data as a whole would be via box plots, where the full statistical distribution of the data can be represented by a single graphic. In this manner, concerning a single metric, the results of all 20 trials could be presented in a series of six box plots, one for each motion segment. Three box plots are generated, one showing the VDV metric with weighted acceleration(Figure 3), one showing the VDV metric calculated with unweighted accelerations (Figure 4), and one showing the RMS metric of the gyroscope data (Figure 5). Note that in order to simplify the presentation of the results, the three axes of measurement were combined into a parameter by calculating the norm. Furthermore, when calculating the VDV, the frequency-weighted acceleration was used, but no frequency weighting was applied to the gyroscope data (The frequency content of

the gyroscope was almost exclusively below 4 Hz, therefore applying frequency weighting resulted in vectors of essentially all zeros). Next, the results of the JE metric are presented for the head, chest and pelvis body segments as boxplots (Figure 6, Figure 7, and Figure 8). The rest of the body segments are not included due to irrelevance or lack of variation from the chest plot.

After providing an overall view of the data via the boxplots, it was determined that a metric showing how, for all the trials as a whole, the input (Litter VDV) manifested in the outputs (Body Segment VDVs). This was calculated by dividing the mean of the output values by the mean of the input values, resulting in a rough analogue of transmissibility. Transmissibility is a transfer function that expresses how an input (such as vibration) is mapped to (i.e. does it amplify, mitigate, or leave unchanged) the output(s). This approach was broken out over all five of the output segments for each of the six motion segments (Figure 10). In order to give a sense of the data's variability, standard deviation bars were placed on each bar of the bar graph.

The final graphic displayed in the Results section provides a qualitative and quantitative overview of how actions of the loading crew manifest themselves in the inertial data, ultimately showing the effect of an unintended action (such as dropping the litter) on the manikin. To accomplish this, the acceleration data from a specific trial and body segment (in this case, the Chest in Trial 2 – more such plots can be found in the Appendix), is displayed broken out into the X, Y, and Z axes. In order to differentiate the different motion segments that occurred during the trial, the data from each motion segment is plotted in a different color (the black plot underneath is the complete data set). Finally, actions identified by watching the video corresponding to the trial that were unintended (such as hitting the litter against the wall or partially dropping the litter) are marked with asterisks and corresponding labels.

Trials 4 and 19 were not included in the calculations. Trial 4 appeared to be an outlier, and Trial 19 did not have a complete video recording and could not be properly segmented.

3 Results

The results presented in this report fall into two sections. The first characterizes the overall biodynamic response using quantitative metrics and qualitative analysis. The gathered data is analyzed using multiple methods with the intent of elucidating the type of vibratory motion encountered in the kind of experiment, how standard metrics (such as those in the ISO documentation) describe (or fail to describe) the data, and how utilizing a non-standard metric (Jolt Exposure) offers a potentially more useful analysis method.

The second section is concerned with statistical analysis. Specifically, the effects of the tested parameters (such as MEDEVAC platform, loading height, etc) in terms of statistical significance and magnitude.

3.1 Biodynamic Characterization

The results of this section offer an overall characterization of the recorded motion. With the exception of Figure 11, in which data from a single trial and single body segment are shown, all of the graphs show the distribution of data over the full set of trials (with the exception of Trial 4 (outlier, likely due to sensor error) and 19 (incomplete video data)). Furthermore, Figure 3 to Figure 7 are divided into subplots for each motion segment. In this manner, the distribution of calculated metrics for each trial in terms of each body segment and motion segment can be succinctly reviewed.

In the interest of clarity, the boxplot methodology employed in this report were elucidated. Each box and whiskers element shows the data distribution. The red line in the center of the box plot indicates the median value. The lower and upper lines of the box (closest to the median line) indicate the 25^{th} and 75^{th} percentile of

the data respectively. The lower and upper whiskers indicate the 5th and 95th percentile of the data respectively. Finally, points marked with a red plus symbol are values that were determined to be outliers compared to the rest of the data.

The plots below depicting the results of this study are formatted in a manner the authors thought most effective for communicating information. However, if different formatting is desired, the original MatLab figures used to generate these images can be provided by ABM. Furthermore, the Jolt Exposure metric is displayed in the global CS, as will be explained before the graphs are presented.

Weighted VDV Norm

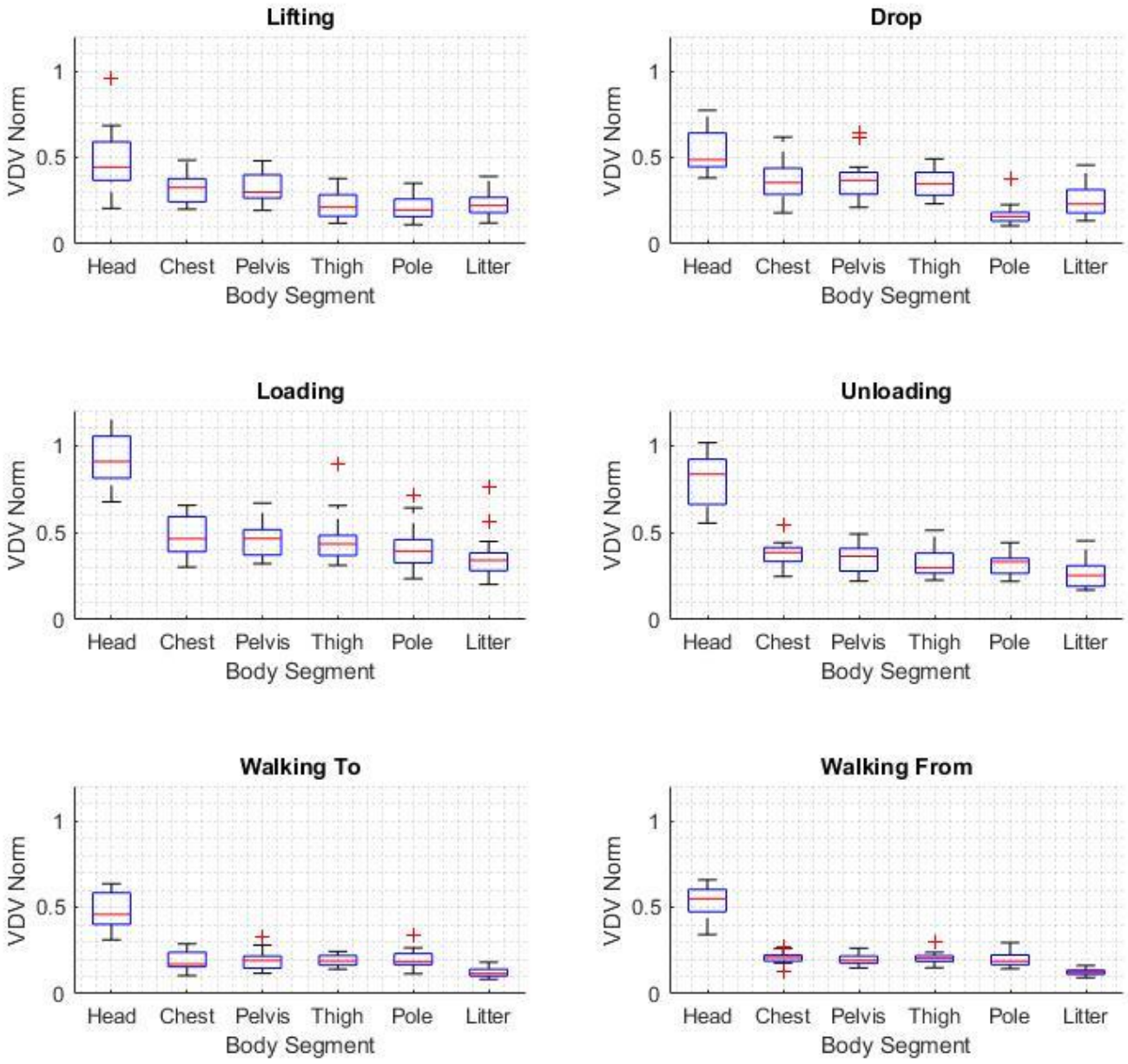

Figure 3: Compilation of box plots showing the statistical distribution of the VDV Norm (weighted) over all the trials. The metric is broken out by both body segment (within each sub-boxplot) as well as motion segment (one motion segment per boxplot).

Unweighted VDV Norm

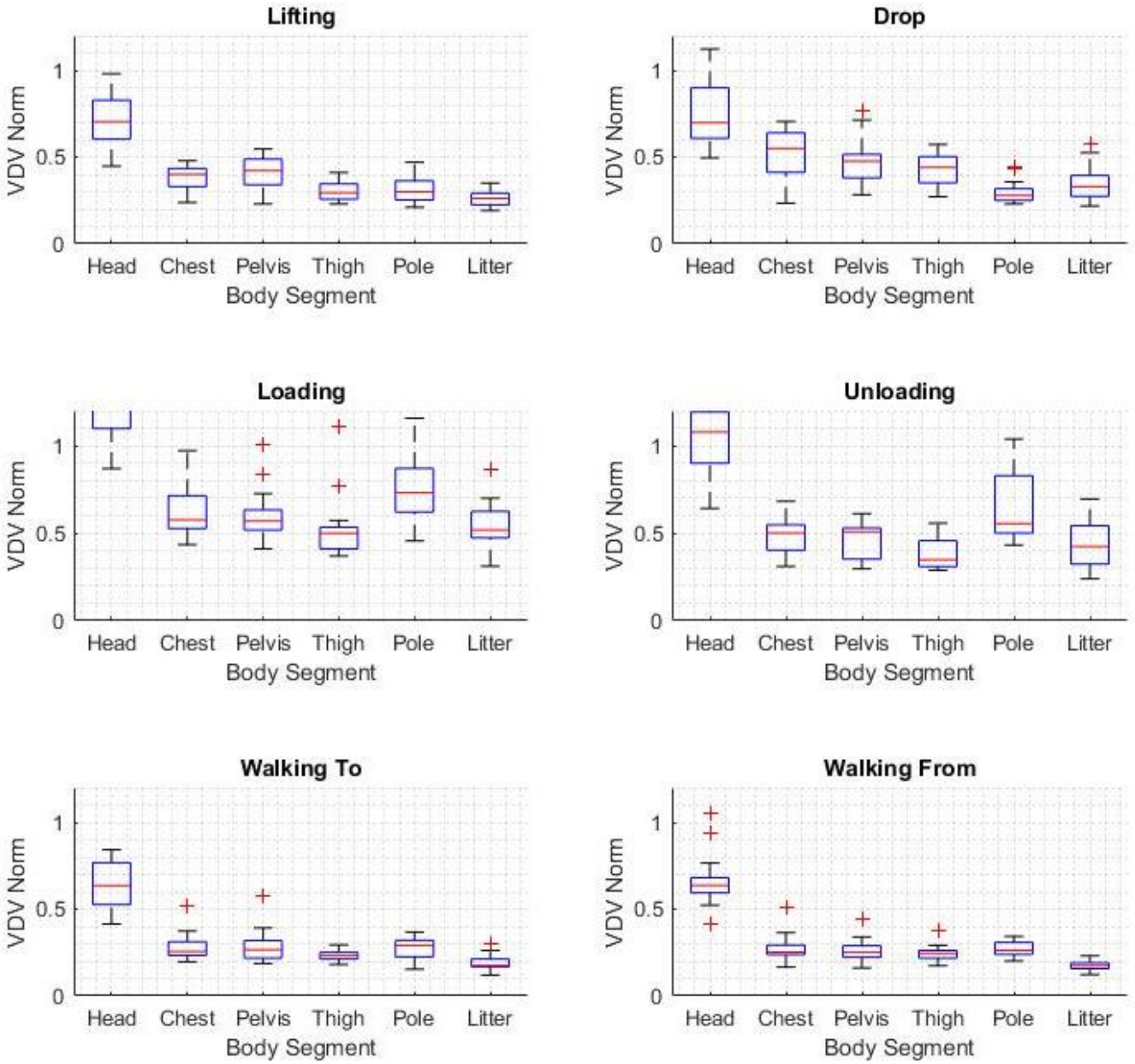

Figure 4: Compilation of box plots showing the statistical distribution of the VDV Norm (unweighted) over all the trials. The metric is broken out by both body segment (within each sub-boxplot) as well as motion segment (one motion segment per boxplot).

Unweighted Gyroscope RMS Norm

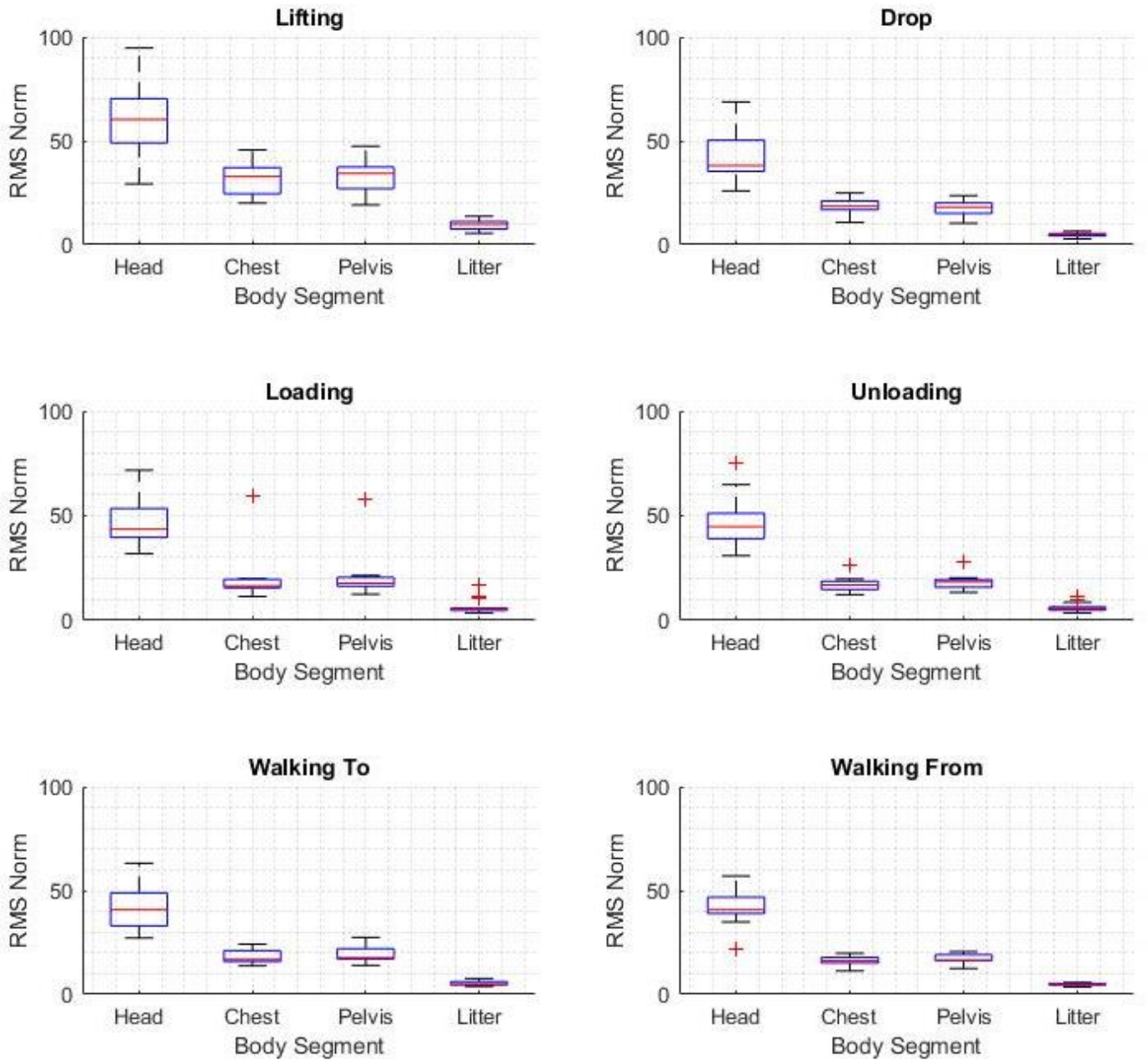

Figure 5: Compilation of box plots showing the statistical distribution of the Gyroscope RMS Norm over all the trials. The metric is broken out by both body segment (within each sub-boxplot) as well as motion segment (one motion segment per boxplot).

The following plots depicting JE exhibit a wide range of Y values. As such, the Y axes for each plot is unique, which must be considered when interpreting the results. Furthermore, the results are presented in a global CS, (as described by the top image of Figure 1). In this CS, the Z axis is always aligned vertically with gravity, the X axis longitudinally traverses the litter, and the Y axis represents lateral motion on/of the litter.

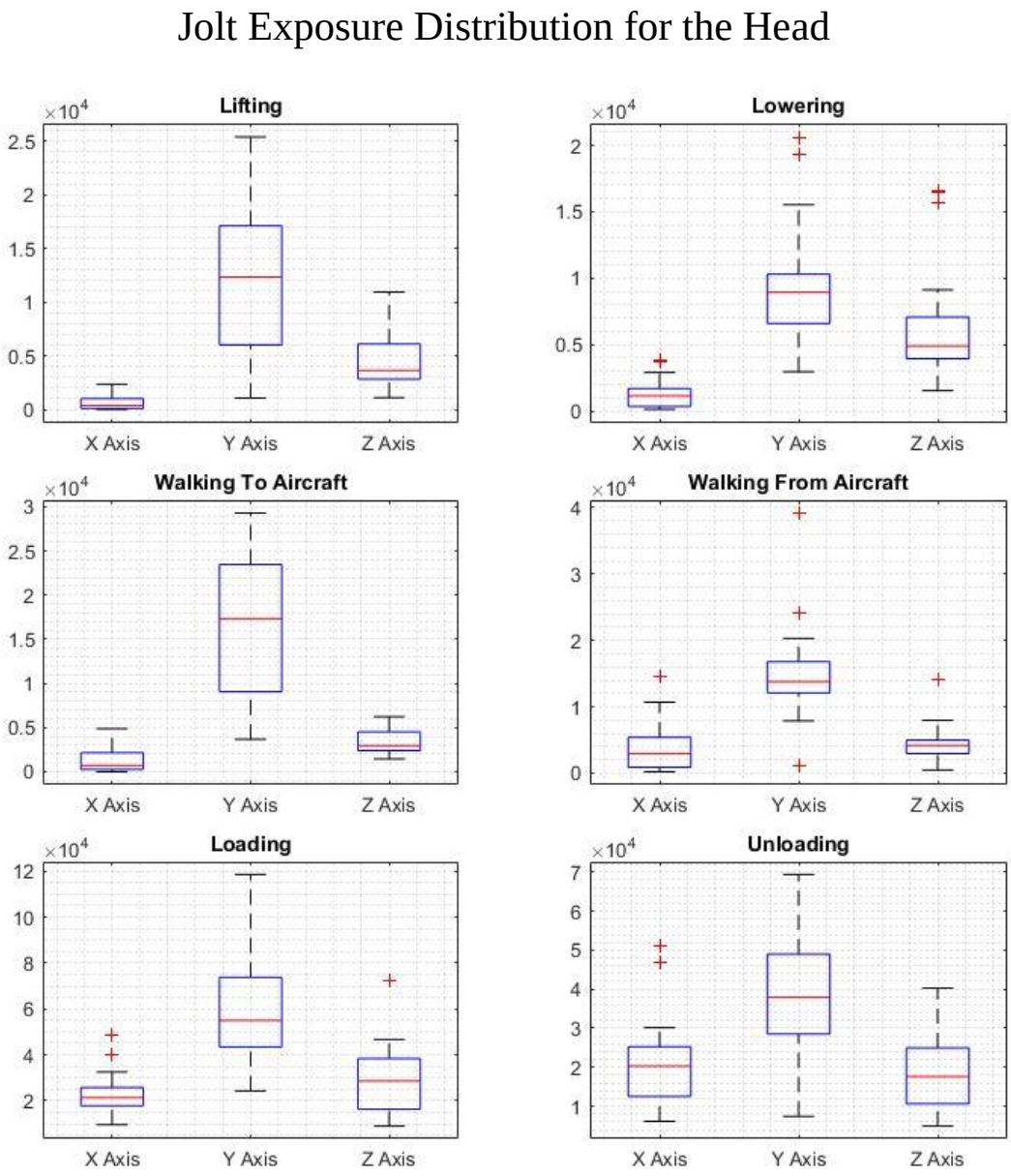

Figure 6: Boxplot showing the distribution of the Jolt Exposure Metric over all trials for each motion segment and the head body segment.

Jolt Exposure Distribution for the Chest

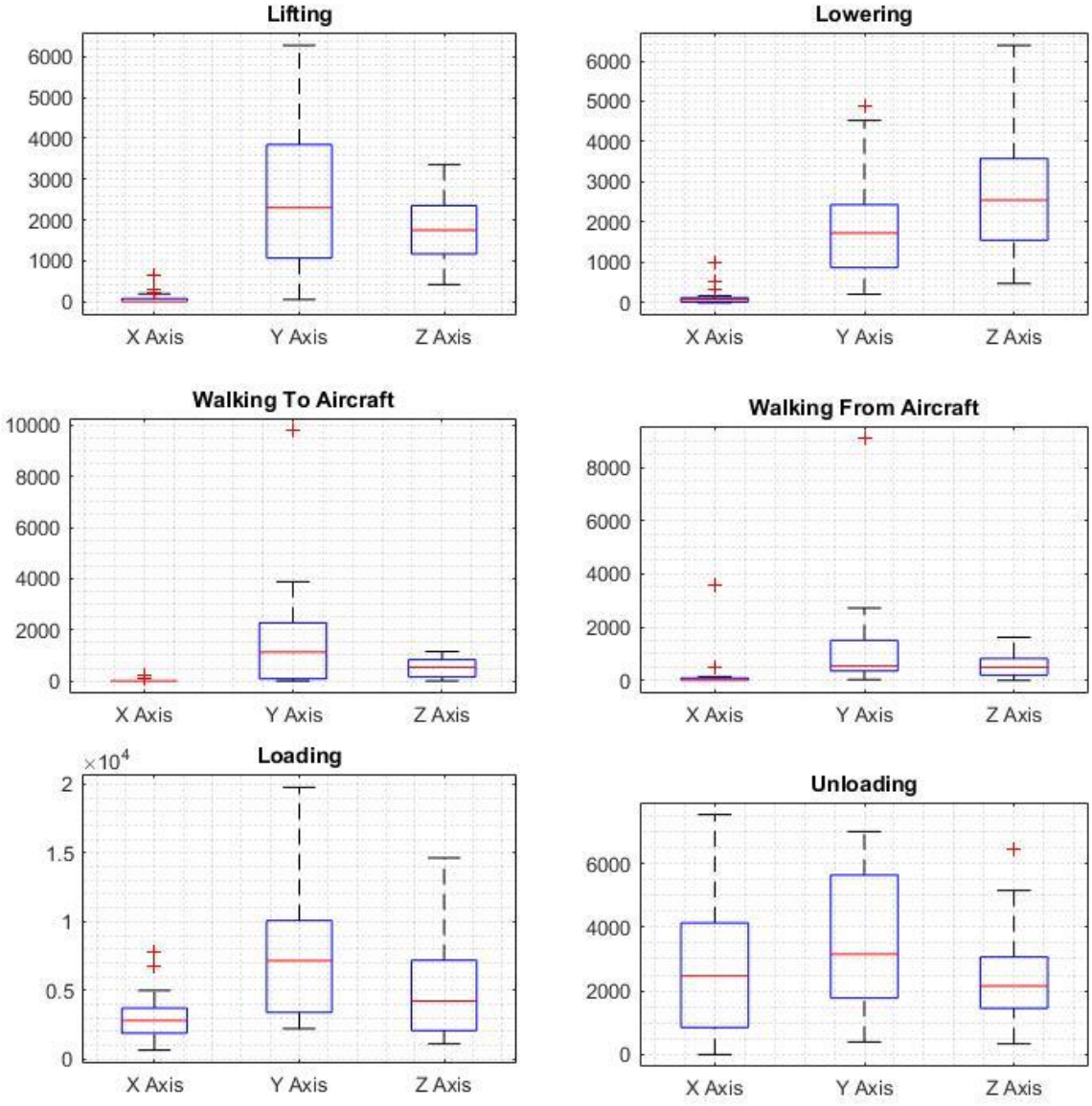

Figure 7: Boxplot showing the distribution of the Jolt Exposure Metric over all trials for each motion segment and the Chest body segment.

Jolt Exposure Distribution for Pelvis

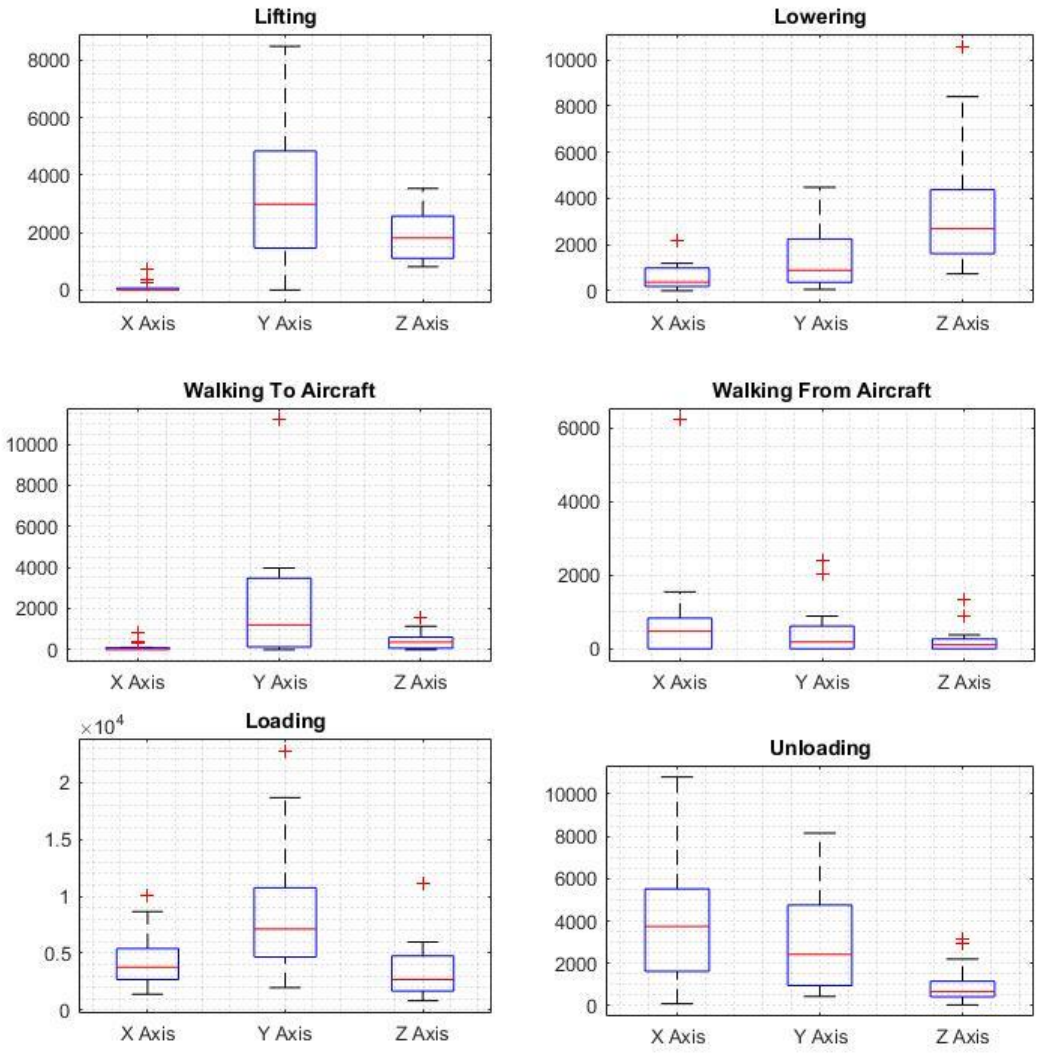

Figure 8: Boxplot showing the distribution of the Jolt Exposure Metric over all trials for each motion segment and the Pelvis body segment.

Figure 9 shows the maximum acceleration values (defined by the norm and in units of g) that were encountered during each segment of each trial. Please note that the color-coding was applied to make table interpretation easier – color has no bearing on the "risk" or "exposure" of a certain value. Color was assigned on a scale from dark green (lowest observed acceleration) to dark red (highest observed acceleration). As mentioned earlier, trials 4 and 19 are not included.

Maximum Acceleration (Norm in gs) of Each Segment for All Trials

Head

	Lifting	Walking To	Loading	Unloading	Wlaking From	Lowering
Trial 1	0.528	0.918	0.364	0.298	0.088	0.850
Trial 2	0.569	1.133	0.593	0.534	0.433	0.697
Trial 3	0.647	0.656	0.646	0.431	0.183	1.107
Trial 4	·	·	·	·	·	·
Trial 5	0.462	0.675	0.391	0.224	0.169	0.593
Trial 6	0.347	0.994	0.342	0.293	0.084	0.898
Trial 7	0.481	1.305	0.640	0.376	0.103	0.707
Trial 8	0.413	0.821	0.213	0.309	0.086	0.763
Trial 9	0.334	0.761	0.741	0.325	0.107	0.760
Trial 10	0.498	1.560	0.342	0.404	0.152	0.664
Trial 11	0.383	0.590	0.508	0.436	0.094	0.880
Trial 12	0.354	0.957	0.508	0.500	0.166	1.654
Trial 13	0.313	1.296	0.755	0.459	0.194	0.611
Trial 14	0.382	1.199	0.335	0.374	0.100	0.937
Trial 15	0.348	1.221	0.401	0.262	0.167	0.958
Trial 16	0.419	1.178	0.347	0.431	0.194	1.058
Trial 17	0.365	1.515	0.457	0.420	0.047	1.240
Trial 18	0.356	1.114	1.114	0.684	0.882	0.822
Trial 19	·	·	·	·	·	·
Trial 20	0.368	1.063	0.376	0.198	0.058	0.768

Chest

	Lifting	Walking To	Loading	Unloading	Wlaking From	Lowering
Trial 1	0.655	0.532	0.364	0.406	0.104	0.342
Trial 2	0.685	0.446	0.282	0.723	0.554	0.259
Trial 3	0.766	0.454	0.376	0.447	0.117	0.317
Trial 4	·	·	·	·	·	·
Trial 5	0.732	0.277	0.310	0.242	0.067	0.233
Trial 6	0.488	0.413	0.169	0.492	0.055	0.312
Trial 7	0.776	0.510	0.274	0.746	0.042	0.414
Trial 8	0.670	0.558	0.175	0.357	0.038	0.294
Trial 9	0.529	0.385	0.308	0.386	0.093	0.391
Trial 10	0.669	0.591	0.315	0.697	0.092	0.364
Trial 11	0.458	0.402	0.402	0.485	0.054	0.263
Trial 12	0.341	0.524	0.531	0.643	0.071	0.606
Trial 13	0.401	0.630	0.293	0.549	0.198	0.335
Trial 14	0.625	0.491	0.159	0.296	0.055	0.267
Trial 15	0.458	0.474	0.435	0.302	0.092	0.412
Trial 16	0.507	0.614	0.287	0.659	0.092	0.351
Trial 17	0.275	0.563	0.380	0.297	0.027	0.613
Trial 18	0.454	0.452	0.430	0.701	0.405	0.332
Trial 19	·	·	·	·	·	·
Trial 20	0.293	0.577	0.296	0.185	0.071	0.290

Pelvis

	Lifting	Walking To	Loading	Unloading	Wlaking From	Lowering
Trial 1	0.550	0.652	0.406	0.266	0.159	0.322
Trial 2	0.479	0.429	0.317	0.223	0.198	0.243
Trial 3	0.725	0.443	0.260	0.207	0.126	0.270
Trial 4	·	·	·	·	·	·
Trial 5	0.539	0.424	0.202	0.516	0.175	0.191
Trial 6	0.492	0.469	0.169	0.219	0.103	0.361
Trial 7	0.475	0.579	0.265	0.550	0.027	0.263
Trial 8	0.394	0.563	0.159	0.266	0.084	0.243
Trial 9	0.504	0.366	0.303	0.201	0.075	0.386
Trial 10	0.556	0.635	0.342	0.262	0.094	0.254
Trial 11	0.400	0.325	0.290	0.181	0.088	0.214
Trial 12	0.307	0.504	0.518	0.227	0.097	0.551
Trial 13	0.352	0.786	0.340	0.370	0.202	0.302
Trial 14	0.493	0.603	0.149	0.162	0.030	0.336
Trial 15	0.433	0.514	0.398	0.249	0.216	0.491
Trial 16	0.409	0.705	0.276	0.175	0.093	0.343
Trial 17	0.367	0.506	0.358	0.257	0.056	0.505
Trial 18	0.398	0.428	0.386	0.274	0.489	0.300
Trial 19	·	·	·	·	·	·
Trial 20	0.412	0.657	0.424	0.276	0.074	0.378

Thigh

	Lifting	Walking To	Loading	Unloading	Wlaking From	Lowering
Trial 1	0.386	0.463	0.463	0.194	0.172	0.388
Trial 2	0.332	0.459	0.193	0.123	0.098	0.254
Trial 3	0.389	0.348	0.195	0.150	0.078	0.279
Trial 4	·	·	·	·	·	·
Trial 5	0.295	0.378	0.219	0.555	0.158	0.197
Trial 6	0.358	0.409	0.165	0.150	0.116	0.345
Trial 7	0.292	0.724	0.142	0.405	0.085	0.316
Trial 8	0.258	0.607	0.082	0.267	0.151	0.367
Trial 9	0.304	0.371	0.275	0.164	0.105	0.270
Trial 10	0.326	0.531	0.151	0.230	0.181	0.237
Trial 11	0.332	0.436	0.264	0.157	0.161	0.245
Trial 12	0.307	0.395	0.277	0.220	0.074	0.484
Trial 13	0.283	0.411	0.147	0.286	0.211	0.329
Trial 14	0.368	0.545	0.118	0.117	0.058	0.376
Trial 15	0.430	0.569	0.327	0.232	0.226	0.706
Trial 16	0.297	0.435	0.178	0.128	0.071	0.284
Trial 17	0.396	0.401	0.285	0.293	0.127	0.357
Trial 18	0.286	0.454	0.126	0.225	0.314	0.319
Trial 19	·	·	·	·	·	·
Trial 20	0.402	0.429	0.415	0.258	0.100	0.229

Pole

	Lifting	Walking To	Loading	Unloading	Wlaking From	Lowering
Trial 1	0.216	0.430	0.386	0.146	0.136	0.362
Trial 2	0.188	0.410	0.278	0.142	0.135	0.302
Trial 3	0.230	0.332	0.253	0.142	0.127	0.340
Trial 4	·	·	·	·	·	·
Trial 5	0.166	0.397	0.320	0.277	0.251	0.298
Trial 6	0.177	0.313	0.234	0.191	0.128	0.286
Trial 7	0.185	0.657	0.134	0.438	0.122	0.263
Trial 8	0.181	0.670	0.194	0.153	0.165	0.404
Trial 9	0.157	0.376	0.208	0.156	0.128	0.296
Trial 10	0.210	0.615	0.237	0.144	0.348	0.271
Trial 11	0.263	0.416	0.280	0.036	0.035	0.261
Trial 12	0.075	0.274	0.224	0.050	0.042	0.378
Trial 13	0.081	0.346	0.212	0.071	0.050	0.267
Trial 14	0.099	0.447	0.215	0.052	0.029	0.326
Trial 15	0.094	0.606	0.342	0.053	0.043	0.309
Trial 16	0.288	0.489	0.274	0.052	0.104	0.265
Trial 17	0.154	0.432	0.134	0.113	0.055	0.331
Trial 18	0.100	0.435	0.171	0.241	0.547	0.343
Trial 19	·	·	·	·	·	·
Trial 20	0.121	0.540	0.314	0.068	0.146	0.294

Litter

	Lifting	Walking To	Loading	Unloading	Wlaking From	Lowering
Trial 1	0.416	0.431	0.426	0.157	0.101	0.268
Trial 2	0.389	0.315	0.236	0.073	0.093	0.205
Trial 3	0.563	0.358	0.209	0.143	0.073	0.214
Trial 4	·	·	·	·	·	·
Trial 5	0.339	0.267	0.215	0.345	0.145	0.162
Trial 6	0.363	0.272	0.171	0.173	0.085	0.170
Trial 7	0.288	0.517	0.202	0.180	0.010	0.223
Trial 8	0.278	0.529	0.168	0.199	0.053	0.269
Trial 9	0.366	0.329	0.281	0.148	0.063	0.291
Trial 10	0.335	0.333	0.296	0.176	0.148	0.175
Trial 11	0.260	0.329	0.263	0.082	0.097	0.157
Trial 12	0.257	0.348	0.349	0.137	0.062	0.277
Trial 13	0.297	0.274	0.219	0.236	0.190	0.200
Trial 14	0.334	0.492	0.113	0.081	0.037	0.204
Trial 15	0.379	0.382	0.326	0.177	0.161	0.335
Trial 16	0.356	0.378	0.092	0.115	0.073	0.248
Trial 17	0.321	0.347	0.225	0.144	0.062	0.279
Trial 18	0.259	0.368	0.196	0.212	0.397	0.189
Trial 19	·	·	·	·	·	·
Trial 20	0.331	0.416	0.418	0.227	0.062	0.187

Figure 9: Table listing the maximum value of the free acceleration norm for each body segment in each trial. The table is color-coded such that the lower the blue denotes low acceleration, and red denotes high acceleration.

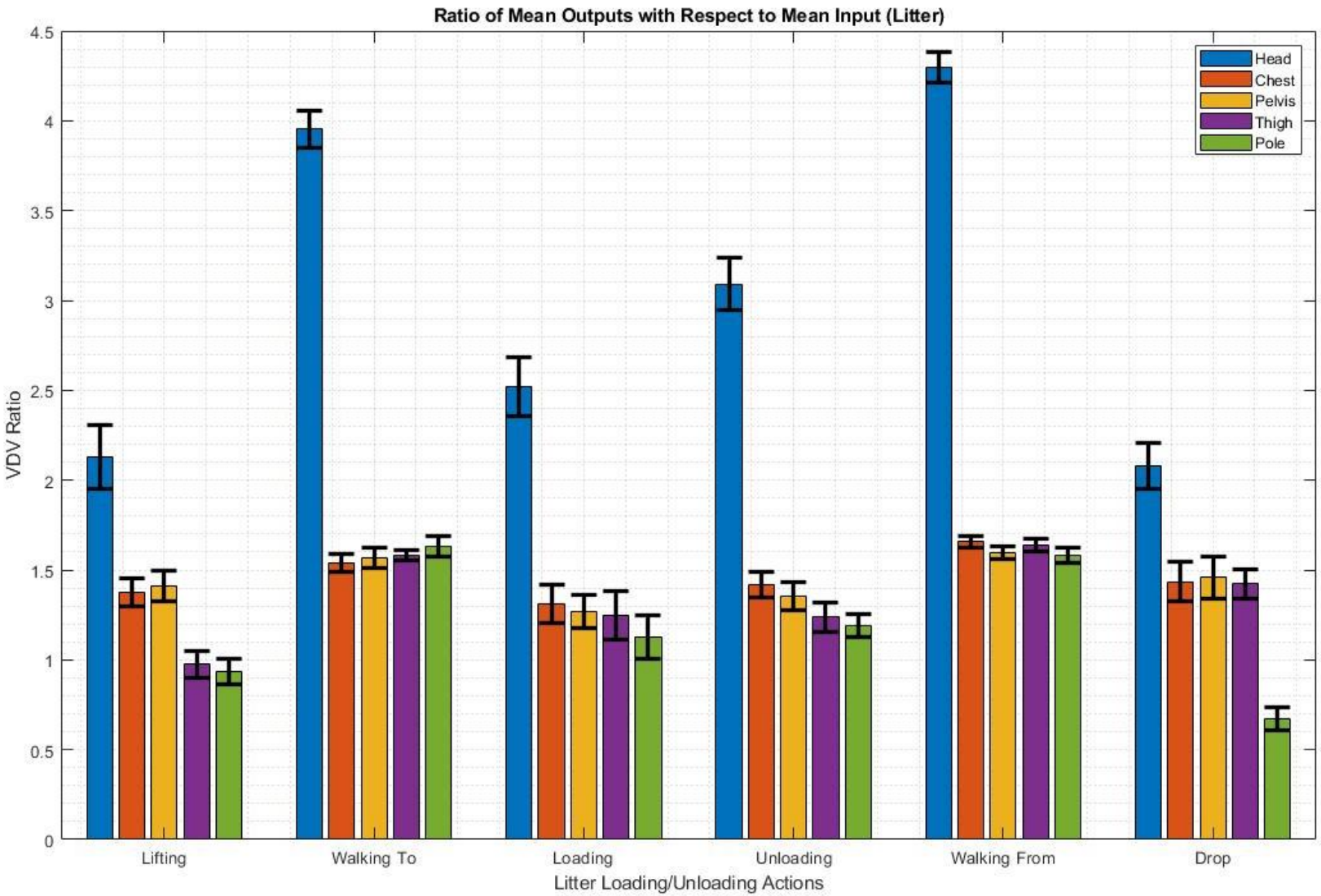
Ratio of Mean Outputs with Respect to Mean Input (Litter)
VDV Ratio
4.5
4
3.5
3
2.5
2
1.5
1
0.5
0
Head
Chest
Pelvis
Thigh
Pole
Lifting
Walking To
Loading
Unloading
Walking From
Drop
Litter Loading/Unloading Actions

Figure 10: A bar graph displaying a rough approximation of the transmissibility metric is shown. The values of this plot were calculated by normalizing the outputs (non-litter segments) against the inputs (litter segment). This effectively shows how the energy/acceleration inputted to the manikin are amplified or attenuated for each segment in each of the six motion segments. The black error bars indicated the range of the standard deviation for the corresponding bar. Note that the VDV Ratio was calculated from frequency-weighted acceleration data

Figure 11 shows the acceleration of the manikin's chest segment in the X, Y, and Z axes (Global CS). The chest segment was selected as qualitative examination showed it to be the segment most indicative of the manikin's overall motion response. Here the Z axis acceleration is shown to center around one rather than zero. This was included to underscore that these plots are in the global CS. The acceleration due to gravity was removed in all calculations. Events identified through visual analysis of the corresponding video as likely mechanical shock events are marked in vertical black lines in the figure.

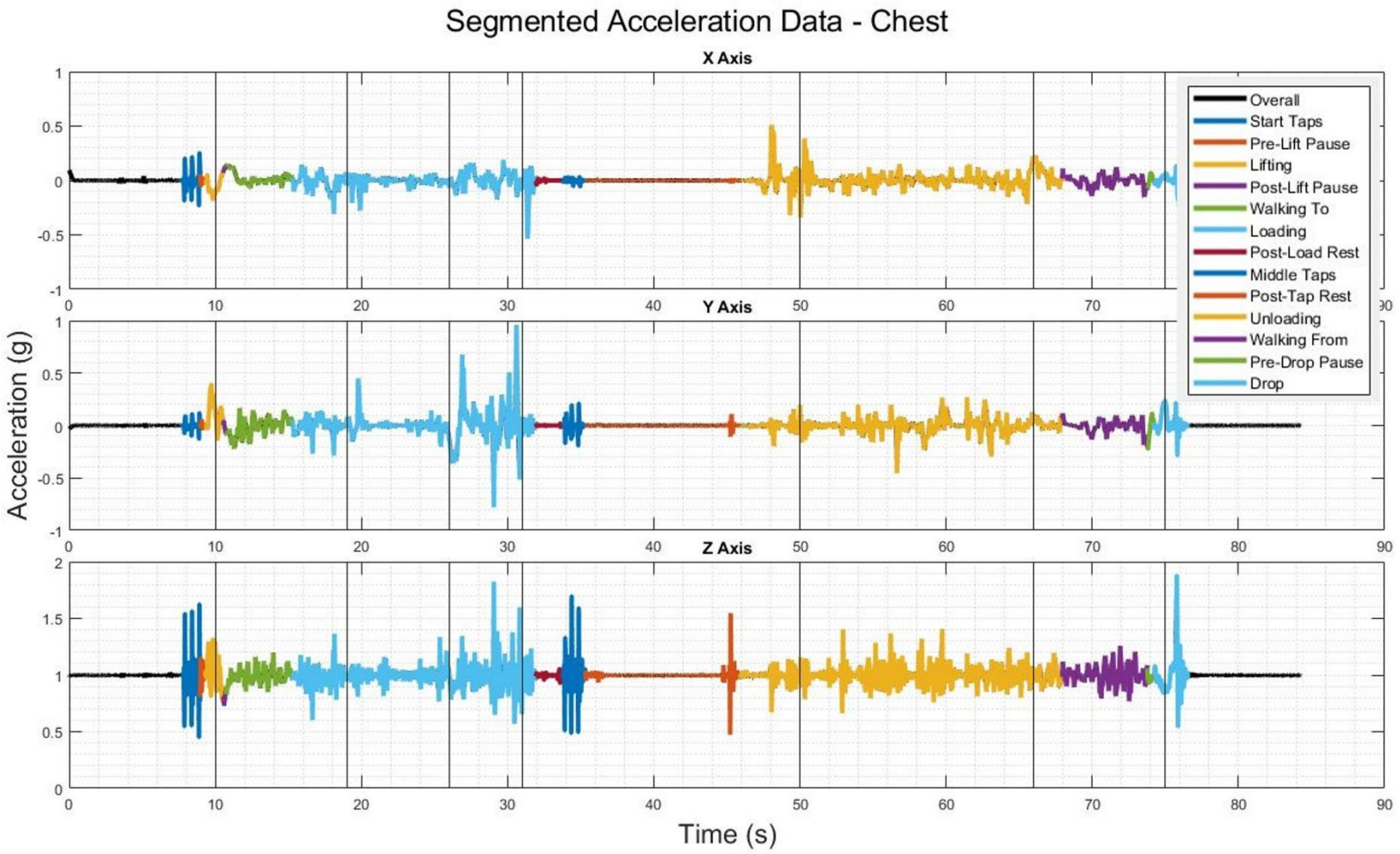

Figure 11: Events causing potentially detrimental motion/vibration during the loading process were identified by examination of the video data and marked by vertical black lines. The corresponding time stamps of said events were synced with the inertial data and used to label the inertial data to quantitatively examine the effects of the identified events on the acceleration experienced by the manikin.

3.2 Statistical Analysis Results

In addition to biodynamic characterization, another goal of this study was to statistically compare the results based on the several tested parameters to assess if said parameters caused a statistically significant difference. To accomplish this, a t-test between the two parameters being compared was performed to compare the means. To ensure a rigorous comparison, the parameters were compared 16 times by leveraging multiple metrics and all body segments (including the pole and litter). The metrics used for comparison are listed below:

- Head VDV Norm, Chest VDV Norm, Pelvis VDV Norm, Pole VDV Norm, and Litter VDV Norm
- Head Gyroscope RMS Norm, Chest Gyroscope RMS Norm, Pelvis Gyroscope RMS Norm, and Litter Gyroscope RMS Norm,
- Head JE Norm, Chest JE Norm, Pelvis JE Norm, Thigh JE Norm, Pole JE Norm, and Litter JE Norm.

The results displayed in this section will, in general, adhere to the following format. First the compared parameters will be introduced and discussed. Second, bar plots of the 16 metrics (split into three subplots) will be presented. The values of each plotted bar were obtained by averaging the values of said metric over all the trials (error bars showing the standard deviation are overlayed on the graph). Note that there were no gyroscope measurements taken on the pole or thigh, therefore the bar graphs for the gyroscopic metrics will not contain these segments. The purpose of this graphic is to provide the reader with general insight into how the parameters impacted the different metrics, by what magnitude they were impacted, and whether the difference is statistically significant. With reference to the statistical significance, for this study, p-values below 0.05 was considered statistically significant, and p-values between 0.05 and 0.1 was considered marginally significant. To show which metrics are statistically significant, the "*" symbol was placed above the bars with statistically significant differences, and the "^" symbol was placed above the bars with marginally statistically significant differences. Finally, the results encompassed by the graphic were enumerated.

3.2.1 Walking vs Loading Motions

Perhaps the most important objective of this report is to establish whether or not the process of loading supine humans expose them to vibratory motion in a statistically significant manner. To establish this, the data from the two motion segments concerning the loading process, loading and unloading, were compared with the two motion segments concerning walking, walking to and from the aircraft. The walking segments were chosen as the comparator as they should ideally constitute a process of minimal exposure to vibration.

For this comparison, the loading and unloading motion segments for all trials were combined into a single dataset, termed the "Loading Set" (LS), and the walking to and walking from motion segments were combined into a single dataset, termed "Walking Set" (WS).

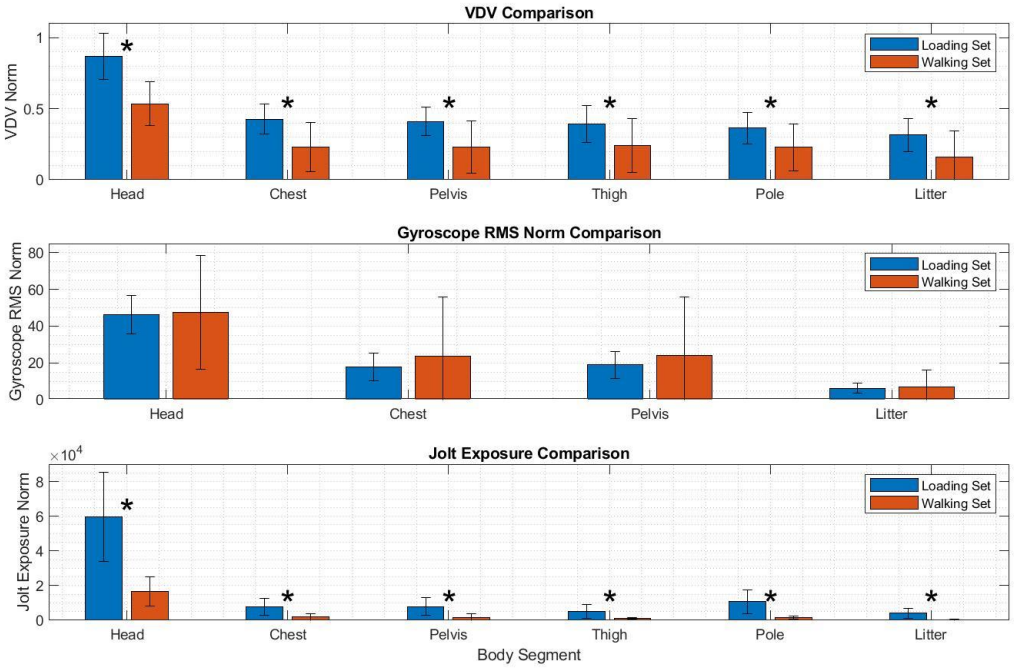

Figure 12: Comparison of the mean Jolt Exposure in the Loading Set and Walking Set.

All six VDV metrics and all six JE metrics were found to be significantly different between LS and WS. Differences in the Gyroscope RMS Norm were not statistically significant. Furthermore, the differences between the VDV norm for the WS and LS were large (LS was between 1.5 and 2 times greater); the differences between JE were larger (LS was between 3 and 11 times greater).

3.2.2 Inboard vs Outboard Litter Pole Sensor Placement

The location of the sensor on the litter pole was varied through the testing such that half of the trials placed the sensor on the outboard side of the MEDEVAC platform, and half on the inboard side. The plots of the mean values can be seen below in Figure 13.

Comparison of Inboard and Outboard Litter Pole Sensor Placement

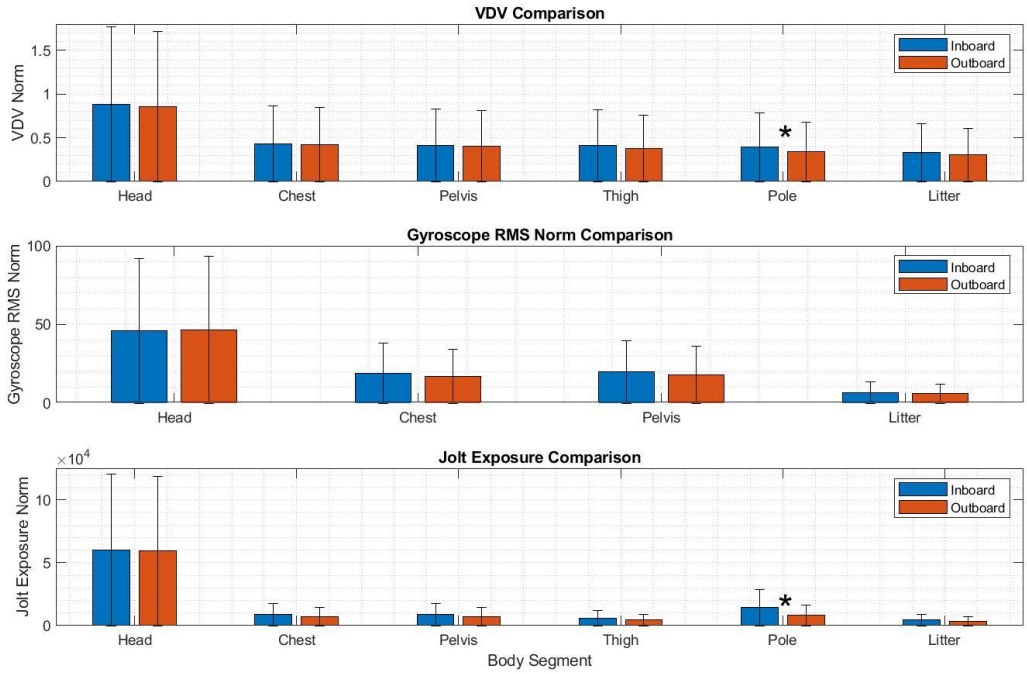

Figure 13: Comparison of the mean values of several metrics between inboard and outboard placement of the litter pole sensor. The symbols "*" and "^" represent statistically significant ($p<0.05$) and marginally statistically significant ($0.05 \leq p < 0.1$) respectively.

The t-test revealed two statistically significant results, The pole VDV and the pole JE. Outside of these two metrics, the metrics for the two cases were generally very similar and exhibited high and similar standard deviations.

3.2.3 Effect of MEDEVAC Platform

Two MEDEVAC platforms were utilized in this project, HH-60 with the BMI and the UH-60 with the IMMSS, referred to as BMI and IMMSS respectively, and trial data was sorted along these lines to allow for statistical comparison. Mean values of the 16 compared components over all trials are shown in Figure 14.

BMI vs IMMSS Comparison

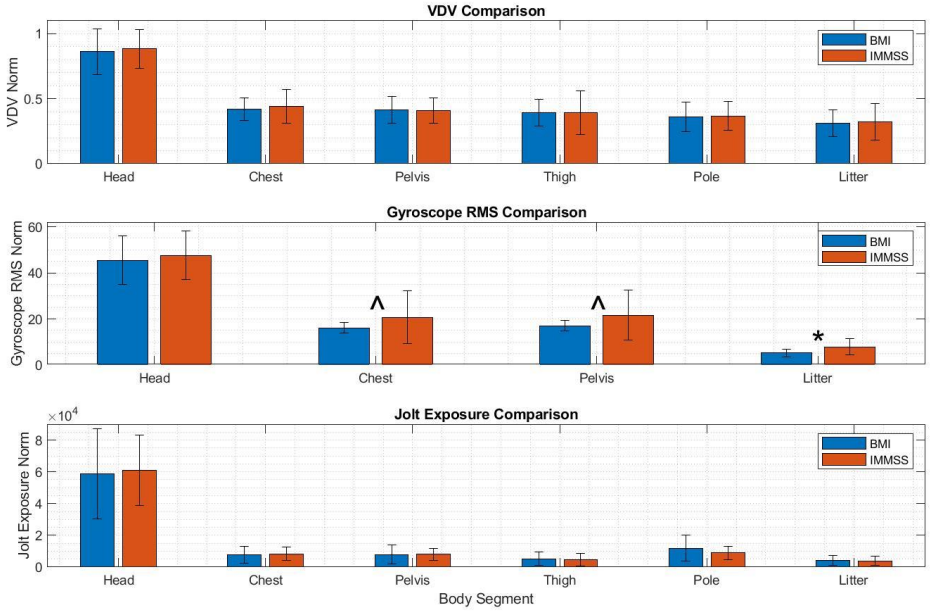

Figure 14: Comparison of the mean values of several metrics between the BMI and IMMSS MEDEVAC platforms.

The t-test results showed one statistically significant difference (Gyro/Litter) and two margninally statistically significant differences (Gyro/Chest and Gyro/Pelvis). It is worth noting that the IMMSS gyroscope data had significantly larger standard deviations than the corresponding BMI data, though this pattern does not seem to extend to any of the other metrics, not even the gyroscope head segment.

3.2.4 Effect of Loading Direction – Head First vs Feet First

Two methods of loading the litter were employed in this study, one where the manikin's head was loaded first, and one where the manikin's feet were loaded first. Figure 15 shows the mean values of the compared metrics for each method.

Comparison – Loading Head First vs Loading Feet First

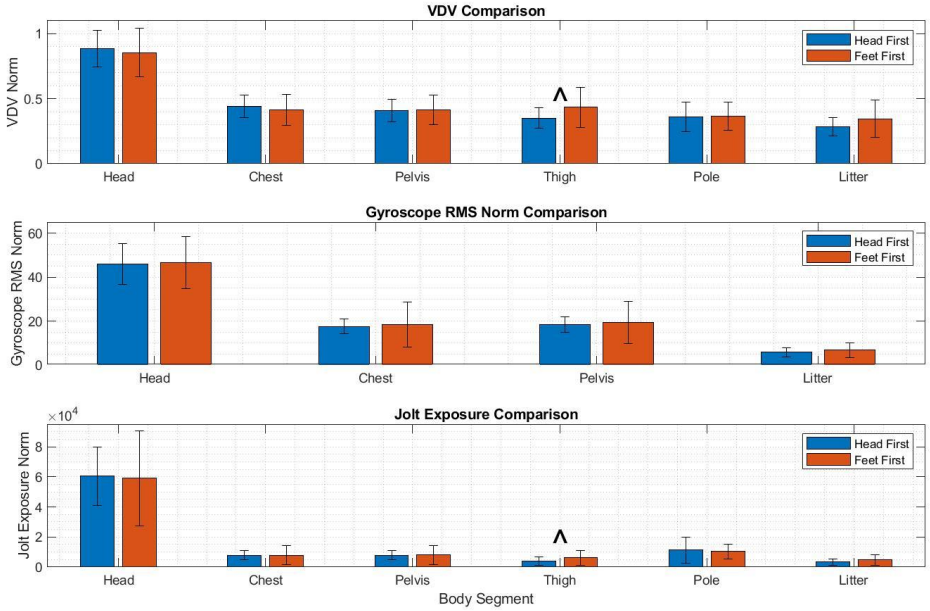

Figure 15: Comparison of the mean values of several metrics between loading the manikin head first vs feet first.

The results of the comparative t-test revealed two marginally statistically significant differences between the two methods, both occurring at the thigh and both based on accelerometric metrics. The thigh was not instrumented with a gyroscope, so it is unknown if a significant difference occurred in the thigh's angular velocity RMS Norm. The feet first data generally admitted to larger standard deviations than the head first data.

3.2.5 Top vs Bottom Litter Loading Heights

The height of litter loading was varied during testing. In the BMI, the top, middle, and bottom litter pan heights were used, and in the IMMSS the top and bottom heights were used. As the middle height was only used on one platform (for a total of four trials), this analysis will eschew that data and compare only the top and bottom heights. Based on this analysis, the relevance of comparing the middle litter height will be considered. The plots of the mean values can be seen below in Figure 16.

Top vs Bottom Litter Loading Heights

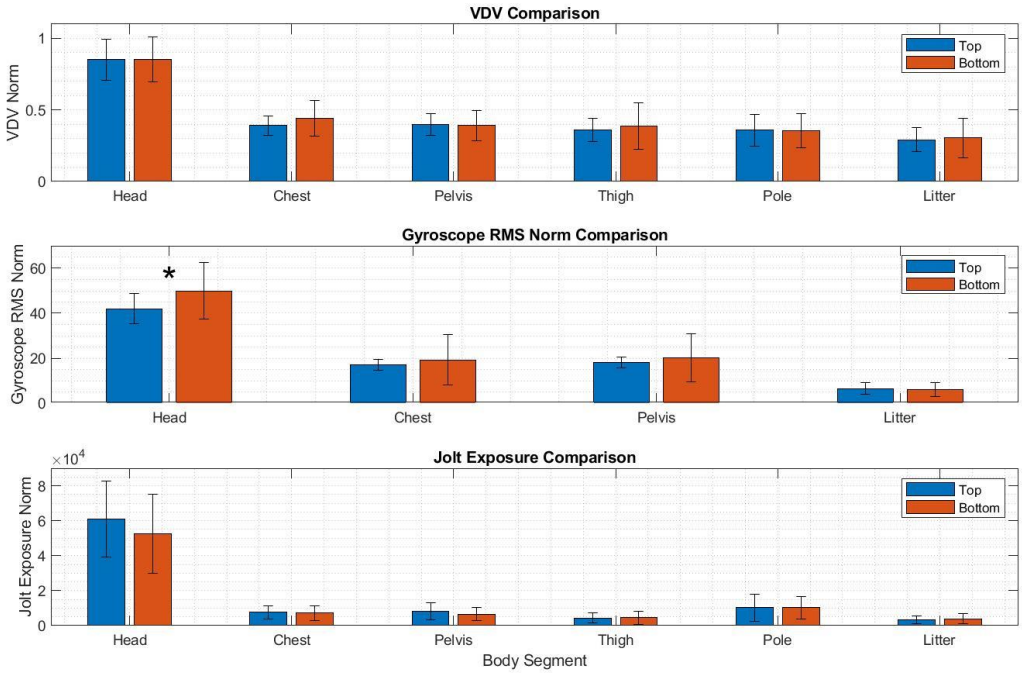

Figure 16: Comparison of the mean values of several metrics between top and bottom litter loading heights. The symbols "*" and "^" represent statistically significant ($p<0.05$) and marginally statistically significant ($p<0.1$) respectively.

The results shown in Figure 16 admitted one statistically significant difference, the Head Gyroscope RMS Norm metric, where the bottom height metric was 1.19 times that of the top height. Another potentially noteworthy difference was that the standard deviations of the chest and pelvis gyroscope metrics were several times larger for the bottom height when compared to the top height. The VDV metrics for the head were essentially identical. The JE metric was 1.17 times greater for the top height, but this was not statistically significant.

3.2.6 Loading vs Unloading Motion Segments

Analysis of the data suggested that the loading motion segment and the unloading motion segment exhibited different exposure profiles, with the loading motion segment appearing to impart greater exposure. An example can be seen in (Will need to reference what is currently figure 12 in the main report). To test this hypothesis, the data from these two motion segments were compared. The plots of the mean values can be seen below in Figure 17.

Loading vs Unloading Motion Segments

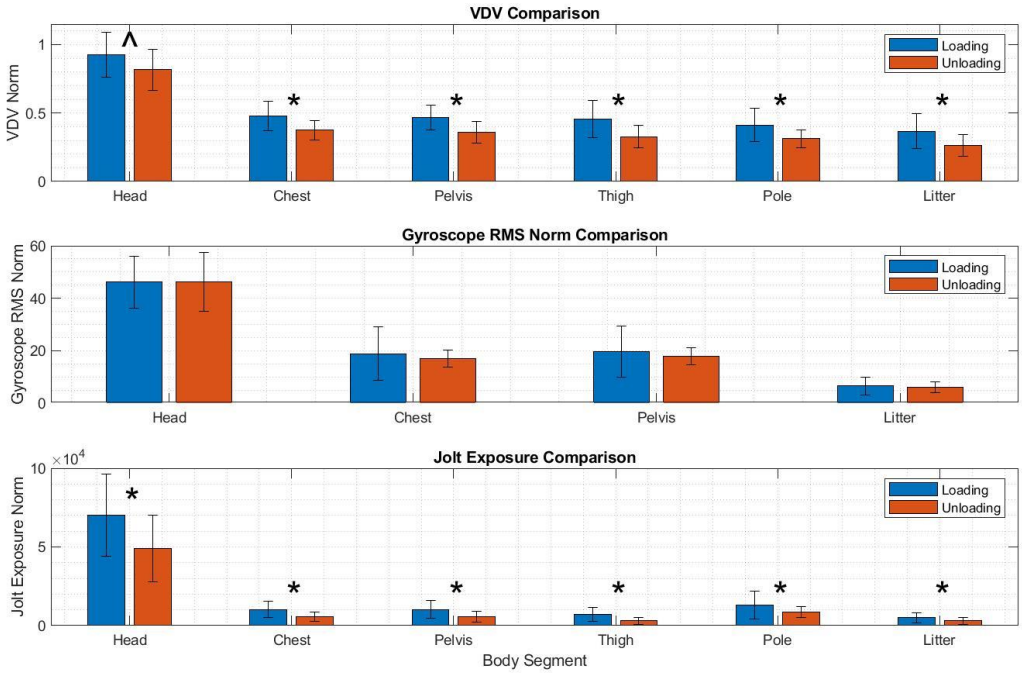

Figure 17: Comparison of the mean values of several metrics between top and bottom litter loading heights. The symbols "*" and "^" represent statistically significant ($p<0.05$) and marginally statistically significant ($p<0.1$) respectively.

The results of Figure 17 showed that there were significant statistical differences in eleven of accelerometric metrics, with the last of the 12 accelerometric metrics (Head VDV Norm) admitting marginal statistical significance. In all 12 cases, the loading motion segment metrics were greater than the unloading motion segment metrics. In terms of JE, the loading metrics were between 1.4 and 2.4 times greater for the loading data.

4 Discussion

4.1 Overall Results

Based on the calculated values for frequency-weighted VDV, unweighted VDV, and Gyroscope RMS norms (Figure 3, Figure 4, and Figure 5 respectively), the body segment most impacted was the head and the loading motion segment generates the most vibration/shock, though the unloading motion segment was a close second.

In terms of weighted VDV, unweighted VDV, and the Gyroscope RMS Norm, the median head values were approximately twice that of the other body segments in all three cases. This corroborates the video observations. When interpreting these results, it should be considered that while the ISMv1.2 has been validated to exhibit the same vibrational response as a human, the contraction of muscles in a human can alter their response. This is most relevant at the head, as the manikin does not have any neck muscles to contract to stabilize itself. Therefore, while it seems reasonable to extend the aforementioned results to unconscious or limp humans, the vibration response could be different outside those conditions.

The results can be differentiated into three categories: Shock (described by VDV (Figure 3 and Figure 4) and JE (Figure 6, Figure 7, and Figure 8), Rotation (described by the Gyroscope RMS Norm (Figure 5)) and max

acceleration (Figure 9). In terms of shock, the loading and unloading motion segments have the largest VDVs, which is corroborated by similar results in the JE values. In terms of rotation, the lifting motion segment generated the largest RMS norm values, particularly at the head. In terms of max acceleration, the Lifting and Walking To motion segments, especially for the head, exhibit the largest values. The Lowering segment for the head also exhibits high max accelerations.

The standard deviation of the metric means were large – in the most extreme cases the standard deviation could be as large as the metric it describes. This indicates there is a large variation in imparted exposure that is dependent on the litter-bearers' performance. The large standard deviations show that while the litter-bearers can cause an increase in vibratory exposure by their actions, they can also decrease it. This suggests that the most important factor in controlling exposure is the quality of the litter bearers' performances. In the authors' opinion, the most expedient method of reducing exposure would be to improve the experience, training, and teamwork of the litter bearers. However, regardless of the litter-bearers' experience and abilities, their anthropometry will likely be a factor. Height and size impact maneuverability of a litter-bearer in and around the MEDEVAC platform, likely impacting the imparted exposure. Furthermore, anthropometric variability within the litter-bearer team likely contributes to overall performance. However, variability of litter-bearer experience and anthropometry is outside the scope of this study and could be a topic of future research.

4.2 Recommended Methods of Interpretation

The primary goal of this study was to investigate the biodynamic effects of the MEDEVAC litter loading and unloading process. This was motivated by subjective observations of mechanical shock occurring during this process and lack of known previous investigation quantifying the issue. This lack of known prior quantification has complicated the interpretation of the inertial data from this study. When the protocol for this study was developed, it was determined that the analysis of the data would begin with a general inspection the inertial data, a subjective visual analysis of the captured video data, and a calculation of quantifiable ISO metrics, such as Crest Factory, RMS, VDV, and Acceleration Dose (ISO 7096, 2631-1, and 2631-5). Once these metrics were determined, it became clear that these metrics did not fully represent the effects implied by the raw inertial and visual data. Namely, the inertial and visual data suggested that the overall exposure of the manikin to shocks, vibration, and motion was greater than suggested by the ISO metrics.

It was determined that because the manikin was not experiencing continuous/consistent transient vibrations or shocks, due to the many pauses in the loading and unloading process, metrics like the Vibration Dose Value and Acceleration Dose were being diluted by the averaging effect that occurs when a continuous time-varying signal is condensed into a scalar. To address this issue, a new metric was developed, Jolt Exposure. JE ignores any acceleration below a certain threshold (1.6 m/s2 in this case) to minimize this averaging effect. Furthermore, as it is reasonable to expect "exposure" is not linearly related to acceleration, namely a 2g acceleration will likely generate more than twice the exposure of a 1g acceleration, the acceleration values were squared to act as a representative weighting function. The calculated JE values, in the authors' opinions, offered useful interpretation of the data in addition to that of the ISO metrics.

4.3 Jolt Exposure

Examination of Figure 6, Figure 7, and Figure 8 show that the loading and unloading motion segments generate by far the most JE. Compared to the walking motion segments, the loading and unloading motion segments had higher JE values several multiples higher in all three axes and both the head and chest body segments. Overall, JE was highest in the Y axis (global CS), corresponding to the manikin moving side-to-side with respect to the litter. During the loading and unloading motion segments, the litter was often tilted, jerked, and caught on the

platform. The reaction forces from these actions would logically be focused in the horizontal plane and specifically in the Y axis. Further, the litter mesh can absorb/dampen motion applied perpendicularly to its plane (generally the global Z axis) but offers little to no resistance against in-plane motion.

The JE metric showcased significant variability across trials in most, if not all, aspects. Examining the data in Figure 11 shows that effect of unintended mechanical jolts on acceleration, as well as the cause of the jolts. The jolts are directly manifested in the JE metric, and the large variability in said metric is evidence of the variability of these jolts in the loading and unloading motion segments.

It is difficult to interpret the meaning of JE, as there is no known reliable method for quantifiably predicting its correlation with injury. However, two conclusions can be drawn from the JE data. First, the JE of the Loading and Unloading motion segments were several multiples that of the walking motion segments, supporting the claim that the former are potentially hazardous to patient health, and likely warrant further investigation. Second, the large variability in JE shows that it can be mitigated (or exacerbated), i.e. in terms of JE the training/experience of the litter bearers has a large impact on patient exposure.

4.4 Statistical Results Discussion

4.4.1 Walking Set vs Loading Set

The results of comparing the WS and the LS (Figure 12) visually suggest that the LS offered far more exposure than the WS. This observation is corroborated by the statistical significance of all 12 accelerometric metrics (all six segments for both VDV and JE metrics). The LS VDV Norms were greater by at least 1.5 times than the corresponding values for the WS. This result is made more relevant by the observation that the WS tend to exhibit relatively consistent acceleration, whereas the LS tend to contain shocks and vibration interspersed with periods of very low acceleration (see Figure 11). The VDV metric is normalized against the number of samples, lending it an averaging effect. The VDV norms for the LS are up to two times as high as for the WS, despite the interspersed periods of low vibration lowering the average value. To support this, JE can be used, as it does not have an in-built averaging mechanism. Examining the JE values of Figure 12, the differences identified by the VDV have been amplified. In terms of mean JE, the head body segment was exposed 3.6 times as much in the LS than in the WS. The largest ratio was that of the litter, where the LS exhibited 10.7 times the JE as the WS. All other ratios fell between those two values (3.6 and 10.7). These quantitative results, along with their statistical significance, offer strong evidence that the act of loading and unloading into the MEDEVAC platform imparts far more vibration exposure to the subject than the act of walking to and from the MEDEVAC platform. This motivates the need to further examine the loading and unloading motion segments, as was done in the other statistical analyses.

Despite this strong evidence, it is interesting to note that the gyroscopic metrics comparing the LS and WS were not different in a statistically significant manner. Furthermore, the Gyroscope RMS Norm was greater for all four measured segments. This suggests that the centripetal and tangential acceleration caused by non-zero rotational velocities – that is acceleration caused by rotation – did not contribute to the acceleration values VDV and JE are constructed from. Therefore, the high VDV and JE values were likely the result of translational accelerations (such as those caused by hitting the litter against parts of the MEDEVAC platform).

4.4.2 Inboard vs Outboard Sensor Placement

The results shown in Figure 13, that the outboard side experienced a higher VDV Norm and JE Norm, were likely the most predictable of all the comparison. Given that the only parameter changed was the placement of

the pole sensor, statistically significant differences should manifest only in the measurements of the pole sensor. This was corroborated by the results. Furthermore, a reasonable hypothesis is that the outboard case will experience higher values of VDV and JE than the inboard, as it is more likely to contact the MEDEVAC platform. This was also corroborated by the results.

Several conclusions can be drawn from these results. First, the lack of statistically significant differences in the non-pole metrics should improve confidence in the reliability of the testing and veracity of the subsequent calculations. Second, these result offers strong evidence that the outboard side of the litter is a greater source of vibration exposure than the inboard side, providing any efforts at mitigating said exposure a reliable starting point. Third, the usefulness of the JE metric, designed specifically for this experiment, is potentially supported by this result. The VDV metric had a mean outboard pole value 1.146 times that of the inboard with an associated p-value of 0.0284. Comparatively, the JE metric had a mean outboard pole value 1.748 times that of the inboard with an associated p-value of 0.0129. This larger ratio and smaller p-value suggest that the JE metric could be more useful in quantifying the vibration exposure examined in this study.

4.4.3 BMI vs IMMSS

Assessing the effect of which MEDEVAC platform imparts greater exposure to the subject is of obvious import. The results of Figure 14 looked similar across all accelerometric metrics. The only statistically significant differences occurred in the gyroscopic metrics, and two of those results were only marginally significant. The litter exhibited the only $p<0.05$ significant difference in the Gyroscope RMS Norm, but this result cannot be offered as evidence of a difference in exposure as the litter is the input. Overall, the data offered little evidence of a difference in vibration exposure between these two MEDEVAC platforms.

4.4.4 Loading Head First vs Feet First

Loading patients head first is the norm, so it would be useful to know if loading feet first offered less vibration exposure. The results of Figure 15 admitted little evidence for this. Loading feet first did offer a lower VDV norm and JE norm that was marginally significant for the thigh, but this was the only statistically significant result. It is interesting to note that the feet first data tended to have larger standard deviations than the head first data. Given the ease with which a subject can be switched from head first to feet first loading, a larger study could be warranted to see if differences exist. However, no such distinction can be made based on the gathered data.

4.4.5 Top vs Bottom Loading Heights

The results shown in Figure 16 offered little evidence of significant differences between the top and bottom litter loading heights. The statistically significant results for the gyroscopic head metric did not lead to/manifest as statistically significant differences in the accelerometric metrics for the head, so its effect on vibratory exposure is questionable. It is interesting to note that the head gyroscope metric was greater for the bottom height, but the JE metric was greater for the top height (though this second difference was not deemed statistically significant). This could be interpreted as further evidence that rotation-induced acceleration has a potentially negligible impact on the accelerometric metrics, as previously hypothesized in the discussion of the WS vs LS data.

4.4.6 Loading vs Unloading Motion Segments

The results of Figure 17 offer strong evidence that the loading motion segment imparts significantly greater vibratory exposure than the unloading motion segment. In terms of JE, the body segment with the least difference was the head, which was 1.44 times greater for the loading segment. Based on the measured accelerations of the trials (see, for example, Figure 11), a likely explanation for this is that lifting the litter into the litter pan is more difficult for the medics than lowering it out of the pan. This manifests as loading sometimes taking a longer amount of time than unloading and a greater likelihood of imparting unintentional shocks/drops to the litter during lifting. That the JE metrics admits greater differences than the VDV metrics potentially support the hypothesis that the loading portion generally takes longer.

5 Works Cited

Barazanji K, Jonathan D, Frick E, Rahmatalla S, Kinsler R. "Biodynamically Validated Instrumented Supine Manikin for Evaluation of Patient Systems," oral presentation at Military Health System Research Symposium, Kissimmee, Florida, August 2019.

DeShaw, J., & Rahmatalla, S. (2012). Comprehensive Measurement in Whole-Body Vibration. *Journal of Low Frequency Noise, Vibration and Active Control*, 31(2), 63-74.

DeShaw, J., Rahmatalla, S. (2016). Predictive discomfort of supine humans in whole-body vibration and shock environments. *Ergonomics*, 59(4), 568-581.

Deshaw, J, Frick, E., Rahmatalla, S., Kinsler, R., and Barazanji, K. (2019). Biodynamically Validated Instrumented Supine Manikin for Evaluation of Patient Systems. Abstract, Military Health System Research Symposium, Kissimmee, FL, August 2019.

International Organization for Standardization, "ISO 7096:2020, Earth-moving machinery – Laboratory evaluation of operator seat vibration," Switzerland, 2020.

International Organization for Standardization, "ISO 2631-1: 1997, Mechanical Vibration and Shock - Evaluation of Human Exposure to Whole-body Vibration," Switzerland, 1997.

International Organization for Standardization, "ISO 2631-5: 1997, Mechanical Vibration and Shock - Evaluation of Human Exposure to Whole-body Vibration – Part 5: Method for evaluation of vibration containing multiple shocks.," Switzerland, 1997.

Kinsler, R. and Barazanji, K. (2011). *Assessment of fixed position litter loading in the HH-60M MEDEVAC helicopter*. Fort Rucker, AL: U.S. Army Aeromedical Research Laboratory. USAARL Technical Memorandum 2011-19.

Kinsler, R., Barazanji, K., Lee, J., Fulton, L., & Hatzfeld, J. (2015). *Analysis of Two Surveys Examining Enroute Care Technologies, Platforms, and Space Requirements.* Poster Presentation at Military Health System Research Symposium, August 2015.

Kinsler, R., Khouri, R., Squire, C., Conti, S., & Wurzbach, J. (2018). [Immobilization and Vibration Mitigation Systems: Test and Evaluation of Current and Developmental Products]. Unpublished report. Fort Rucker, AL: U.S. Army Aeromedical Research Laboratory.

Meusch, J., & Rahmatalla, S. (2014a). 3D Transmissibility and Relative Transmissibility of Immobilized Supine Humans during Transportation. *Journal of Low Frequency Noise, Vibration and Active Control*, 33(2), 125-138.

Meusch, J., & Rahmatalla, S. (2014b). Whole-body vibration transmissibility in supine humans: effects of board litter and neck collar. *Applied Ergonomics*, 45 (3), 677–685.

Ratanalert, S., Phuenpathom, N., Saeheng, S., Oearsakul, T., Sripairojkul, B., Hirunpat, S. (2004). ICP Threshold in CPP Management of Severe Head Injury Patients, Surg Neurol, 61(5):429-34.

Reno, J. (2010). Military aeromedical evacuation, with special emphasis on craniospinal trauma, Neurosurg Focus 28 (5):E12.

S. O. H. Madgwick, A. J. L. Harrison and R. Vaidyanathan, "Estimation of IMU and MARG orientation using a gradient descent algorithm," *2011 IEEE International Conference on Rehabilitation Robotics*, 2011, pp. 1-7, doi: 10.1109/ICORR.2011.5975346.

6 Appendix

6.1 Description of Segmentation Process

The process of segmenting the inertial data into different motion segments is described here. Said segments had to both allow for straight-forward syncing of the inertial data with the video data, as well as a robust method of isolating the inertial data associated with the six motion segments of interest: Lifting, Walking To, Loading, Unloading, Walking From, and Dropping. Therefore a small protocol was setup for identifying the different motion segments.

A total of 13 motion segments were defined. The extra seven segments allowed for the entire set of inertial data (with the exception of the static data at the start and end of the trial) to be assigned a motion segment. The definitions of the 13 segments are as follows:

- Syncing Start Taps - Begins before first tap touches and ends after third tap
- Pre-lift Pause - Time after taps, but before the ISMv1.2 has been moved by the lifting motion
- Lifting - Time from when ISMv1.2 leaves ground until the upward motion is complete and rolling/pitching motions have settled
- Post-lift pause - Time after lift and before the walking of the ISMv1.2 to the aircraft is initiated
- Walking to - Time the walking of the ISMv1.2 to the aircraft begins until the time that the orientation/height of the litter is changed to begin the process of loading (typically this occurs when the carrier closest to the aircraft begins to lift his/her litter handle
- Loading - Time from end of walking until the ISMv1.2 is fully in the pan (adjustments of the ISMv1.2 count as part of loading) and the ISMv1.2 has stopped shaking/come to rest
- Post load Pause - Time from end of loading until beginning of taps
- Syncing Middle Taps - Time right before first tap to the time after third tap
- Post tap Pause - Time from the end of the Syncing Middle Taps to start of unloading.
- Unloading - Time from when ISMv1.2 is in the litter pan until changes in orientation/height become that of walking
- Walking from - Time from start of walking until the litter bearers are standing stationary at the drop point
- Pre-drop Pause - Time between walking from and dropping
- Drop - Time from the start of lowering the ISMv1.2 until all litter-bearer hands have been removed from litter and/or the ISMv1.2 has stopped moving as a result of the drop

Note that the pause segments are not necessarily present in every trial, as sometimes the litter bearers moved from one motion segment directly into another. The pause motion segment only exists to excise the pause segments from the inertial analysis (if they are present).

6.2 Populated Protocol Table for Statistics Calculations

Phase	Litter Position	Loading Direction	Litter Pole Sensor Placement	Loading/Unloading Trial	Head VDV	Chest VDV	Pelvis VDV	Thigh VDV	Pole VDV	Litter VDV	Head Gyro RMS	Chest Gyro RMS	Pelvis Gyro RMS	Litter Gyro RMS	Head SE	Chest SE	Pelvis SE	Thigh SE	Pole SE	Litter SE
BMI (three litter positions)	Top Litter Position	Head First	Outboard	Loading	0.921102	0.476506	0.476002	0.36804	0.234585	0.281338	51.86647	19.63063	20.55783	5.760143	48204.23	7558.968	8090.973	3651.712	3185.707	2095.059
				Unloading	0.658532	0.405415	0.357828	0.238209	0.221353	0.18987	41.2827	18.69648	19.34213	5.35347	73677.01	8459.734	8056.879	1347.235	3587.583	1063.206
			Inboard	Loading	1.058816	0.488192	0.516298	0.522849	0.440745	0.413822	31.93018	11.40874	12.49671	3.506984	79432.32	8296.594	10614.44	11106.49	32550.25	7531.736
				Unloading	0.920252	0.429564	0.409079	0.340099	0.339466	0.247449	44.92348	19.52537	20.04131	5.660463	48648.81	8275.285	9203.108	4001.751	12841.47	3636.22
		Feet First	Outboard	Loading	0.891901	0.428711	0.468259	0.483463	0.389087	0.448254	39.61775	15.67166	16.45338	5.33202	72101.32	9814.785	12630.42	9207.876	18423.25	6616.502
				Unloading	0.876393	0.398794	0.387316	0.381605	0.351704	0.27542	50.04022	17.90772	18.82319	5.13026	72183.3	7737.556	6442.675	4359.697	6630.103	2578.671
			Inboard	Loading	0.873626	0.452881	0.501477	0.431899	0.45979	0.339618	38.21995	16.18304	17.73985	4.885056	90915.32	15522.54	20392.09	6581.696	9917.954	4630.749
				Unloading	0.570106	0.265594	0.274	0.273242	0.237551	0.170552	30.89997	15.4339	16.22541	4.437225	17351.23	997.1179	1841.814	1396.664	8332.239	381.7182
	Middle Litter Position	Head First	Outboard	Loading	1.070254	0.591641	0.556244	0.446304	0.399969	0.357933	55.82878	17.56161	18.15713	5.022555	83482.27	13464.73	11979.82	6476.074	14021.99	4225.898
				Unloading	0.861231	0.410945	0.405378	0.380087	0.441527	0.366306	33.3171	13.46178	13.81699	3.981711	43885.3	5153.683	7527.357	3544.705	17487.67	7477.066
			Inboard	Loading	*	*	*	*	*	*	*	*	*	*	*	*	*	*	*	*
				Unloading	*	*	*	*	*	*	*	*	*	*	*	*	*	*	*	*
		Feet First	Outboard	Loading	0.675811	0.363774	0.442737	0.461736	0.309009	0.324715	40.72823	14.96406	17.31814	4.977809	44099.5	3768.77	5132.277	6385.194	4419.803	3622.02
				Unloading	0.947493	0.441745	0.460514	0.512902	0.344402	0.452711	51.15082	16.13924	16.28766	9.507006	79370.74	9489.738	8572.561	8714.081	8943.774	6366.259
			Inboard	Loading	1.315845	0.620669	0.66799	0.653767	0.528819	0.566709	53.46759	19.62353	20.72302	10.24456	144578.6	25095.06	25720.73	19271.83	23201.26	13106.02
				Unloading	0.89575	0.413122	0.454969	0.400111	0.388886	0.309079	44.63766	17.21755	18.67177	5.056856	56304.61	6809.065	7005.1	4542.514	9498.981	3271.078
	Bottom Litter Position	Head First	Outboard	Loading	0.786911	0.389815	0.370511	0.348083	0.334556	0.291718	40.06442	13.50981	14.43823	4.01572	56709.16	6359.24	6993.186	3337.34	6617.06	3188.714
				Unloading	0.633337	0.361513	0.27885	0.266837	0.284043	0.199948	39.02929	14.25867	14.80788	3.980693	20242.83	2327.526	983.8273	979.3019	10520.56	853.0241
			Inboard	Loading	0.982719	0.525317	0.486751	0.393593	0.715294	0.381034	59.74868	16.41861	17.68403	5.039567	61954.77	8187.174	6857.759	3736.587	30641.38	6496.038
				Unloading	0.79438	0.344493	0.254326	0.249021	0.333688	0.183456	55.65344	18.24295	18.19793	4.925458	44038.64	5653.136	3225.286	2151.648	6413.956	2322.314
		Feet First	Outboard	Loading	0.689401	0.344669	0.321717	0.371424	0.285033	0.264388	35.31528	15.53282	15.83225	4.422194	32311.3	3910.432	3875.956	4157.936	5680.599	2417.788
				Unloading	1.014481	0.353111	0.365819	0.429162	0.331903	0.316062	75.11881	15.92245	18.33296	5.282263	63939.92	5636.015	5236.374	4489.216	7172.443	6850.493
			Inboard	Loading	0.856884	0.439638	0.354142	0.425326	0.325908	0.278449	46.39083	16.45366	16.47616	4.666626	35705.03	3590.13	3060.842	5921.69	12272.95	3036.232
				Unloading	0.661051	0.27944	0.272241	0.255441	0.236206	0.190405	40.66469	12.30655	13.34931	3.590881	26134.95	1286.803	1720.98	1241.299	10225.4	1143.111
IMMSS (two litter positions)	Top Litter Position	Head First	Outboard	Loading	0.684305	0.300583	0.349617	0.311652	0.362625	0.201993	39.46746	17.21906	18.76346	5.197785	63932.13	7523.789	8445.823	2866.789	6360.151	1727.168
				Unloading	1.000212	0.371423	0.364181	0.325433	0.280266	0.272981	41.64604	18.96589	20.10692	5.95044	37622.89	3267.956	4376.022	1683.023	3080.086	2354.177
			Inboard	Loading	1.052261	0.447504	0.456489	0.437689	0.427988	0.341151	53.83898	19.94691	21.48278	10.53881	80406.5	10836.68	9973.885	7330.073	15544.24	4754.353
				Unloading	0.807229	0.334582	0.312498	0.297793	0.280182	0.266953	38.96657	14.81051	14.99683	11.299	42190.18	4425.439	3380.888	2075.118	8263.195	1988.415
		Feet First	Outboard	Loading	0.812714	0.369228	0.365126	0.355756	0.64107	0.382524	40.10787	17.11629	17.81242	11.47603	85776.59	10306.28	9711.056	4440.194	9012.248	4464.6
				Unloading	0.797273	0.307024	0.328472	0.28965	0.351404	0.254397	44.99362	16.6774	17.33854	6.426645	42265.93	2565.621	2160.963	1852.069	7723.11	1872.888
			Inboard	Loading	*	*	*	*	*	*	*	*	*	*	*	*	*	*	*	*
				Unloading	*	*	*	*	*	*	*	*	*	*	*	*	*	*	*	*
	Bottom Litter Position	Head First	Outboard	Loading	0.890634	0.528016	0.456988	0.348667	0.323122	0.263499	45.19927	19.84107	20.95635	5.730731	58566.23	9342.274	8228.744	3885.224	7962.615	2371.571
				Unloading	1.007642	0.540974	0.443339	0.300767	0.266006	0.252936	64.8948	26.22771	27.56749	7.488299	81316.46	9131.996	11355.27	3366.047	5423.566	2415.218
			Inboard	Loading	0.999358	0.590965	0.516284	0.465929	0.397822	0.375863	42.00839	15.75104	16.29318	4.839226	92214.72	12900.82	12627.56	7588.818	6507.485	4880.766
				Unloading	0.78356	0.402082	0.364189	0.271288	0.415331	0.2345	47.16511	19.79447	20.26552	5.726137	70292.94	9897.402	11037	1218.461	12242.71	2245.008
		Feet First	Outboard	Loading	1.054887	0.654924	0.46262	0.497891	0.343091	0.318849	46.82898	13.89511	14.33802	5.164028	81692.51	12769.65	8471.144	5991.237	9275.96	5120.596
				Unloading	0.913046	0.433881	0.491621	0.455969	0.331559	0.379393	55.10405	17.14997	19.46322	8.637204	45505.3	5804.776	7845.659	6174.016	6750.563	5896.005
			Inboard	Loading	1.010274	0.629512	0.595713	0.896944	0.512625	0.760085	71.73568	59.1315	57.71526	16.70855	54321	15832.97	12214.56	16250.84	19479.35	12465.42
				Unloading	0.553828	0.248003	0.22032	0.227297	0.219297	0.191031	34.21677	13.64323	15.83297	5.874389	17023.7	1809.9	2143.453	1025.538	8884.349	936.604

Figure 18: This table is equivalent to Table 1 of the protocol, populated with the calculated metrics for each body segment *during the loading and unloading motion segments*. The symbol "*" is used to denote cells where values from the removed trials 4 and 19 would go.

Phase	Litter Position	Loading Direction	Litter Pole Sensor Placement	Walking To/From Trial	Head VDV	Chest VDV	Pelvis VDV	Thigh VDV	Pole VDV	Litter VDV	Head Gyro RMS	Chest Gyro RMS	Pelvis Gyro RMS	Litter Gyro RMS	Head SE	Chest SE	Pelvis SE	Thigh SE	Pole SE	Litter SE
BMI (three litter positions)	Top Litter Position	Head First	Outboard	To	0.583842	0.287971	0.281136	0.208485	0.216812	0.133844	45.90229	21.92417	22.52855485	6.212999166	29339.15	2918.366	2084.579	1010.841	2373.703	948.62
				From	0.470239	0.177462	0.177361	0.205634	0.197108	0.140956	42.00824	15.69855	15.61459453	4.49216125	13782.83	840.5334	1353.078	2004.724	1723.036	1067.656
			Inboard	To	0.594796	0.171783	0.147039	0.177175	0.125513	0.109362	52.58634	17.40635	17.53534855	4.957631276	19770.49	2276.273	2459.547	388.6473	260.3457	265.829
				From	0.602882	0.222435	0.218413	0.225042	0.199482	0.135553	56.99814	19.59118	20.6704445	5.78903364	18871.97	933.9401	837.002	976.3959	1995.937	54.43439
		Feet First	Outboard	To	0.560248	0.238673	0.218861	0.218432	0.194626	0.148152	44.07296	15.80318	17.15103868	4.831337821	20402.23	1760.493	1613.436	1407.616	2399.626	547.2304
				From	0.452834	0.177752	0.164544	0.203657	0.173507	0.114014	36.56061	15.17177	16.27658162	4.608035138	11026.46	1010.973	487.5519	1064.558	1242.215	178.0875
			Inboard	To	0.403059	0.197186	0.214662	0.234723	0.338569	0.141595	33.07376	13.86328	15.1116303	4.030179137	7111.499	1244.823	868.7564	347.2204	1300.798	84.04005
				From	0.473671	0.211079	0.219049	0.20983	0.154244	0.11681	35.47831	15.11081	16.67966996	4.68190261	10067.65	603.7816	676.4214	676.4816	460.4206	0
	Middle Litter Position	Head First	Outboard	To	0.63523	0.160675	0.117834	0.160689	0.174367	0.082728	63.15019	18.76349	18.35013862	5.103453525	29664.79	426.7395	395.5494	334.8375	1571.488	0
				From	0.648874	0.234073	0.180874	0.193212	0.295701	0.163396	39.45247	15.19422	15.67303448	4.43196903	15838.72	608.4852	0	731.2539	2913.52	79.84038
			Inboard	To	*	*	*	*	*	*	*	*	*	*	*	*	*	*	*	*
				From	*	*	*	*	*	*	*	*	*	*	*	*	*	*	*	*
		Feet First	Outboard	To	0.625233	0.247519	0.327533	0.219923	0.231693	0.132522	48.93197	21.47289	22.54882424	6.30703498	17882.53	1876.851	3478.087	1016.266	468.4658	146.476
				From	0.579911	0.219215	0.251938	0.239828	0.232964	0.14602	44.94921	19.79952	20.33560687	5.789448039	17353.92	988.0285	2396.059	1675.395	1212.68	200.1778
			Inboard	To	0.454546	0.190949	0.194393	0.193313	0.16889	0.122123	38.57972	16.69989	17.3422732	4.810688648	10249.59	864.3187	499.9622	1066.613	1916.033	328.7978
				From	0.492524	0.216252	0.188038	0.187188	0.167882	0.1294	47.36857	15.83799	16.3301352	4.510670965	15504.37	1664.965	878.8119	1354.914	1090.782	784.0066
	Bottom Litter Position	Head First	Outboard	To	0.436013	0.147448	0.164533	0.157547	0.265826	0.104054	37.80887	15.90163	16.17133791	4.449238076	11234.51	528.2341	591.6702	726.6059	3295.41	251.2384
				From	0.635928	0.214905	0.185732	0.201198	0.175081	0.118109	39.22678	16.27244	16.49914176	4.634446999	14537.3	766.215	773.3181	1156.8	1693.829	226.8064
			Inboard	To	0.386899	0.172051	0.137624	0.165591	0.115382	0.09967	27.21581	15.95767	17.03654418	4.562236174	4904.486	639.4007	75.66515	724.7183	*	66.21261
				From	0.601753	0.190862	0.199003	0.163834	0.171709	0.113474	52.92174	19.47908	19.09902173	5.251430519	15968.98	1522.189	841.3163	321.1078	1457.683	29.00961
		Feet First	Outboard	To	0.396979	0.167986	0.189928	0.165273	0.167598	0.133736	29.4359	14.5495	15.45661001	4.34496609	9202.633	1625.886	1600.958	215.3118	681.9252	372.9536
				From	0.544132	0.23064	0.217344	0.301005	0.191252	0.155005	39.16	17.86754	19.72519076	5.487721519	13519.8	1198.644	769.5013	1999.802	845.9012	443.4069
			Inboard	To	0.461101	0.187288	0.195433	0.173157	0.184919	0.111928	45.69224	24.17789	27.46050973	7.644184402	10497.03	685.7884	1025.348	1164.048	2102.471	445.9462
				From	0.553633	0.195838	0.155844	0.198153	0.203583	0.132542	46.80743	16.67479	16.34030246	4.68317509	17780.42	994.3249	377.1213	1429.313	2135.039	414.6385
IMMSS (two litter positions)	Top Litter Position	Head First	Outboard	To	0.336781	0.144062	0.204927	0.194066	0.17699	0.102401	31.00987	17.05732	18.83980527	5.187695784	17427.15	288.5224	313.009	987.8711	583.9335	192.5206
				From	0.486955	0.208788	0.215954	0.20574	0.223389	0.108542	39.38419	16.52653	17.59352424	4.790973938	13874.2	1706.933	1743.797	908.5851	1673.115	147.5683
			Inboard	To	0.602675	0.260595	0.239344	0.24204	0.264395	0.182684	49.79638	21.5442	22.00595259	6.217756701	29767.33	3908.373	3952.962	1014.588	4153.947	270.7519
				From	0.604999	0.195057	0.197259	0.219382	0.18402	0.132228	45.3862	17.07227	17.57515027	4.98325827	25516.17	2716.53	1645.979	921.2015	631.9663	67.31703
		Feet First	Outboard	To	0.312303	0.104197	0.16943	0.230569	0.250274	0.141828	29.02872	13.76354	13.95705356	3.876327672	4571.62	761.0095	625.6591	1174.117	3535.257	573.9473
				From	0.48539	0.177339	0.149062	0.150483	0.262087	0.092439	38.984	13.79236	14.08879558	4.056417936	14346.89	470.3383	0	391.2634	438.5311	0
			Inboard	To	*	*	*	*	*	*	*	*	*	*	*	*	*	*	*	*
				From	*	*	*	*	*	*	*	*	*	*	*	*	*	*	*	*
	Bottom Litter Position	Head First	Outboard	To	0.537339	0.158245	0.151919	0.174861	0.168207	0.097399	53.42324	21.16218	22.61151696	6.181774165	18450.06	06.193	3856.059	529.0411	3264.704	416.6697
				From	0.449045	0.18967	0.171606	0.186216	0.156229	0.109333	34.88215	15.47751	16.25403612	4.529852199	8600.62	545.3895	371.0553	448.3824	519.7752	0
			Inboard	To	0.558251	0.259552	0.217326	0.24406	0.223549	0.157888	42.2203	17.43872	18.25782505	5.011762181	24139.61	3439.603	4024.029	1907.916	1087.366	789.5937
				From	0.589931	0.261265	0.262589	0.203435	0.144346	0.12675	45.9913	16.33921	16.60292665	4.534576764	44141.43	9776.157	6545.23	629.0516	2065.215	708.0519
		Feet First	Outboard	To	0.423784	0.156441	0.139347	0.184298	0.147469	0.092538	39.30778	16.43584	17.82495724	4.8976412	28566.31	9830.109	11343.42	731.6564	849.8608	2404.543
				From	0.658698	0.275137	0.256512	0.237376	0.166644	0.122441	50.24865	18.60457	19.77307885	5.611620543	22435.6	2416.26	1596.147	1289.452	870.7355	153.7588
			Inboard	To	0.401126	0.141418	0.143496	0.141429	0.183491	0.10912	33.80897	16.34642	17.02530417	4.775145324	7713.656	1136.979	1142.387	1109.76	2559.943	1035.109
				From	0.341228	0.131634	0.178513	0.157118	0.265693	0.093548	21.91204	11.35386	12.46163936	3.539158805	3783.419	32.17866	90.94215	271.8954	2533.072	0

Figure 19: This table is equivalent to Table 1 of the protocol, populated with the calculated metrics for each body segment *during the walking to and walking from motion segments*. The symbol "*" is used to denote cells where values from the removed trials 4 and 19 would go.

U.S. Army Aeromedical Research Laboratory
Fort Rucker, Alabama

All of USAARL's science and technical information documents are available for download from the Defense Technical Information Center.

https://discover.dtic.mil/results/?q=USAARL

Army Futures Command
U.S. Army Medical Research and Development Command